POLITECNICO DI TORINO

Collegio di Ingegneria Chimica e dei Materiali

**Corso di Laurea Magistrale
in Ingegneria Chimica e dei Processi Sostenibili**

Tesi di Laurea Magistrale

Production and characterization of sawdust-derived biocarbon monolith

Relatore

Prof. Alberto Tagliaferro

Correlatore

Prof Charles Q. Jia

Candidato

Elena Guazzo

Marzo 2019

ABSTRACT

Renewable energies have usually the problem that their supply is intermittent. They need energy storage systems (ESSs), that can capture energy at any time, store it and release it when it is necessary. Supercapacitors could be a good solution because of their long cycle-life, fast charging and discharging time and satisfactory values of energy and power densities. This thesis is focused on the study of a new, eco-friendly and cheap material for supercapacitor applications: biochar.

Biochar is a carbon-rich porous solid material obtained from pyrolysis of biomass. In this case the feedstock was lignocellulosic biomass, in particular sugar maple sawdust. Biochar has always been used in agricultural systems to improve soil fertility. In the last decades interest in biochar has grown a lot thanks to its ability to face some important problems such as the climate change and water pollution and to be used as sustainable material in energy applications. This work is a first step of a project focused on the production of electrodes for supercapacitors. Sawdust-derived biocarbon monolith were produced from delignified, compressed and pyrolyzed sawdust. The research was conducted in the Green Technologies Lab of the Department of Chemical Engineering of the University of Toronto under the supervision of the Professor Charles Q. Jia.

This research studies the feasibility in terms of production and characterization of sawdust-derived biocarbon monolith. The sawdust has undergone a pre-treatment process, has been compressed to produce pellets and has undergone a pyrolysis process. Physical and electrical properties of the sawdust-derived biocarbon monolith has been investigated. The main goal was to understand how the change in pressure applied during the compression and the pyrolysis conditions can affect the physical and electrical properties of the final biocarbon structure. The idea of using compressed sawdust instead of monolith pieces of wood could have some advantages such as valorising a waste of the wood industry, producing a homogeneous and more uniform material, with the possibility to make the material repeatable, without depending on the original tree structure and producing a dense material, denser than the original wood.

ESTRATTO IN ITALIANO

1.PREMESSA

Il biochar è un materiale solido carbonioso e poroso ottenuto dalla pirolisi di materiale organico. Con il termine pirolisi si intende un processo di decomposizione termica condotta in parziale o totale assenza di ossigeno. Dalla pirolisi di biomassa si ottengono tre prodotti: bio-oil (olio pirolitico), bio-gas e biochar. I primi due vengono principalmente utilizzati come combustibili mentre il residuo solido, biochar, ha trovato moltissimi campi di applicazione, alcuni molto recenti e di particolare interesse.

Negli ultimi decenni l'interesse per il biochar è cresciuto molto, grazie alla sua abilitá di affrontare problematiche attuali come la mitigazione dei cambiamenti climatici, il trattamento delle acque, la bonifica dei terreni, ed essere utilizzato per la produzione di energia o come filler di polimeri biocompositi. Ad oggi l'applicazione principale è ancora quella di ammendante per terreni, tuttavia aree di applicazioni meno tradizionali si stanno sviluppando. In particolare, in questa tesi l'interesse è rivolto all'utilizzo del biochar come materiale di partenza per elettrodi di supercondensatori. Questa applicazione è molto recente e il biochar viene considerato altamente funzionale grazie alla qualitá di essere facilmente ottenibile, economico e soprattutto environmentally friendly. Il suo prezzo di mercato è di circa 250 US\$/ton.

Le sue proprietá fisiche, chimiche e meccaniche dipendono dal tipo di materia prima scelta. La biomassa di partenza gioca un ruolo fondamentale nel processo perché influisce sulle proprietá del prodotto finale. In questo caso la materia prima è il legno, in particolare la segatura.

2. OBIETTIVI E METODOLOGIA

Poiché il biochar è sempre stato utilizzato come combustibile solido e fertilizzante per terreni, molte delle sue proprietá, tra cui la conducibilitá elettrica, non sono mai state studiate. Solo negli ultimi anni è nato l'interesse verso questo materiale e verso la possibilitá di utilizzarlo come elettrodo nei supercondensatori.

Il Green Technologies Lab della University of Toronto, sede in cui è stato condotto il lavoro presentato in questa tesi, ha dedicato la sua attivitá di ricerca nello studio della conducibilitá elettrica di biochar monolitico e delle sue prestazioni come materiale elettrodico. Prima di questo studio, la conducibilitá elettrica è sempre stata studiata su polveri compresse; per la prima volta si è cercato di collegare la conducibilitá del biochar alla sua struttura, che dipende fortemente dalla biomassa da cui esso deriva.

Lo studio eseguito per questa tesi puó essere considerato il primo step di un progetto che ha come obiettivo principale l'analisi della conducibilitá elettrica di biochar derivante da pellets prodotti da segatura compressa, e non da pezzi monolitici di legno. L'idea di utilizzare segatura nasce dal fatto che essa sia uno scarto dell'industria e il biochar derivante da essa sarebbe un materiale economico ed ecosostenibile. Tutti i lavori che si possono trovare in letteratura riguardanti la compressione di segatura per la produzione di pellets hanno come obiettivo la produzione di combustibile. Per questo motivo non si hanno informazioni riguardanti la pirolisi e la conducibilitá elettrica di questo tipo di biochar.

Quindi, i principali obiettivi che si pone questo lavoro sono:

- La valorizzazione di un waste come la segatura, invece di utilizzare legno come negli studi precedenti che sono stati condotti alla University of Toronto;
- Produrre un materiale che sia il piú omogeneo e uniforme possibile, con la possibilitá di mischiare differenti tipi di segatura derivanti da differenti tipi di albero e rendere il materiale ripetibile, senza dipendere dalla struttura originale dell'albero;
- Produrre un materiale denso, piú denso del legno originale da cui proviene la segatura e questa è la proprietá che ci si aspetta essere responsabile di una buona conducibilitá elettrica.

Poiché il lavoro è il primo step di questo progetto, esso prevede la produzione, la caratterizzazione e la misura della conducibilitá elettrica di pellets pirolizzati derivanti da segatura compressa.
La procedura sperimentale seguita puó essere riassunta nei seguenti punti:

1- Selezione della materia prima
2- Pretrattamento della segatura
3- Compressione della segatura a 100°C e produzione dei pellets
4- Pirolisi e produzione del biochar
5- Misure di conducibilitá elettrica
6- Caratterizzazione fisico-chimica del biochar

La prima parte del lavoro ha riguardato la produzione di pellets senza l'utilizzo di leganti. L'attenzione è stata rivolta alla possibilitá di ottenere una struttura densa e compatta senza l'aiuto di leganti. Nell'ultima parte del lavoro la lignina è stata aggiunta come legante durante la produzione dei pellets. Si vedrá in seguito come l'aggiunta di lignina influisca sulle proprietá fisiche ed elettriche del biochar. Poiché il numero di parametri coinvolti nel lavoro è molto alto, solo tre di essi sono stati scelti come variabili da studiare, mentre gli altri sono stati fissati.
In particolare, sono stati fissati i seguenti parametri: il tipo di materia prima, la dimensione delle particelle di segatura, il tipo e la durata del pretrattamento, il contenuto di umiditá e la temperatura utilizzata durante la compressione.
Le variabili scelte sono state: la pressione applicata durante la compressione della segatura, le condizioni adottate durante il processo di pirolisi e la percentuale di lignina aggiunta negli ultimi due set di campioni.

Il lavoro si basa su 54 campioni: 9 set da 6 campioni ciascuno.
I primi 42 campioni sono pellets pirolizzati derivanti da segatura compressa. All'interno di ogni set i campioni si distinguono per l'utilizzo di differenti pressioni adottate durante la compressione e produzione dei pellets. I set si distinguono uno dall'altro per l'adozione di differenti condizioni di pirolisi durante la produzione del biochar.
Gli ultimi 12 campioni sono pellets pirolizzati derivanti da segatura compressa con aggiunta di lignina come legante. I due set si distinguono per la diversa percentuale di lignina aggiunta. Come per i precedenti, all'interno di ogni set i campioni si distinguono per l'utilizzo di differenti pressioni adottate durante la produzione dei pellets.
Si sono quindi studiate le proprietá fisiche ed elettriche del biochar ottenuto al variare della pressione applicata, delle condizioni di pirolisi adottate e dal contenuto di lignina aggiunto.

3.ATTIVITÁ DI RICERCA

3.1 SELEZIONE DELLA MATERIA PRIMA

La materia prima scelta per questo lavoro è stata segatura derivante da acero, Acer Saccharinum. È stata fornita dalla Faculty of Forestry della University of Toronto. L'acero appartiene alla categoria degli hardwood e la sua densitá è di circa 0.733 g/cm^3. La scelta è stata dettata dal fatto che, negli studi portati avanti alla University of Toronto negli ultimi anni, è stato dimostrato che il biochar monolitico derivante da acero fosse il piú conduttivo.

La segatura è stata setacciata per mezzo di setacci U.S.A standard testing di VWR Scientific. Il range scelto per la dimensione delle particelle è stato 212-600 μm.

3.2 PRETRATTAMENTO DELLA SEGATURA

Per ottenere pellets da segatura, una rimozione parziale della lignina (e dell'emicellulosa) dalla struttura è necessaria, al fine di rendere la compressione piú semplice ed efficiente. In caso contrario, le particelle non riuscirebbero a formare una struttura compatta, e la compressione richiederebbe una temperatura di centinaia di gradi. La biomassa lignocellulosica è formata principalmente da 3 componenti: cellulosa, emicellulosa e lignina. La lignina è la componente che conferisce rigiditá alle pareti cellulari e resistenza alla compressione. La sua rimozione è uno step cruciale in questo lavoro in quanto uno dei principali obiettivi è quello di ottenere un materiale piú denso e un miglior contatto tra le particelle. Tuttavia, questa rimozione deve essere parziale e non totale in quanto lignina ed emicellulosa agiscono da agenti cementificanti: l'effetto combinato di pressione e temperatura adottati durante la produzione dei pellets, causa il rilascio della lignina contenuta ancora nelle strutture cellulari che agisce come collante tra le particelle di segatura, favorendo la compressione e aumentando la densitá dei pellets. Questo step si basa su lavori precedenti, le cui referenze sono [53] e [54]. Il metodo si basa principalmente su due step: un trattamento chimico in soluzione alcalina seguito da compressione e densificazione della segatura.

La segatura é stata sottoposta ad un pretrattamento in una soluzione acquosa in ebollizione composta da una miscela 1:1 in volume di 2.5 M di NaOH e 0.4 M di Na_2SO_3, della durata di 2 ore. Solitamente 20-30 gr di segatura sono immersi in 400 mL di soluzione. In seguito, è stata immersa numerose volte in acqua deionizzata in ebollizione per rimuovere i residui di soluzione. A seguito di ogni immersione, la segatura è stata separata dalla parte liquida grazie all'utilizzo di un filtro in fibra di vetro e di una pompa da vuoto. Successivamente, la segatura ha subito numerosi lavaggi con acqua deionizzata fino a quando la conducibilitá elettrica dell'acqua post-lavaggio non mostrasse un valore molto vicino a quella dell'acqua deionizzata (8 μS/cm). In figura 5.6 è possibile notare il cambiamento di colore della segatura a seguito dei vari lavaggi: da un colore marrone scuro dovuto al pretrattamento e alla rimozione della lignina, si schiarisce fino ad assumere un colore giallo dorato.

L'analisi TGA è stata eseguita su un campione di segatura prima e dopo il pretrattamento al fine di avere un'idea della decomposizione dei componenti lignocellulosici nelle due differenti situazioni. L'analisi termogravimetrica è una tecnica che monitora la massa di un campione in funzione della temperatura e del tempo quando il campione è sottoposto ad un programma di temperatura controllata in atmosfera controllata. Confrontando le curve TGA prima e dopo il pretrattamento con curve trovate in letteratura, si possono notare le regioni di temperatura in cui i componenti del legno si degradano.

Il contenuto di lignina nei campioni di segatura prima e dopo il pretrattamento è stato calcolato in laboratorio tramite processo Klason. Esso è un metodo che permette di calcolare il contenuto di lignina insolubile nel legno.

3.3 COMPRESSIONE A 100°C

Il secondo step della procedura sperimentale prevede la compressione della segatura e la produzione dei pellets. Prima della compressione la segatura è stata posta in forno a 110°C, monitorandone il peso, per un tempo tale per cui il contenuto di umidità fosse nel range 8-8.5%. Questo valore è stato scelto sulla base di altri lavori trovati in letteratura riguardanti le condizioni ottimali per raggiungere alte densità durante la produzione di pellets utilizzati poi come combustibili. La compressione è stata eseguita con una pressa meccanica manuale Carver in cui è stato inserito un set-up formato da una cavità cilindrica riscaldata e da un pistone, per la produzione di pellets. Come menzionato in precedenza, ogni set contiene 6 campioni, che sono stati ottenuti a 6 differenti pressioni:

1) 500 psi (3.45 MPa)
2) 1000 psi (6.89 MPa)
3) 1500 psi (10.34 MPa)
4) 2000 psi (13.79 MPa)
5) 2500 psi (17.24 MPa)
6) 3000 psi (20.68 MPa)

Ad ogni campione è stata assegnata una sigla X.Y dove X sta ad indicare la condizione di pirolisi adottata e Y indica la pressione alla quale è stato prodotto il pellet. Ad esempio, il campione 3.6 è il campione prodotto ad una pressione di 3000 psi e pirolizzato alla condizione di pirolisi n.3 (che verranno descritte a breve).

I campioni con lignina aggiunta sono stati prodotti aggiungendo 10 e 20% in peso di lignina. La lignina è stata miscelata con le particelle di segatura ed in seguito è stata compressa per la produzione di pellets. Dalla figura 5.12 si può notare come i campioni prodotti con aggiunta di lignina possiedano un colore marrone scuro conferito dalla lignina.
Le dimensioni (spessore e diametro) e la massa dei pellets sono stati misurati e volume e densità sono stati calcolati. Questi parametri saranno importanti perché saranno poi confrontati con quelli misurati in seguito al processo di pirolisi.

3.4 PIROLISI E PRODUZIONE DI BIOCHAR

Il terzo step adottato in questa procedura sperimentale prevede che i campioni siano sottoposti a pirolisi. La composizione e le proprietà del biochar sono fortemente dipendenti dalle condizioni di pirolisi. Essa è un processo di degradazione termochimica che avviene in atmosfera inerte a temperature superiori ai 300-400°C. È stato utilizzato un reattore verticale in quarzo inserito in una fornace (figura 5.14). Per assicurare un'atmosfera inerte nel reattore, ed evitare la combustione dei campioni, un flusso di azoto di 400 mL/min è stato utilizzato.
La produzione di campioni di biochar si è focalizzata sul controllo dei seguenti parametri:

- Temperatura massima di pirolisi (HTT): sono state scelte come temperature massime 1000 e 1200°C. Alla temperatura di circa 700-800°C la quasi totalità della componente organica è eliminata. Dopo l'iniziale evaporazione dell'acqua, emicellulosa, cellulosa e lignina iniziano a degradarsi. Aumentando la massima temperatura di pirolisi, le catene carboniose alifatiche si convertono gradualmente in gruppi carboniosi aromatici, causando successivamente l'inizio della grafitizzazione della microstruttura quando la temperatura finale supera i 1000°C. Tuttavia si arriva a strutture grafitiche ordinate quando la temperatura raggiunge i 2000-2500°C.
- Velocità di riscaldamento (HR): poiché l'interesse principale è rivolto verso il prodotto solido della pirolisi, basse velocità di riscaldamento (pochi °C/min) devono essere adottate per aumentare la resa in biochar e ottenere una struttura esente da cricche. Tutti i lavori condotti

nel Green Lab della University of Toronto, hanno sempre adottato HR inferiori ad 1°C/min. Poiché questo lavoro si basa su pellets derivanti da segatura compressa, velocitá di riscaldamento fino a 2°C/min sono state testate: l'umiditá contenuta nei pellets infatti possiede molti piú percorsi disponibili per lasciare la struttura del pellet, a differenza del biochar monolitico.

- Tempo di mantenimento (HT): è il tempo al quale viene mantenuta la HTT. Aumentando il tempo di mantenimento, accrescono le probabilitá di reticolazione e ciclizzazione dei polimeri in decomposizione. Le molecole organiche si organizzano in strutture condensate, accrescendo la possibilitá di formare una microstruttura piú ordinata. Vedremo in seguito che aumentare il tempo di mantenimento è piú efficace nel migliorare la conducibilitá elettrica rispetto alla diminuzione della velocitá di riscaldamento.

Nella sezione 5.4.1 sono descritte le 6 differenti condizioni di pirolisi adottate in questo lavoro.

Successivamente al processo di pirolisi, la *char yield* e il ritiro percentuale radiale e assiale sono stati calcolati. Come si puó notare dalla figura 5.16 infatti, il campione pirolizzato ha subíto un ritiro in entrambe le direzioni. Inoltre, la perdita di massa è superiore rispetto alla diminuzione del volume: vedremo infatti che i valori di densitá post-pirolisi sono inferiori a quelli dei pellets.

3.5 MISURE DI CONDUCIBILITÁ ELETTRICA

La conducibilitá elettrica del biochar è stata misurata con un metodo *two probes*.
La figura 5.17 riporta uno schema della misura della resistività elettrica con il metodo two probes: una differenza di potenziale ai capi del campione e una corrente attraverso esso sono misurati. Due differenti set-up sono stati utilizzati, al solo scopo di avere maggiore conferma dei risultati sperimentali. Qui verrà riportata la descrizione del primo set-up, da cui sono stati ricavati i risultati presentati nella sezione 6.4. La descrizione del secondo set-up è riportata nella sezione 5.5.
Il campione è stato posizionato tra due elettrodi di tin foil (carta stagnola) fissati su due piastre di plexiglass. Poiché i campioni non hanno superficie liscia, per migliorare il contatto tra il campione e il collettore di corrente, una leggera pressione è stata applicata durante la misura, posizionando un pesetto di rame al di sopra della piastra superiore del set-up. La resistenza elettrica del campione è stata misurata da un multimetro Hewlett Packard 34401A DC. La resistività è stata calcolata attraverso la seconda legge di Ohm, conoscendo le proprietá geometriche (area di base e spessore) del campione di biochar. A questo punto la conducibilitá elettrica è stata calcolata.

È importante definire la differenza tra *bulk conductivity* e *skeletal conductivity*. La conducibilitá di bulk è la conducibilitá misurata, quella "apparente" in quanto tiene conto dell'intera struttura del campione composta da solido (biochar) e aria (porositá all'interno della struttura). La conducibilitá skeletale è la conducibilitá effettiva del solo materiale solido, senza tenere conto della presenza di aria all'interno della struttura del campione. Per calcolarla, si parte dall'assunzione che la struttura del biochar ottenuto (con HTT di 1000 e 1200°C) sia quasi completamente amorfa. La frazione in volume del biochar puó essere calcolata dividendo la densità del campione per la densità del biocarbon amorfo. A questo punto la conducibilitá di bulk misurata in precedenza viene divisa per questo valore, ottenendo la conducibilitá skeletale. Alla fine della sezione 5.5 si puó trovare una descrizione piú dettagliata del calcolo eseguito.

È importante sottolineare come in letteratura non esistano lavori riguardanti misure di conducibilitá elettrica di biochar monolitici derivanti da segatura compressa. Le misure di conduttività elettrica di biochar sono sempre state ottenute da polveri di biochar compresse: il biochar veniva prodotto, frantumato e in seguito le misure di conduttività elettrica erano effettuate.

3.6 CARATTERIZZAZIONE FISICO-CHIMICA DEL BIOCHAR

La caratterizzazione del biochar comprende: analisi termogravimetriche, analisi elementale, analisi XRD e spettroscopia Raman. Le informazioni ricavate dalla caratterizzazione sono state utili per riuscire a spiegare i risultati di conducibilitá elettrica ottenuti.

4. RISULTATI

4.1 ANALISI TERMOGRAVIMETRICHE

In figura 6.1 e 6.2 sono riportate le curve TGA e DTG (derivata prima della curva TGA) della segatura prima e dopo il pretrattamento. Le componenti della biomassa si decompongono in fasi ben distinte: a 70-80°C viene eliminata l'umiditá, a 200°C emicellulosa e cellulosa iniziano la decomposizione e nel range tra i 200 e 400°C, il 70% della massa viene persa. La degradazione della lignina avviene invece piú lentamente coinvolgendo un range di temperature molto piú ampio: da 300 a 700-800°C. La segatura post-trattamento presenta un comportamento differente: se prima si distinguevano due picchi per la decomposizione di emicellulosa e cellulosa, dopo il trattamento si puó notare solo il picco della cellulosa. Inoltre, le aree sottese dalle curve DTG evidenziano differenti percentuali di emicellulosa e lignina rispetto al caso prima del trattamento. Esso infatti ha rimosso parzialmente la lignina e l'emicellulosa dalla biomassa.

4.2 RIMOZIONE DI LIGNINA

Con il metodo Klason è stata calcolata la percentuale in peso di lignina contenuta nella segatura prima e dopo il pretrattamento. La percentuale di lignina passa dal 31.4% al 13.7% in peso. In figura 6.3 sono riportati gli spettri IR della segatura trattata e non: essi sono molto simili eccetto per la scomparsa del picco a 1729 cm^{-1} per la segatura trattata. Questo segnale rappresenta lo stretching del legame C=C, gruppo funzionale tipico degli anelli aromatici contenuti nella struttura della lignina.

4.3 PROPRIETÁ DEI PELLETS

La tabella 6.2 riporta un esempio di massa, spessore, volume e densitá dei pellets. Come atteso, a parità di massa, aumentando la pressione applicata durante la produzione dei pellets, lo spessore va a diminuire, cosi come il volume, mentre la densitá aumenta. I valori di densitá ottenuti si trovano nel range 1.00-1.29 g/cm^3, valori molto piú alti della densitá del legno di partenza. I campioni ottenuti con aggiunta di lignina come legante hanno mostrato una densitá piú elevata: il range di valori è infatti 1.12-1.34 g/cm^3 e il set di campioni contenente il 20% di lignina presenta densitá maggiori di quello ottenuto con il 10%. La presenza della lignina comporta un aumento della densitá dei pellets: questo potrebbe essere dovuto al fatto che la lignina si trovi in forma di polvere e particelle piú piccole rispetto a quelle della segatura, se compresse, presentano densitá piú elevate. La parziale rimozione di lignina è un punto chiave in questo lavoro: essa ha favorito la compressione delle particelle di segatura ottenendo densitá di 1.3 g/cm^3 applicando una pressione di 20.68 MPa; in letteratura (ref. [62]) si trovano, a parità di altre condizioni durante la produzione di pellets, densitá di 0.9 g/cm^3 ottenute a 191 MPa. Sono state ottenute denitá piú elevate a pressioni applicate inferiori.

4.4 PROPRIETÁ DEL BIOCHAR

In tabella 6.3 sono riportati i valori di char yield, ritiro percentuale assiale e radiale e perdita percentuale in volume per il set di pellets sottoposto alla condizione di pirolisi n.1, pirolisi lenta. Come si puó notare, non c'è alcuna dipendenza di questi parametri dalla pressione applicata durante la produzione di pellets. I valori di char yield sono coerenti con quelli ottenuti nei precedenti lavori delle ref. [33] e [63]. Il ritiro assiale è piú marcato rispetto a quello radiale: questo risultato porta all'ipotesi che ci sia un'orientazione preferenziale nella struttura. La riduzione della struttura del biochar è quindi anisotropa. Nel caso di biochar monolitico (ref. [63]), il ritiro assiale è inferiore rispetto a quello radiale. Una possibile

spiegazione è che l'applicazione della pressione durante la produzione dei pellets favorisca un'orientazione delle fibre in direzione radiale, ovvero perpendicolare alla direzione della pressione applicata. Durante il processo di carbonizzazione, cellulosa ed emicellulosa si decompongono, rilasciando prodotti e restringendo le pareti cellulari. In figura 6.7 è riportato un confronto fra le densitá dei pellets derivanti da segatura compressa e quelle del biochar che ne deriva. La densitá del biochar è inferiore a quella dei pellets in quanto la perdita di massa prevale sulla diminuzione del volume. Il trend della densitá in funzione della pressione applicata viene mantenuto anche dopo il processo di pirolisi. La densitá post-pirolisi è circa il 70% di quella pre-pirolisi. Il range di valori ottenuti è 0.65-0.98 g/cm^3, superiore a quello del biochar derivanti da monoliti dello stesso tipo di legno, 0.552 g/cm^3.

In seguito, sono stati confrontati char yield e ritiri di campioni sottoposti a differenti condizioni di pirolisi, per valutare l'effetto della HTT, della velocitá di riscaldamento e del tempo di mantenimento. Nella sezione 6.3 sono riportati i risultati di questo confronto. L'aumento del tempo di mantenimento a 1000°C da 6 a 60 minuti sembra non avere effetto sul char yield o sul ritiro radiale e assiale. Per quanto riguarda invece la velocitá di riscaldamento, possiamo concludere che velocitá piú basse e una pirolisi piú lenta causano l'aumento del ritiro assiale, mentre non hanno alcun effetto sul ritiro radiale. Lo stesso effetto viene causato da un incremento della HTT: passando infatti da 1000 a 1200°C, il ritiro assiale passa da un 23-25% ad un 30-32%. Aumentando la massima temperatura di pirolisi, si favorisce la condensazione delle molecole aromatiche in strutture sempre piú ordinate.

L'aggiunta di lignina causa un incremento della resa in char: la lignina infatti, è la piú responsabile per la resa in char tra i componenti lignocellulosici. Ancora una volta il ritiro radiale possiede gli stessi valori visti in precedenza, mentre il ritiro assiale è superiore rispetto ai casi senza lignina: i valori sono nel range 32-36%. La lignina quindi subisce un maggior effetto di ritiro una volta sottoposta a pirolisi. Poiché la perdita in massa è minore rispetto ai casi di pellets senza lignina aggiunta, la densitá del biochar ottenuto con lignina aggiunta è piú alta rispetto agli altri campioni: il range di valori è infatti 1.03-1.08 g/cm^3.

4.5 CONDUCIBILITÁ ELETTRICA

Si sono studiati gli effetti dell'HTT, velocitá di riscaldamento, tempo di mantenimento, pressione applicata durante la produzione dei pellets e aggiunta di lignina sulla conducibilitá elettrica del biochar derivante da segatura compressa.

Tutti i set, sottoposti a differenti condizioni di pirolisi hanno mostrato lo stesso andamento di conducibilitá di bulk e skeletal: all'aumentare della pressione applicata durante la produzione dei pellets e quindi della densitá, la conducibilitá elettrica diminuisce.

In figura 6.12 la conducibilitá skeletale del set n.1 è riportata in funzione della densitá dei pellets: è possibile osservare la diminuzione di conducibilitá all'aumentare della densitá. Il range di valori è 56-91 S/m. La conducibilitá elettrica di biochar monolitico derivante dallo stesso tipo di biomassa è stata studiata in precedenti lavori nel Green T. Lab: 1233 S/m è stato il valor medio misurato, dieci volte superiore rispetto a quello del biochar derivante da segatura compressa.

L'aumento del tempo di mantenimento alla massima temperatura di pirolisi (figura 6.12 e 6.13) ha causato un incremento della conducibilitá da 56-91 S/m a 85-124 S/m. L'aumento del tempo da 6 a 60 minuti permette agli atomi di carbonio di organizzarsi in una struttura grafitica maggiormente ordinata e quindi piú conduttiva. L'aumento del tempo a 1000°C da un'ora a 6 ore ha portato ad un incremento di conducibilitá elettrica da 74-119 a 92-132 S/m.

All'aumentare della velocitá di riscaldamento (figura 6.13, 6.14 e 6.16), a parità di altre condizioni, passando da una condizione di pirolisi lenta ad una di pirolisi convenzionale, la conducibilitá elettrica diminuisce, in quanto i campioni di biochar sono prodotti in un tempo minore e gli atomi di carbonio hanno minor tempo di organizzarsi in una struttura piú ordinata e conduttiva.

L'aumento della massima temperatura di pirolisi (figura 6.15 e 6.17) da 1000 a 1200°C comporta un aumento della conducibilitá da 92-132 S/m a 89-163 S/m. Anche in questo caso la conducibilitá del biochar derivante da pellets prodotti per compressione di segatura è di un ordine di grandezza inferiore a quella misurata su biochar monolitici derivanti dallo stesso legno, 1763 S/m.

L'aggiunta di lignina ha causato una forte diminuzione nella conducibilità elettrica dei campioni di biochar. La tabella 6.8 mostra questa diminuzione, a parità di altre condizioni, passando da campioni ottenuti senza addizione di lignina a campioni ottenuti con il 20% di lignina aggiunta. Questo risultato è spiegato con il fatto che la lignina è la piú amorfa tra i componenti lignocellulosici. La cellulosa possiede la struttura piú ordinata e cristallina, precursore della struttura grafitica e conduttiva che si forma durante il processo di pirolisi. La presenza di maggiore lignina nel campione comporta la formazione di una struttura principalmente amorfa.

In figura 6.18 è rappresentato il tipico andamento della conducibilità elettrica in funzione della pressione applicata durante la produzione dei pellets. All'aumentare della pressione applicata, e quindi della densitá dei pellets, i campioni mostrano una conducibilitá inferiore.

Alcune ipotesi sono state formulate a spiegazione di questo fenomeno:

1- Grado di carbonizzazione: l'aumento della pressione durante la produzione dei pellets potrebbe ostacolare la riuscita del processo di carbonizzazione, in quanto all'interno di pellets piú densi i prodotti di pirolisi potrebbero avere maggiori difficoltá a lasciare la struttura.
2- Grado di grafitizzazione: l'aumento della pressione durante la produzione dei pellets potrebbe ostacolare il processo di grafitizzazione e lo sviluppo di nano-cristalli di grafite all'interno della struttura del biochar, causandone la minor conducibilitá.
3- Presenza di micro-cricche nella struttura: l'aumento di pressione durante la produzione dei pellets potrebbe causare la formazione di cricche nelle particelle di legno e quindi in quelle di biochar. In letteratura è stato mostrato come la presenza di cricche nella struttura del biochar sia considerata un punto di discontinuitá nella struttura, che abbassa la conducibilità elettrica. Inoltre, durante il processo di pirolisi, umiditá e prodotti di pirolisi volatili potrebbero avere piú difficoltá a lasciare la struttura dei pellets piú densi causando la formazione di cricche durante la carbonizzazione.
4- Presenza di umidità: i pellets prodotti a minori pressioni presentano una minor densitá e questo potrebbe favorire l'adsorbimento di umiditá dall'ambiente esterno, incrementandone la conducibilitá elettrica: le molecole di acqua potrebbero avere il ruolo di ponti di collegamento tra le particelle di biochar, favorendo il passaggio di corrente.
5- Resistenza di contatto tra le particelle: aumentando la pressione durante la produzione dei pellets potrebbe causare un aumento della resistenza di contatto, abbassandone la conducibilitá.

Grazie alla caratterizzazione e a lavori trovati in letteratura, 4 delle 5 ipotesi sono state confutate.

L'analisi elementare ha rilevato che il contenuto di carbonio e i rapporti H/C e O/C, indici del grado di carbonizzazione e aromatizzazione del biochar, dipendano dalle condizioni di pirolisi, in particolar modo dalla HTT ma non dalla pressione applicata. Infatti, il contenuto di carbonio è lo stesso per tutti i campioni appartenenti allo stesso set. Per i campioni pirolizzati a 1000°C il contenuto in carbonio è del circa 93%, mentre per quelli pirolizzati a 1200°C esso si trova nel range 94-98%. Questo risultato spiega come i campioni del set n.6 siano piú conducibili di quelli appartenenti al set n.5.

Le analisi XRD e la spettroscopia Raman hanno confutato l'ipotesi n.2. Dalla caratterizzazione infatti, emerge che esistano dei nano-cristalli all'intero della struttura, ma che la loro presenza dipenda dalla HTT adottata e non dalla pressione applicata. Non esiste infatti alcun legame tra la dimensione dei cristalli calcolata attraverso l'equazione di Scherrer e la pressione applicata durante la produzione dei pellets. I due picchi principali degli spettri XRD si trovano nelle regioni $2\vartheta= 20°\text{-}30°$ e $2\vartheta= 40°\text{-}50°$ e si

riferiscono alle direzioni cristallografiche {002} e {100} della grafite, rispettivamente la direzione perpendicolare e parallela ai piani grafitici. Le dimensioni dei cristalli lungo le due direzioni si trovano nel range 1.1-1.7 nm, e sono coerenti con le dimensioni ottenute in biochar monolitici pirolizzati alle stesse temperature. Le dimensioni dei cristalli sono molto simili tra di loro e non permettono di individuare un certo trend di valori al variare della pressione applicata.

La spettroscopia Raman è stata impiegata per analizzare lo sviluppo di un ordine strutturale nel biochar, confermando i risultati delle analisi XRD. Le caratteristiche più importanti dello spettro Raman per materiali carboniosi sono le bande G e D, i cui picchi si trovano a 1560 e 1360 cm^{-1} (figura 6.20 e 21). Il picco G è legato allo stretching dei legami tra atomi di carbonio ibridati sp^2 sia nelle catene che negli anelli e rappresenta l'ordine della struttura analizzata. Il picco D è indice del grado di disordine della struttura. Passando dai campioni pirolizzati a 1000°C a quelli a 1200°C, è possibile notare un restringimento del picco D e una diminuzione delle inter-componenti tra i due picchi. Questo suggerisce che all'aumentare della HTT, la struttura è più ordinata, in accordo con altri risultati di letteratura. Tuttavia, la spettroscopia Raman non ha mostrato alcun legame tra l'ordine della struttura e la pressione applicata durante la produzione dei pellets. Gli spettri dei campioni appartenenti a ciascun set infatti, si sovrappongono quasi perfettamente, senza mostrare alcuna differenza.

L'ipotesi n.4 è stata confutata testando i campioni appartenenti al set n.6, i più conduttivi. Essi sono stati posti in forno per 3 ore a 110°C e la massa e la conducibilità elettrica sono state nuovamente misurate. La percentuale rappresentante la perdita di massa a seguito dell'essicamento è dell'1.3%, indice del fatto che i campioni non hanno adsorbito umidità dall'ambiente esterno. Inoltre, i valori di conducibilità non hanno mostrato un decremento uniforme: per alcuni campioni si è registrato un valore inferiore di circa 1.2% rispetto al valore iniziale mentre altri campioni si sono mostrati leggermente più conduttivi.

L'ipotesi n.5 è stata confutata dal fatto che in letteratura si siano trovati lavori recenti (ref. [64]) riguardanti la compressione di polveri nanostrutturate di materiali carboniosi e la dipendenza della conducibilità elettrica dalla pressione applicata. Applicando pressioni da 0 a 80 MPa, la conducibilità elettrica ha sempre mostrato un incremento, stabilizzandosi asintoticamente quando le pressioni fossero molto alte. La spiegazione riportata è stata il miglior contatto tra le particelle a seguito della compressione, che ha favorito la conducibilità.

5.CONCLUSIONI

Il biochar è tra i materiali del futuro, in quanto sia sostenibile, economico e facilmente ottenibile. Inoltre, puó essere prodotto a partire da tantissime materie prime e i campi di applicazione sono i piú svariati: mitigazione dei cambiamenti climatici, trattamento delle acque e decontaminazione dell'aria, produzione di energia etc. In questa tesi il campo di interesse è rivolto allo stoccaggio di energia: possiamo utilizzare il biochar come elettrodo per supercondensatori? Poiché esiste la necessitá di immagazzinare l'energia derivante da fonti rinnovabili, i supercondensatori potrebbero essere una buona soluzione in termini di densitá di energia, densitá di potenza e ciclo di vita.

Tutti gli studi precedenti riguardanti biochar ottenuto da legno, con l'intento di trovare un materiale elettrodico, hanno rivolto la loro attenzione sul biochar monolitico ottenuto da pezzi monolitici di legno. In questo lavoro, il principale obiettivo è stato quello di studiare la fattibilitá in termini di produzione e caratterizzazione di biochar monolitico derivante da segatura compressa. Utilizzare la segatura è un buon metodo per riciclare un waste, economico ed inoltre la compressione della segatura e la produzione dei pellets produce un materiale piú denso del precursore, aiutando a raggiungere maggiori densitá di energia. Questo studio consiste nella parziale rimozione della lignina, compressione della segatura e produzione di pellets, pirolisi e produzione di biochar ed infine caratterizzazione del biochar ottenuto. In particolare, siamo interessati alla conducibilità elettrica del materiale in quanto sia una delle proprietá richieste per essere un elettrodo nei supercondensatori. Inoltre, è stato studiato l'effetto dell'aggiunta di un legante (lignina), nella struttura del biochar.

Le principali conclusioni di questo studio possono essere cosí riassunte:

La parziale rimozione della lignina è un punto chiave in questa ricerca in quanto aiuta la compressione delle particelle, aumentando la densitá dei pellets. La lignina conferisce rigiditá alle pareti cellulari e la sua rimozione rende la segatura piú compressibile.

Aumentando la pressione durante la produzione dei pellets a 100°C, la densitá aumenta raggiungendo valori fino a 1.3 g/cm^3, ben piú alti della biomassa di partenza (0.733 g/cm^3).

Le condizioni di pirolisi influenzano le proprietá fisiche ed elettriche del biochar. L'aumento della HTT migliora la conducibilità elettrica. Il tempo di mantenimento e la velocitá di riscaldamento giocano un ruolo importante nella determinazione della conducibilità elettrica del biochar, ma in misura minore rispetto alla HTT. In particolare, l'aumento del tempo di mantenimento alla HTT risulta essere piú efficace della diminuzione della velocitá di riscaldamento. I campioni piú conduttivi sono quelli appartenenti al set n.6, pirolizzati fino a 1200°C con un tempo di mantenimento di un'ora. Il piú alto valore di conducibilità elettrica registrato è stato 176.2 ± 4.6 S/m.

La conducibilità elettrica del biochar derivante da segatura compressa è inferiore a quella del biochar monolitico derivante dallo stessso tipo di legno: i valori sono di un ordine di grandezza inferiori. Questo puó essere spiegato dal fatto che il biochar monolitico derivante da legno ha una struttura solida continua, conservando le sue strutture e canali dal suo precursore, mentre il biochar derivante da segatura compressa è formato da particelle individuali non ben connesse tra loro.

Il risultato piú interessante ottenuto in questo studio è la dipendenza della conducibilità elettrica del biochar dalla pressione applicata durante la produzione dei pellets. Tutti i set di campioni hanno mostrato lo stesso trend: il campione piú conduttivo è risultato essere quello prodotto a pressione piú bassa mentre quello piú conduttivo è risultato essere quello prodotto a maggiori pressioni. Aumentando la pressione applicata la densitá dei pellets aumenta, ma la conducibilità di bulk e skeletale diminuisce. Il meccanismo che sta alla base di questo comportamento è ancora da confermare ed è stato solamente

ipotizzato: l'applicazione di pressione potrebbe causare la formazione di micro-cricche nella struttura del biochar, elementi di discontinuitá che fanno diminuire la conducibilitá elettrica.

Il contenuto in carbonio e il grado di carbonizzazione è piú elevato per i campioni pirolizzati a temperature piú elevate, tuttavia non esiste alcun legame tra il contenuto in carbonio e la pressione applicata. Le analisi XRD e la spettroscopia Raman hanno mostrato una struttura leggermente piú ordinata per i campioni prodotti a temperature piú alte; tuttavia non c'è alcuna relazione tra il grado di grafitizzazione e la pressione applicata.

I campioni prodotti con addizione di lignina hanno mostrato una char yield piú elevata, una densitá piú elevata e una minore conducibilitá elettrica. La diminuzione di conducibilitá elettrica dovuta all'aggiunta del 10% in peso di lignina è inferiore rispetto a quella dovuta all'aggiunta del 20% in peso di lignina. L'aggiunta di piccole particelle di lignina favorisce la compressione e aumenta la densitá dei pellets, ma le particelle di biochar derivanti da essa sono piú amorfe e meno conduttive rispetto a quelle derivanti da sola segatura pretrattata che contiene principalmente cellulosa ed emicellulosa.

Table of contents

1. INTRODUCTION

1.1 Biochar

1.1.1 Definition of Biochar

Biochar is a carbon-rich porous solid material obtained from pyrolysis of lignocellulosic biomass. Pyrolysis is the thermal decomposition process conducted in the partial or total absence of oxygen. In addition to biochar, this process also yields liquid products (bio-oils) and gaseous products (e.g. CO, CH_4, H_2). The latter are used mainly as fuels [1]. The solid product biochar is used instead in many applications, some of which are very recent and interesting.

In the last decades interest in biochar has grown a lot, thanks to its ability to face some important problems such as the climate change, water pollution, waste management and to be used for energy production, filler for polymer composites, soil improvement etc. [2]. Today, soil amendment is still the main application of biochar, but non-traditional areas applications are catching on. This thesis is focused on sustainable energy applications that involve biochar as a starting material in supercapacitor electrodes. It is a functional material due to its qualities: readily available, inexpensive and environmentally friendly. Its current price is approximately 250 US$/ton, even if the price is often affected by its applications [3].

1.1.2 History of Biochar

The term 'biochar' was coined in recent times, but its origins are ancient. In the central Amazon there are entire regions of Terra Preta (see figure 1.1). It means 'dark earth' in Portoguese and this is a highly fertile dark-coloured soil that has been used for agricultural needs by the Amazonians for centuries. Analysis of the dark soils have revealed high concentrations of charcoal and organic matter, such as plant and animal remains. Interestingly, terra preta exists only in inhabited areas: this is a suggestion that probably humans are responsible for its creation, but it is not clear how it was created so long ago. Some theories suggest the use of the techniques slash-and-burn and slash-and-char. The first one consists in cutting and burning of the vegetation to make way for agricultural activities, while the slash-and-char consists in cutting and igniting it but only allowing the refuse to smoulder [4].

From the last decades of the nineteenth century natural scientists, geographers and anthropologists discovered Terra Preta in Amazon and began to take an interest in it. The existence of a fertile anthropogenic soil in the forest changed completely the common idea that the Amazonian uplands were poor, and that the human civilisation could not have developed in these resource-poor places. It was the proof that people living in the forests didn't adapt to nature but transformed the environment thanks to the technology and engineering. In the last decades of the twentieth century, scientists wanted to replicate this Terra Preta and in 2002 they went to Manaus from Brazil, United States and Europe to discuss its reproduction. Terra Preta Nova was born and became closely connected with ideas of sustainable development and climate change mitigation. After some years the concept of Terra Preta was soon replaced by the concept of biochar. Terra Preta Nova and biochar basically tried to do the same, but Terra Preta Nova was born with the purpose to reproduce 'the old' while biochar was related to the concept of a new technology, a key component to improve soil fertility [5].

Figure 1.1 Anthropogenic Dark Earth, or Terra Preta, in the archaeological site of Hatahara on the middle Amazon, near Manaus, Brazil (Photo by Manuel Arroyo-Kalin)

The IBI (International Biochar Initiative) defines biochar as "a solid material obtained from carbonization thermochemical conversion of biomass in an oxygen-limited environment" [6].

To make things clearer it is appropriate using the right nomenclature. The term biochar is related to the solid product of pyrolysis and the IBI definition is the most adopted.

PCM means "pyrogenic carbonaceous material" and it refers to materials that were produced by thermochemical conversion and contain some organic C, such as charcoal, biochar, char, black carbon, soot, activated carbon.

Char is the material generated by incomplete combustion process that occur in natural and man-made fires.

Charcoal is produced by thermochemical conversion from biomass (mainly wood) for energy generation.

Black carbon is used in the geologic, soil science and environmental literature to refer to PCMs dispersed in the environment from wildfires and fossil fuel combustion.

Soot is a secondary PCM and a condensation product: char, charcoal, biochar and black carbon may contain soot.

Ash is the fraction of biomass or PCM including inorganic oxides and carbonates {all definitions from ref. [2]}.

1.2 Biomass and wood

Biochar is the major solid product of pyrolysis and it contains unconverted organic solids and carbonaceous residues produced from the partial or complete decomposition of biomass components. The physical, chemical and mechanical properties of biochar depend on the type of feedstock [7]. The choice of the biomass plays an important role in the process because it affects the final product desired. The term biomass refers to wood, woody crops, herbaceous species, wood wastes, bagasse, sawdust, grass, wheat, organic waste, nutshells, sewage sludge, bio-solids, waste paper, waste from food processing and many others [8].

Depending on the purpose of use of biomass, the choice will concern a certain type rather than other: the choice of biomass source is influenced by the form in which the energy is required. For instance, high moisture content biomass such as herbaceous plant sugarcane is more suitable for fermentation process, that involves biological reactions in an aqueous environment; on the contrary dry biomass as wood chips is more economically suited to gasification, combustion or pyrolysis because it doesn't require a costly drying process. In addition to the moisture content, another important parameter is the proportion of fixed carbon and volatile matter. The fixed carbon content is the mass remaining after the releases of volatiles, excluding the ash and the moisture content [9]. In order to obtain more gas products, the volatile matter has to be higher whilst the fixed carbon is more important to obtain more solid products. Since in this case the interest is addressed to biochar, the preferred biomass sources are wood and sawdust: they have a high carbon content (about 50 wt%), low moisture content and high content of lignin that increases the char yield [10]. Furthermore, to ensure a final carbon-rich structure, it would be better to avoid biomasses with a high content of mineral components, that would cause an increase in concentration of elements such as phosphorus and potassium (like animal litters) [7]. For these reasons the lignocellulosic biomass is the most suitable to produce biochar.

1.2.1 Composition of wood

Wood is a porous and fibrous structural tissue found in the roots and stems of trees and in other woody plants. In order to understand its properties, it is useful to describe the nature of the molecules of which it is made up and the way in which the different kinds of molecules are arranged in wood cell walls. Basically, wood structure consists in holocellulose (hemicellulose and cellulose), lignin and extraneous materials that are not part of its essential anatomy (see figure 1.2). Some of these components can be dissolved in solvents such as acetone and for this reason they are called extractives. The organic part of extraneous material are the extractives, the inorganic part is obtained as ash. Extractives are usually low molecular weight organic compounds [11].
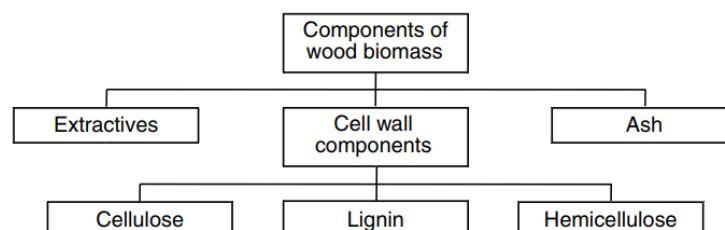

Figure 1.2 Major constituents of a woody biomass. From ref. [12].

Cellulose is a polymer formed by a long linear chain of β-glucose, a hexose sugar; the link between adjacent sugar units is through 1,4 beta glycosidic bonds so it is called β 1-4 glucan [1]. Since it is composed by the repetition of the same monomer, it is a homopolysaccharide (see figure 1.3). The number of monomers in the cellulose molecule is usually variable and in wood it is about 8000 to 10000. It is highly ordered, unbranched and made of only glucose units. This ordered and crystalline structure gives cellulose strength and stability. The cellulose content of wood varies between species in the range 40-50 %.

Cellulose

E. Jaspard (2012)
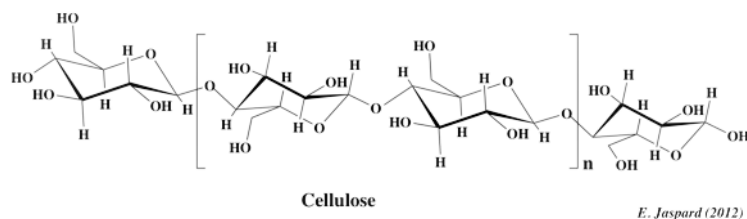
Figure 1.3 The structure of cellulose.

Hemicellulose differs from cellulose by being smaller and branched polymer containing more than one type of sugar. It is a heteropolysaccharide. An example of hemicellulose structure is reported in figure 1.4. The degree of polymerization is in the range of 150-200 and the monomers of which it is made could be hexose sugars as glucose, mannose, galactose and pentose sugars such as xylose and arabinose. It has a more random structure and it is amorphous. It acts as the cement material holding together the cellulose micells and fibers [13].

(i) Xylan

(ii) Glucomannan
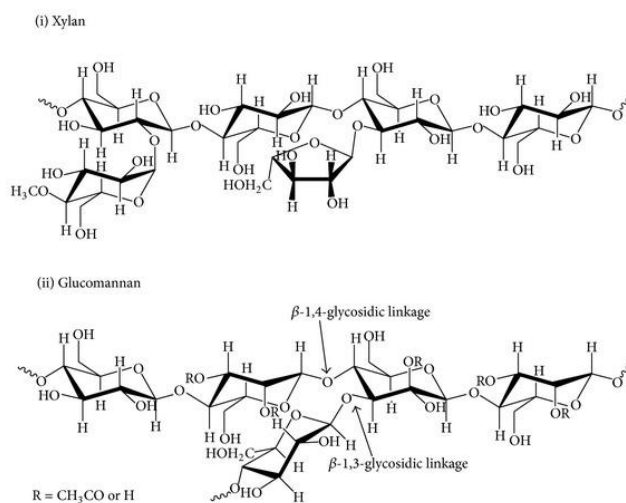
Figure 1.4 An example of the structure of hemicellulose.

Lignin is the last of the three main components of lignocellulosic biomass. Lignin is a cross-linked three-dimensional phenolic polymer (see figure 1.5). It is mainly composed with phenolic compounds of phenyl propionic alcohol such as coumaryl, coniferyl and sinapyl alcohol. They form a complex matrix which contains various kinds of functional group such as hydroxyl, methoxyl and carbonyl [14]. There are a lot of possible lignin structures, there is no a defined one; like the hemicellulose it is an amorphous polymer. It provides structural strength, provides sealing of water conducting systems that link roots with leaves, and protect plants against degradation.
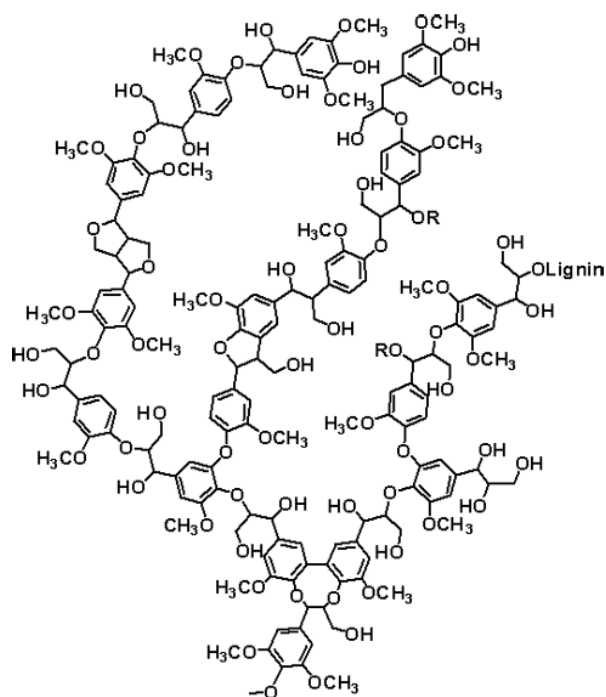
Figure 1.5 An example of the structure of lignin.

Extraneous materials include mineral deposits such as silica, calcium salts, carbonate, phosphate and a great variety of organic substances like oils, fats, flavonols, anthocyanins, tannins, polyphenols, sugars and others. The hydroxyl groups on the glucose molecules of the cellulose let the chains bound to each other through hydrogen bonds. These bonds hold the chain firmly together and form microfibrils, very long and difficult to solve. The microfibrils are so ordered that they confer a crystalline structure to the cellulose, even if small amorphous parts could still exist. Several different structures of cellulose are known, depending on the location of hydrogen bonds between the chains. Cellulose microfibrils are embedded in a matrix of hemicellulose and lignin (see figure 1.9).

Lignin is the material that contains the highest content of carbon atoms and methoxyl groups. During the development of the cells it is incorporated as the last component in the cell walls, interpenetrating the fibrils, strengthening the cell walls [11]. It gives rigidity to cell walls and hence resistance to compression, depending on its structural organization. Lignin, together with hemicelluloses, acts as a cementing agent matrix of cellulose fibers, assuming the function of glue and this will be a very important property in our process [13].

The percentages of these components change accordingly to the type of biomass. They change also from wood to wood, especially from softwood to hardwood.

Table 1.1 Example of different percentages of the main components in hardwood and softwood (wt%). Data from ref. [9]. (See paragraph 1.2.2 for the definition of hardwood and softwood).

Biomass	Lignin (%)	Cellulose (%)	Hemicellulose (%)
Softwood	27-30	35-40	25-30
Hardwood	20-25	45-50	20-25

The percentage of extractives depends on the type of wood and it is in the range 2-7 % (wt%).

From an elemental point of view wood biomass is composed approximately by 50% of C, 42% of O_2, 6% of H_2, 1% of N_2 and 1% of other compounds such as Ca, K, Na, Mg, Fe, Mn [11].

1.2.2 Structure of wood

Wood has a microstructure made by pores, canals and elements that extent both axially (in the tree growth direction) and radially (perpendicular to growth direction), see figure 1.6.
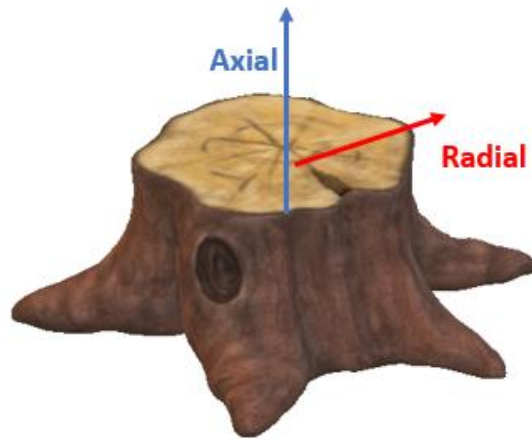

Figure 1.6 Axial and radial directions in the tree trunk.

According to its physical structure, wood is classified into two categories: Softwood and Hardwood.

In figure 1.7 a typical softwood structure is represented. In Softwoods the great majority of the axial elements are tracheids (90 % or more of the volume of softwoods). They are long, narrow cells of a length about 75 – 200 times their diameter (length: 3 – 5 mm, diameter: 0.02 – 0.04 mm). A tracheid is a cell that has developed a thick lignified cell wall. They are very strongly adherent and fit closely together without intercellular space. For this reason, they confer mechanical strength to the wood. The thickness of the cell walls is due to the development of a secondary cell walls during the tree growth. However, there are some areas where the primary wall is thinner than elsewhere and where secondary wall deposition does not occur. These areas in the cell walls are called pits. They form the major pathway for water and solutes from one cell lumen to another. In the radial direction of Softwoods, we can find ray tracheids (very short cells in comparison to axial tracheids) and ray parenchyma (smaller than the other cells with storage function). Examples of softwoods are cedar, pine, redwood, spruce and yew.
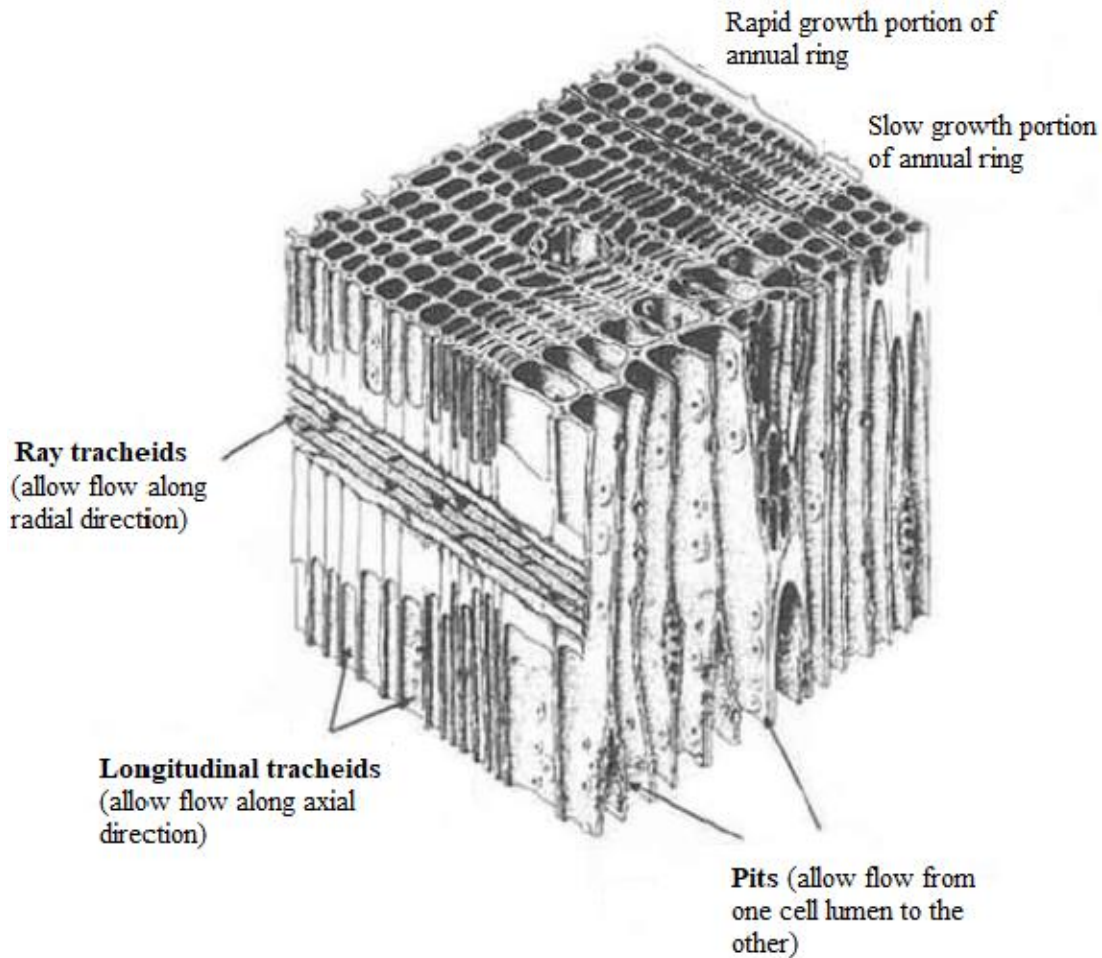
Figure 1.7 Typical structures of softwood species. From ref. [15].

In Hardwoods the cells are more varied, both individually and in their distribution in the wood as a whole. In Hardwoods the axial elements are not only tracheids and parenchyma, but also vessels, fibre-tracheids and fibres (see figure 1.8). It is possible to find these five types of cell in different proportions and patterns. Vessels are pipe-like structures with the main function of carrying water and sap through the tree. They are wider and shorter compared to the tracheids. The end walls of the vessels are open and the area of the adjacent end walls where two vessels are connected to each other is called perforation plate. They could be single or multiple openings. In a few hardwoods, in association with vessels it is possible to find vascular tracheids, small vessels with no perforated ends but with many pits, like tracheids. Axial and ray parenchyma are more abundant in hardwoods than in softwoods. Fibres are particular elements of hardwoods. They are long narrow cells (length 1-2 mm, diameters 0.01-0.05 mm). They have closed ends and their walls may be thick or thin, depending on the period of tree life in which they are formed. Their primary function is to provide mechanical support to the tree. Examples of hardwoods are balsa, beech, sugar maple, oak and walnut [11, 16]. In figure 1.10 a cross section of a hardwood is represented: it is possible to see the difference between rays and vessels.
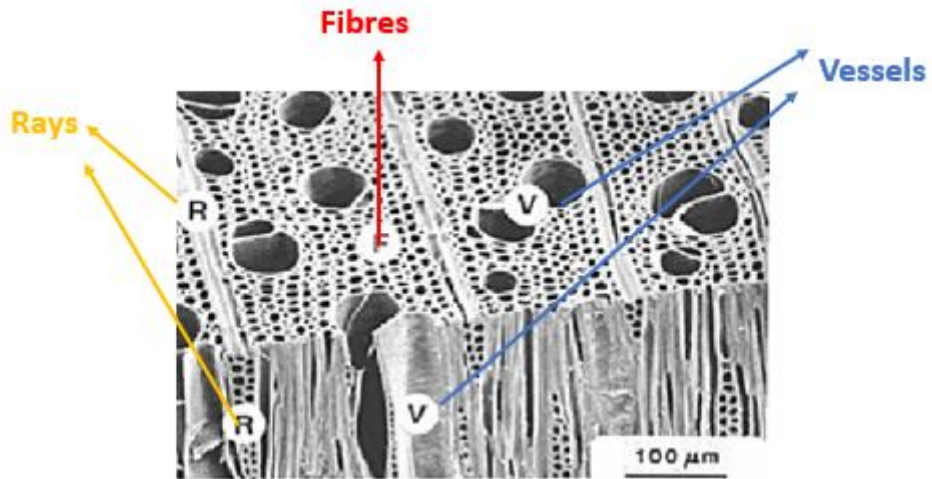
Figure 1.8 SEM of wood rays (R), vessels or pores (V), and wood fibres (F) of soft maple, hardwood. From ref. [17].

The differences between Hardwoods and Softwoods just described, are represented in figure 1.9. Softwoods structure is more uniform and regular, while Hardwoods structure is more complex, it has more elements and larger pores. Through SEM analysis, it is simple to distinguish the two structures because of their differences.
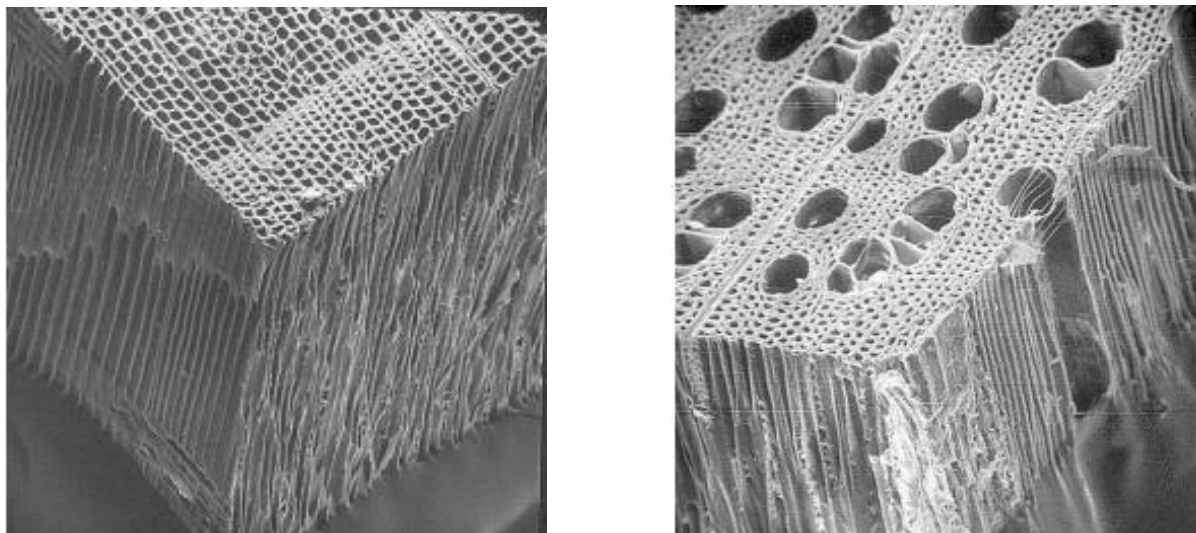

Figure 1.9 Different structures respectively of softwood (maritime pine) and hardwood (beech). From ref. [16].
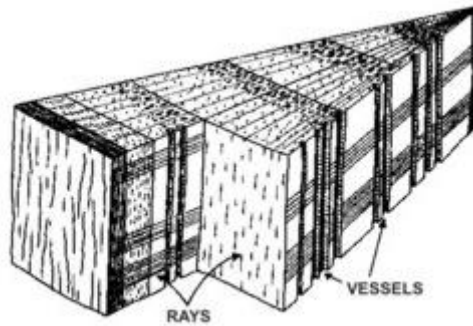
Figure 1.10 Cross-section through hardwood showing rays and vessels.

In Hardwoods vessels elements are called pores. According to the arrangement of these pores, we can divide hardwoods in three main categories: ring-porous, diffuse-porous, semi-ring porous. Some species like oak and ash have a ring-porous structure: the largest pores are in the earlywood while the pores in the latewood are more distributed ad uniform in size. On the contrary, some species as maple, cherry or yellow poplar have a diffuse-porous structure: the pores are fairly distributed both in the earlywood and in the latewood. The third category has the semi-ring porous structure: pores are large in the earlywood and smaller in the latewood but the change from one size to the other is gradual, not well definite. Trees as black walnut and butternut belong to this category [18]. In figure 1.11 the three categories just described are reported.
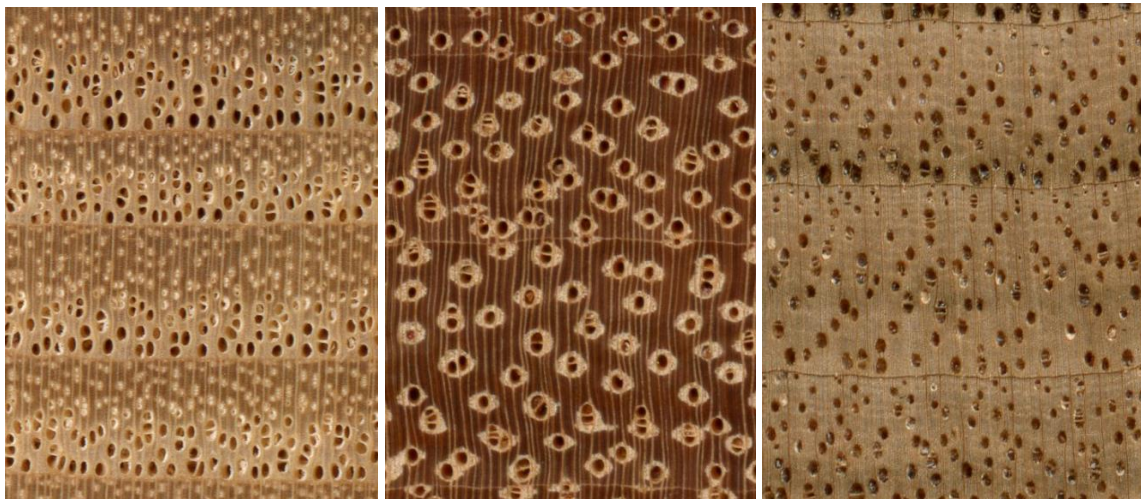

Figure 1.11 Different porous structure of hardwoods: ring-porous, diffuse-porous, semi-ring porous (from the left respectively), end grain 10X

In figure 1.12 it is enclosed what has just been described. The wood vessels are the main components of wood structure and they follow the tree growth direction. The cellulose polymers are arranged in micro fibrils, that are combined into wood cell wall. Cellulose fibrils are embedded in the matrix formed by hemicellulose and lignin.
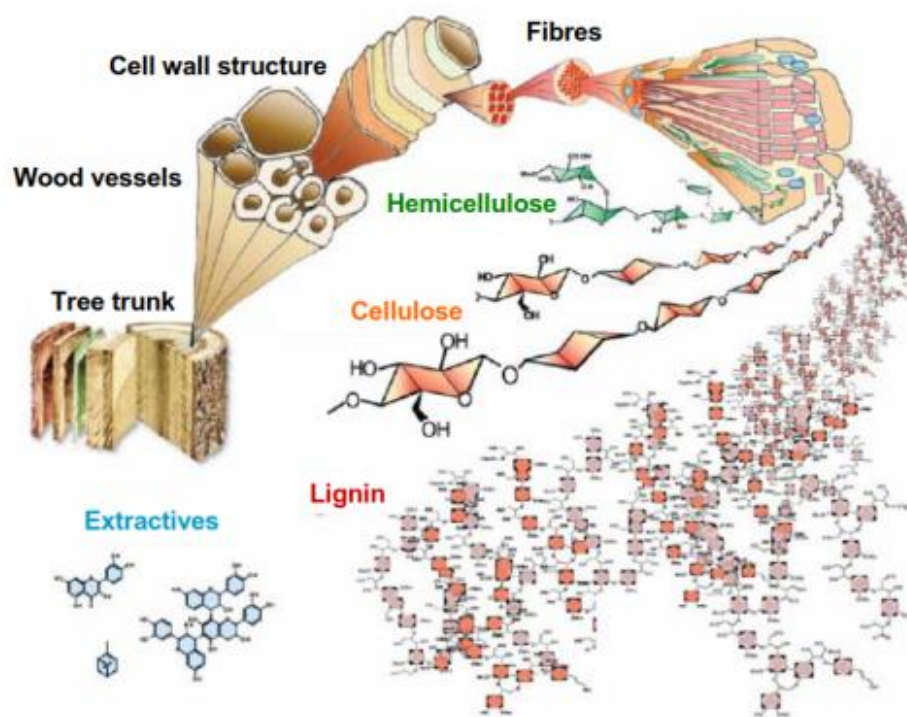

Figure 1.12 Chemical structure of wood. From ref. [19].

1.3 Pyrolysis

1.3.1 Pyrolysis process

Pyrolysis is the thermal decomposition of materials in an oxygen-poor environment, where significantly less oxygen is present than required for complete combustion. Biomass is heated in this type of atmosphere to produce a hydrocarbon-rich gas mixture, a liquid phase called bio-oil and a carbon-rich solid residue. Pyrolysis is the simplest method of processing one fuel in order to produce a better one [8]. In this thesis the interest is focused on the solid product, biochar, and on the study of its electrical properties with the aim to use it as electrode in supercapacitor application. Depending on the type of the product desired, it will be appropriate to vary pyrolysis parameters. The same thing happens depending on the type of biochar desired: changing the pyrolysis parameters affects the final structure and physical and electrical properties of biochar.

Since the biomass used in this case is wood, it is useful to understand how the lignocellulosic components degrade during pyrolysis.

The first stage of biomass decomposition occurs between 120°C and 200°C and may be called prepyrolysis. During this stage some internal rearrangements such as water elimination, bond breakage, appearance of free radicals and formation of carbonyl, carboxyl groups take place [20].

The second stage is the actual pyrolysis and it involves the decomposition of biomass into the final products. The decomposition reactions of biomass components occur at different temperatures and they involve different temperature ranges. In the context of reaction mechanism behind thermal decomposition, cellulose is the most studied and understood. Cellulose and hemicellulose initially break into lower molecular weight compounds. Hemicellulose is the first one that starts its decomposition. A temperature range of 250°C to 350°C is reported for the decomposition of xylan, the most studied of the hemicelluloses. At low temperature xylan undergoes dehydration that leads to the formation of anhydride fragments, water soluble acids, gases, char and water. Cellulose undergoes dehydration reactions below 300°C and leaves solid char, gases and water. Cellulose and hemicellulose dehydration form an activated cellulose which decomposes during the following step of pyrolysis by two competitive reactions: one yields volatiles and the other char and gases. At higher temperature in fact xylan undergoes fragmentation forming volatile organics such as phenolic compounds, levoglucosan and furans meanwhile in the range between 300°C and 450°C the decomposition of cellulose is dominated by depolymerization of active cellulose forming anhydrosugars. The fragmentation process of cellulose reaches its optimum temperature at about 600°C and forms carbonyl compounds [1, 21, 22]. All these reactions just described take place concurrently and consecutively and the temperature ranges in which they take place overlap each other. In the end there is decomposition of lignin: since it is a very stable component, it decomposes over a wider range of temperature, from 200°C to 900°C [23]. Below 500°C dehydration dominates whereas above 500°C it tends to decompose into monomers. Then, above 700°C also the monomers decompose and enter the vapor phase. The main products formed after this decomposition are catechols, vanillins and aromatic carbohydrates [22]. When the temperature increases the pyrolysis enters a third stage in which the char decomposes at a very slow rate and carbon-rich residual solid is produced. Anyhow this description of all reaction mechanisms must be considered generally speaking. The rate and the temperature ranges of degradation of each of these components strictly depend on the process parameters chosen such as reactor type, pressure, temperature, particle size, heating rate, holding time exc.

It is possible to understand the temperature ranges of decomposition reactions of each component through thermogravimetric analysis (TGA). It is a method of thermal analysis in which the mass of the sample is measured over time as the temperature increases. This measurement provides information about physical phenomena, such as phase transitions, desorption or adsorption and chemical phenomena such as chemisorptions, chemical reactions or thermal decomposition (see paragraph 5.1).

In figure 1.13 we can see TGA curves taken from a study in which the three components have been studied separately [23]. The authors have bought powders of each component (cellulose, hemicellulose and lignin) from birchwood and then analysed their behaviour during heating. The samples were heated up to 900°C at a constant heating rate of 10 °C/min; purified nitrogen at a flow rate of 120 ml/min was used as the carrier gas to provide inert atmosphere for pyrolysis [23]. The solid curves of figure 1.13 show the mass percentage in the sample while the temperature is increasing. They are decreasing curves because they represent a mass loss of the sample. The hatched curves are called DTG curves and they represent the first derivative of the solid ones. DTG curves make the noticing small features on TGA curves much easier, because they appear as peaks. They are helpful to identify temperature ranges of decomposition.
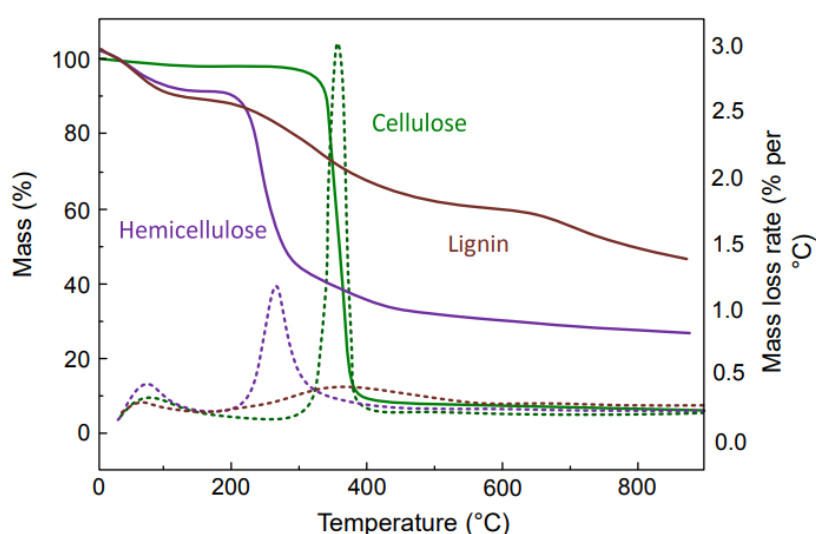

Figure 1.13 Thermal analysis of birchwood components: TGA curves of hemicellulose, cellulose and lignin (solid curves) and DTG curves of hemicellulose, cellulose and lignin (hatched curves). From ref. [23].

As already explained we can see great differences among pyrolysis behaviours of the three components. Hemicellulose starts its decomposition more easily, at low temperature, between 220°C and 315°C. They are mainly formed by different saccharides that create an amorphous structure, rich of branches, which are very easy to remove at low temperature, releasing volatile compounds as CO, CO_2 and hydrocarbons with low molecular weight. Cellulose pyrolysis instead has a wider temperature range until 400°C, and all of it is pyrolyzed as we can see from the solid residue at 900°C: it is only 6% compared with the 20% of hemicellulose. Cellulose is more difficult to decompose than hemicellulose because of its more ordered structure with long polymer chains without branches. Lignin is the most difficult one to decompose: the range is much wider than the previous two and it was pyrolyzed very slowly compared to hemicelluloses and celluloses. Its residue at 900°C is very high, 45%. Lignin is made by aromatic rings and they need higher temperature to be decomposed.

This example is referred to a case in which the three components were studied separately. We have to consider the fact that during this process the three main lignocellulosic components could interact with

each other: it is almost impossible predict the characteristic of biomass pyrolysis simply basing on the thermal behaviour of the three individual separated components. For example, during the process the interaction between hemicellulose and lignin could promote the production of lignin-derived phenols while hindering the generation of hydrocarbons [24]. In figure 1.14 we can see the differential scanning calorimetry analysis (DSC) on the three lignocellulosic components of wood biomass.
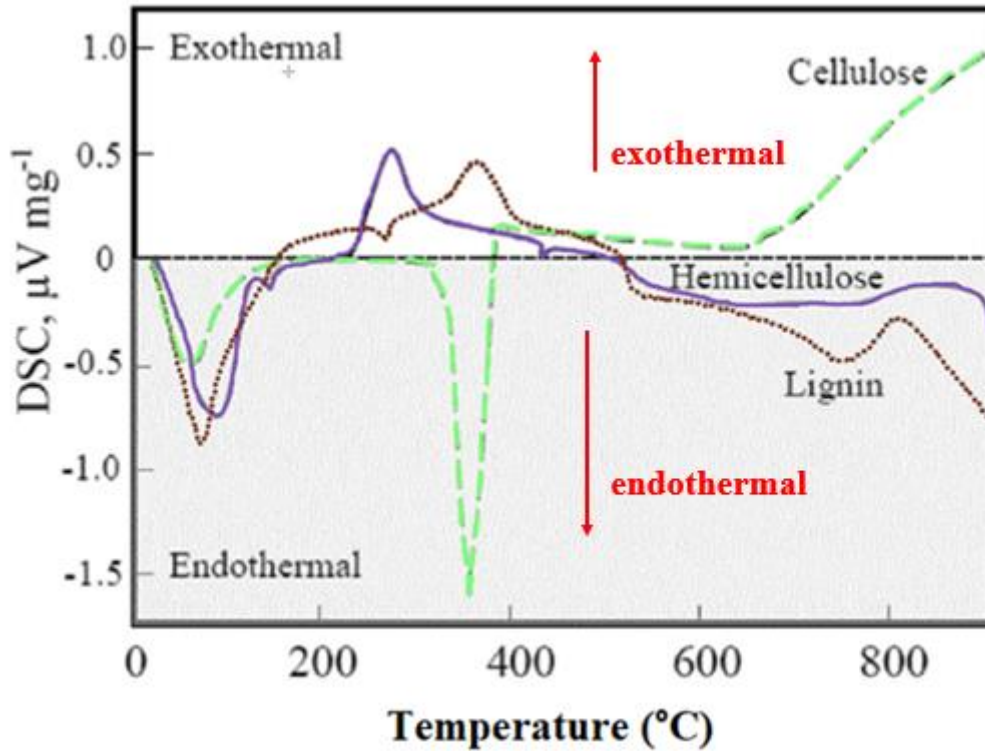

Figure 1.14 Thermal analysis of biomass components: DSC curves of cellulose (green), hemicellulose (violet) and lignin (brown). Data from ref. [25].

DSC is a thermo-analytical technique in which the difference in the amount of heat, required to increase the temperature of a sample and reference is measured as a function of temperature. Both the sample and the reference are kept at the same temperature during the experiment. DSC analysis give important quantitative and qualitative information about physical and chemical changes that involve exothermic or endothermic processes. Through this analysis it is possible to notice that when the temperature is lower than 200°C all the reactions are endothermic: the main reason is the removal of moisture when the sample is heated up. When the temperature increases, the behaviour of the three components is completely different: the cellulose shows a big endothermic peak around at 350°C, unlike lignin and hemicellulose. This means that the pyrolysis of lignin and hemicellulose are exothermic, the one of cellulose is endothermic. A possible explanation for this behaviour is that the charring process is highly exothermal whereas volatilization is endothermal. As mentioned earlier in fact, decomposition of hemicellulose and lignin could be attributed to the charring, while the decomposition of cellulose could be related to quick devolatilization reactions, leading to a very few solid residues left [23]. When temperature is higher than 400°C the curves show an inverse trend. The cellulose decomposition becomes highly exothermal and this might be related to some cracking reactions.

In general, we can divide pyrolysis in three phases: initial evaporation of free moisture and some volatile loss, primary decomposition reactions that lead to primary char formation and secondary reactions such as oil cracking or repolymerisation yielding additional char called secondary char [24].

1.3.2 Pyrolysis parameters

As mentioned earlier, the final biochar properties are strongly affected by pyrolysis process parameters. The three main pyrolysis parameters considered are pyrolysis temperature (HTT, highest treatment temperature), heating rate (HR) and residence time (RT). HTT is referred to the maximum temperature which the biomass is subjected to in the pyrolysis reactor and residence time is referred to pyrolysis vapours flowing in the reactor, it can be considered as the duration of pyrolysis. It should be distinguished from the holding time, representing the time at which a certain temperature is kept constant.

Based on heating rate, pyrolysis may be broadly classified as slow and fast. If the time required to heat the biomass to the pyrolysis temperature is much longer than the characteristic pyrolysis reaction time, it is considered slow, otherwise fast.

Table 1.2 Characteristics of some pyrolysis processes. Data from ref. [1, 12, 13].

Process	Heating Rate	Temperature (°C)	Residence time	Main Products
Slow Pyrolysis (Carbonization)	<1 °C/min	400	days	Charcoal
Conventional Pyrolysis	1-5 °C/min	600	5-30 min	Char, oil and gas
Fast Pyrolysis	10-200 °C/s	650	0.5-5 s	Bio-oil
Gasification	>1000 °C/s	1000	< 1 s	Bio-oil, chemicals, gas

In table 1.2 some of pyrolysis processes are described: this is not a strict classification as we can combine all pyrolysis parameters in different way to obtain different products, with different yields and with different properties. Slow pyrolysis yields the highest amount of solid biochar, whereas fast pyrolysis and gasification favour the production of liquid bio-oil and gas [1].

Carbonization is a slow pyrolysis process conducted in absence of oxygen in which the production of charcoal, the carbonaceous solid residue, is the primary goal. The char yield could be 35% (wt %). The biomass is usually heated very slowly to a relatively low temperature over an extended period of time. We will see subsequently that increasing the final temperature and the holding time is possible to promote the process of graphitization, in which we are interested because it improves the electrical conductivity of biochar. Besides the pyrogenic biochar obtained with a slow pyrolysis process, there is also the hydrothermal biochar obtained with a hydrothermal carbonization. This process is done on biomass soaked with water, at high pressure so that the water remains in the liquid state throughout the range of temperatures used. As in dry pyrolysis, reaction temperature and other parameters determine the production distribution. This process becomes very advantageous when the biomass feedstock is not dry, as hydrothermal carbonization eliminates the need for a drying process [26].

The conventional pyrolysis is a sort of intermediate one between slow pyrolysis and fast pyrolysis. It is a thermal conversion of the biomass that implies slow heating rate, between 1 and 5 °C/min, moderate temperature, up to 600 °C. The residence time could vary from few minutes to hours or days according to the desired product: char, bio-oil or syngas. The char yield could vary from 20 to 35% (wt %) according to the heating rate and residence time chosen.

Fast pyrolysis is a process involving higher heating rates and very short vapor residence time. The main aim of this process is the production of liquid bio-fuels. The liquid product yield could achieve 60-75% (wt %). In the following chapter a brief description of all possible products will be reviewed. To achieve

the high heating rate needed, the process requires intensive heat transfer from heat source to biomass particle. For this reason, as opposed to slow and convention pyrolysis, small particle sizes (1-2 mm) are required, due to low thermal conductivity of biomass. To achieve a good bio-oil quality is important to ensure rapid quenching or cooling of vapors to let them condensate. In this way, unwanted secondary vapor phase decomposition reactions are avoided [27].

The process of gasification can be seen as an extension of fast pyrolysis. It has the main goal to produce chemicals and clean power because it is a process converting biomass into either fuel gas containing hydrocarbons as methane or syngas. The advantage of gasification is that using the syngas is potentially more efficient than direct combustion of the original fuel. Syngas can be burned directly in gas engines, used to produce hydrogen or methanol or converted into synthetic fuel through the Fischer-Tropsch process. It is usually performed with the aid of a gasification agent that can be steam, oxygen or carbon dioxide. The process is performed at very high temperatures, up to 1500 °C and residence times chosen are very short, less than a second. The quality and the composition of the gas product are associated with factors as type of feedstock, particle size, temperature, heating rate, residence time and moisture content [28].

1.3.3 Pyrolysis products

As mentioned earlier the main pyrolysis products are a solid product (char), a liquid product (bio-oil, water) and a gas mixture (CO_2, CO, H_2O, C_2H_2, C_2H_4, C_2H_6, C_6H_6 and other hydrocarbons). The product distribution depends on the type of biomass and on the type of process. In the Table 1.3 we can see the differences in yields product for different pyrolysis process of lignocellulosic biomass.

Table 1.3 Comparison of product distribution of slow pyrolysis, fast pyrolysis and gasification. Data from ref. [26, 29].

Type of process	Product abundance (wt%)		
	Solid (Char)	Liquid (Bio-oil)	Gas
Slow Pyrolysis	35	30	35
Conventional Pyrolysis	25	50	25
Fast Pyrolysis	10	70	20
Gasification	10	5	85

The relative amount of each final product might change depending on other several factors including the heating rate and the final temperature reached by the biomass. If the purpose is to maximize the yield of liquid products resulting from biomass pyrolysis, a moderate final temperature (450-650°C), high heating rate, short gas residence time process would be required. For a high char production, case of our interest, a low final temperature, low heating rate and long residence time process would be chosen. If the purpose is to maximize the yield of fuel gas, a high final temperature (700-900°C), high heating rate process would be preferred [20].

Primary decomposition of biomass produces both condensable gases (vapor) and noncondensable gases (primary gas). The vapors are made of heavier molecules and they condense during cooling, increasing the liquid yield. The noncondensable gas mixture contains lower-molecular-weight gases like carbon dioxide, carbon monoxide, hydrogen, methane, ethane and ethylene. There could be also small amount of other gases as propane, ammonia, nitrogen oxides and alcohols of low carbon numbers. They don't condense during the cooling phase and they increase the gas yield of the process. Additional noncondensable gases are produced through secondary cracking of the vapor and they are called secondary gases [28]. The typical LHVs (lower heating value) of the pyrolytic gas range between 10 and 20 MJ/Nm^3. The LHV is a property of a fuel and it is defined as the amount of heat released by combusting a specified quantity and returning the temperature of the combustion product to 150 °C. Pyrolytic gas has multiple potential applications, such as direct use for production of heat or electricity, production of individual gas components including CH_4, H_2 or other volatiles, or in production of liquid bio-fuels through synthesis [7].

Bio-oil is also referred to as pyrolysis oil, pyrolysis liquid, pyrolysis tar. It is a dark brown liquid mixture containing up to 20% of water. The final water content depends on the initial moisture content of the feedstock and water formation during pyrolysis [7]. It consists of a mixture of complex hydrocarbons and hundreds of organic compounds such as acids, alcohols, ketones, aldehydes, phenols, ethers, esters, sugars exc. The typical LHV of bio-oil is in the range 13-18 MJ/kg. Bio-oil is a microemulsion in which the continuous phase is an aqueous solution of the products of cellulose and hemicellulose decomposition containing a wide variety of organo-oxygen compounds of low molecular weight and small molecules from lignin decomposition. The discontinuous phase is composed of pyrolytic lignin macromolecules containing insoluble organics of high molecular weight [8, 28].

Biochar is the solid yield of pyrolysis and it will be the object of this thesis. It is primarily carbon (85-95%) but it can also contain oxygen and hydrogen. Its LHV is about 32 MJ/kg, which is substantially higher than the biomass which it comes from and the liquid product [28]. This makes it attractive for fuel applications as substitute for coal. It is used for several applications, in completely different field of interest. In the next chapters biochar structures and its main current applications will be analysed.

A way to follow the changes in elemental composition of biochar during pyrolysis is given by van Krevelen diagram. This diagram plots H/C ratio vs O/C ratio while the temperature increases. In figure 1.15 we can observe an example of van Krevelen diagram taken from a study on corn stalk biomass.
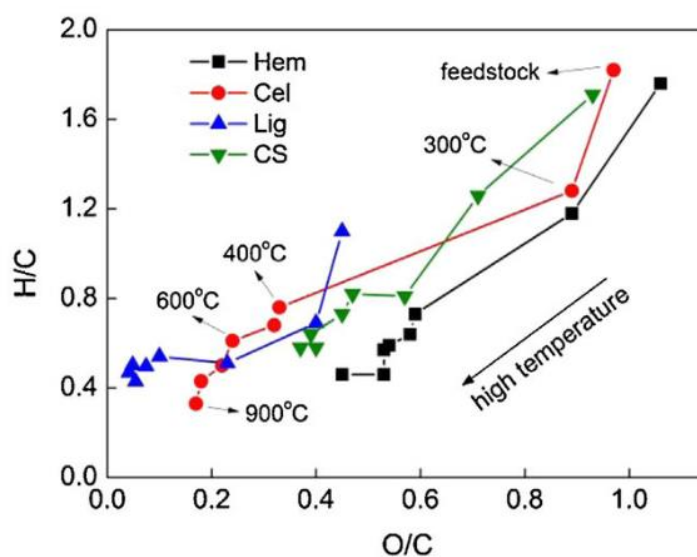

Figure 1.15 Atomic ratios of H/C vs O/C (van Krevelen diagram) of the feedstock and chars obtained at different pyrolysis temperatures. From ref. [30].

It can be observed that elemental composition of original feedstock, hemicellulose, cellulose and lignin was studied at different temperatures. Increasing the temperature, points on the graph moves from the upper to the lower zone and from the right to the left. This means that carbon content is increasing while hydrogen and oxygen contents are decreasing. For hemicellulose and cellulose, because of the dehydration and decarboxylation, the H/C and O/C ratio decrease in the range between 300 °C and 500 °C: the major decomposition of these two components take place in fact in this temperature range. Lignin decomposes at higher temperatures when the fracture of aliphatic functional groups occurs. When the temperature is above 700 °C the O/C ratio of the feedstock is constant, but we can observe that the H/C ratio decreases: the reaction of aromatization and carbonization of char release abundant amount of H_2 and low molecular weight hydrocarbons [30].

In figure 1.16 there is another example of van Krevelen plot referred to pitch pine biomass samples undergone fast pyrolysis.
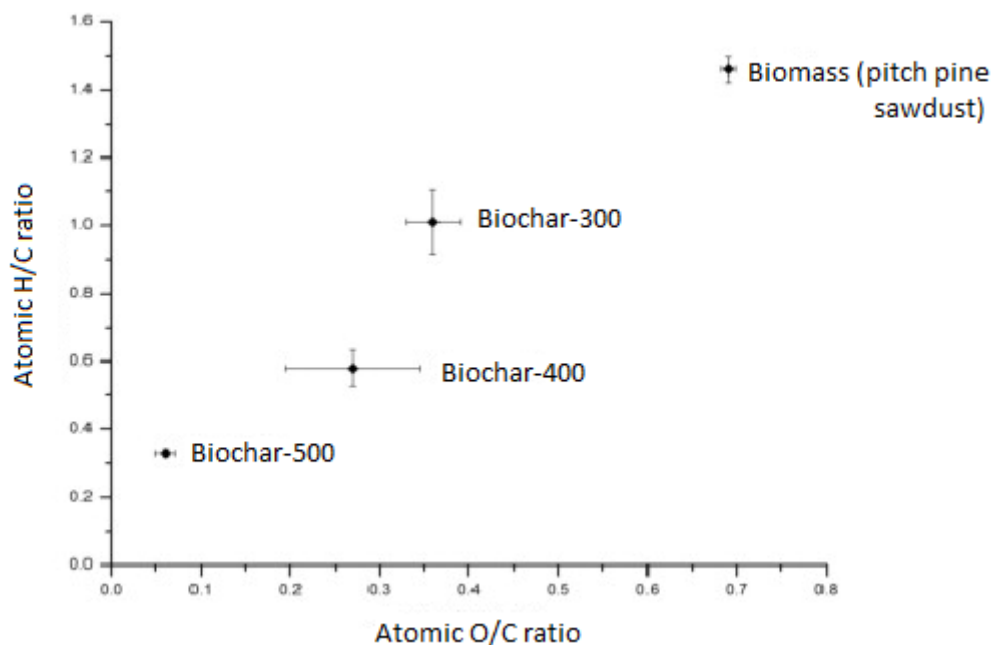
Figure 1.16 Van Krevelen plots of biochars produced at different temperatures (Biochar-300, Biochar-400, Biochar-500 are the biochars produced at pyrolysis temperatures of 300°C, 400°C and 500°C, respectively, and control is pitch pine sawdust). Type of feedstock: pitch pine. From ref. [31].

As the pyrolysis temperature increases it is possible to see that H/C and O/C ratios decrease significantly compared to the parent biomass. The pitch pine sawdust in fact is characterized by a high H/C atomic ratio: this fact means low aromaticity and high aliphatic content compared to biochars samples. Increasing the temperature, the level of aromaticity increases, charring reactions take place leading to a high degree of carbonization. The relatively high H/C and O/C ratios for Biochar-300 can be attributed to residual organic matter such as carbohydrates, that need higher temperature to be degraded [31].

2. STRUCTURE AND APPLICATIONS OF BIOCHAR

Biochar structure depends strictly on the biomass structure which it comes from and on pyrolysis conditions including heating rate, HTT, residence time, reaction pressure. The parameter that is the most responsible for physical change in biochar structure is the HTT. Some studies define its transformation during pyrolysis through a "dynamic continuum" molecular model. The adjective dynamic refers to the fact that polymeric components of biomass undergo a range of molecular transformations and rearrangements as the level of applied thermal energy varies. The transitions in biochar properties and structure are often abrupt, with the possibility that a biochar made at a given temperature may have much different properties compared to a biochar from the identical feedstock that was prepared at slightly lower or higher temperatures [32].

In general, biochars are mostly amorphous in structure with a fraction of crystallinity. Normally the carbonization process tends to enlarge any pre-existing micro-crystallite clusters. The fraction of crystallinity increases as HTT increases.
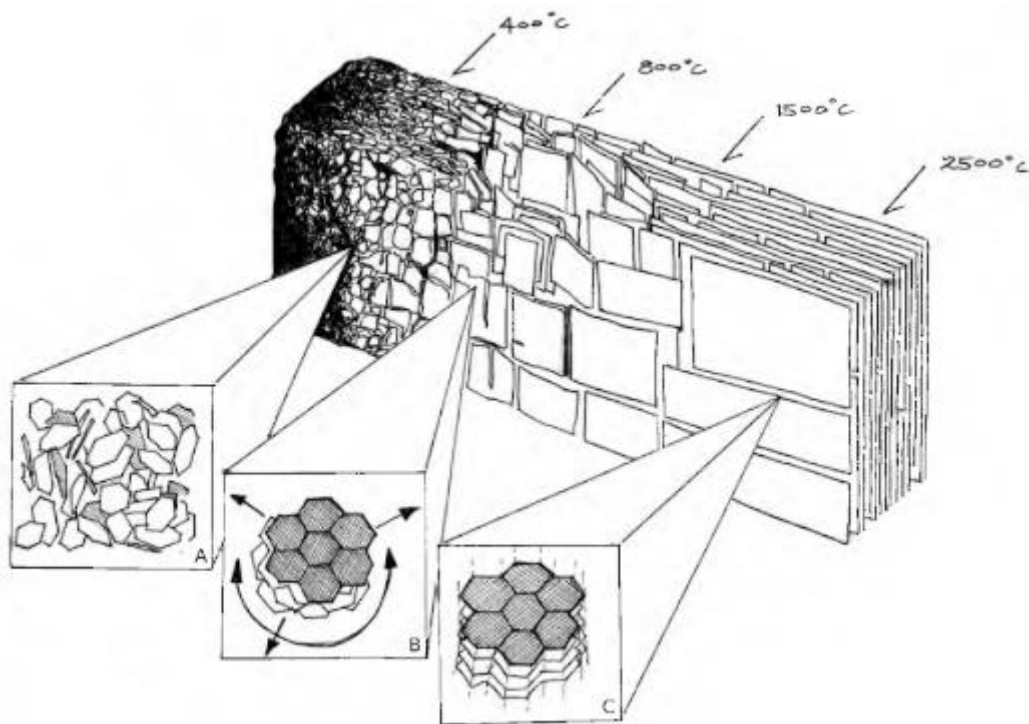
Figure 2.1 Biochar carbon structure relative to highest treatment temperature. From ref. [32].

Increasing the temperature, the structure develops from amorphous to more ordered. In figure 2.1A (400 °C) the degree of aromatic carbon is increasing but the mass is still highly disordered and amorphous. In figure 2.1B (800 °C) the sheets of turbostratic aromatic carbon begin to grow and in figure 2.1C (2500 °C) the structure has become graphitic with a high degree of order: the process has been developed from carbonization to graphitization. This happens when the temperature is above 1500-2000 °C.

2.1 Macrostructure of biochar

From a macroscopic point of view the structure of the biochar doesn't change so much as the HTT increases. Biochar macrostructure is similar to that of its precursor: it is porous. Its morphology is very important to the performance of biochar. Key features often investigated include dimension, shape, distribution, arrangement and interconnectivity of macropores, mesopores and micropores [1]. Its macrostructure is mainly investigated by SEM analysis. In figure 2.2 (left) we can see that the main structures of wood are clearly retained in biochar structure. Tracheids, vessels and rays are the main features of both wood and wood-based biochar. Axial images are indicated with the letter A, radial images are indicated with the letter R. To understand the direction from which the SEM images are taken, see the blue and red arrows in figure 1.6. In figure 2.2A (left) we can see an axial image: vessels are the largest circular features and tracheids are the smallest. The rays run perpendicular to both vessels and tracheids and they are seen as vertical features; in figure 2.2R (left) we can see a radial image: where rays are clearly visible as circular pores [33]. These features may change a little from one biochar to the other depending on the type of wood precursor. In figure 2.2 (right) we can observe that frequently vessels are in clusters of three or four, this means that not all of the structural features are perfectly intact after pyrolysis process. The rays sometimes don't maintain their straightness due to the collapse of the tracheids near them or the deformation of neighbouring vessels [33].
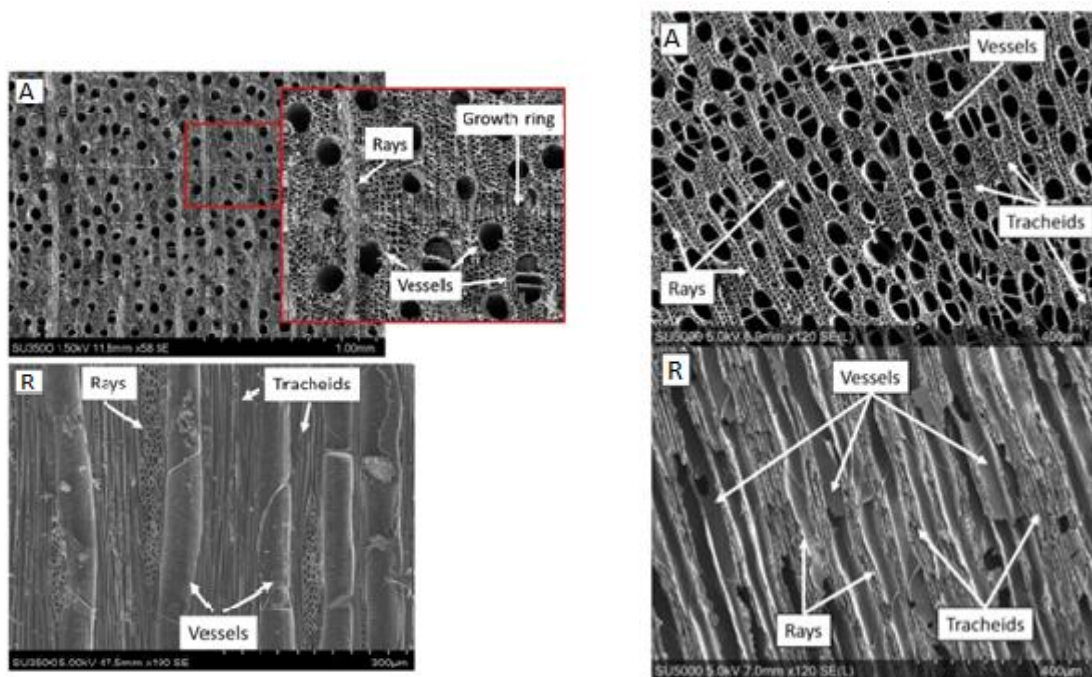
Figure 2.2 SEM images of a commercial biocarbon sample of hardwood (on the left) and SEM images of poplar biocarbon (on the right). (A are axial images, R are radial images). From ref. [33].

Other important features of the macrostructure of biochar are cracks. They are caused by an abrupt release of moisture or volatile compounds during pyrolysis. They also can be caused by a stress induced by the difference of temperature between the surface and the heart of biochar. Wood has a very low thermal conductivity, which improves the gradient of temperature within the piece. Commercial biocarbon used as a fuel have macroscale cracks: for this reason, the damage effects of collapse of tracheids and vessels are not visible in the figure 2.2 on the left. The macroscale cracks relieve internal forces during pyrolysis such that microscale deformation is prevented [33]. In other applications, such

as biochar as electrode for supercapacitors, cracks are unwanted features [1, 33]. In fact, the heating rates chosen are very slow to give time to moisture to be released very slowly, without increasing the pressure and cracking the biochar. We will see in the next chapters that during pyrolysis it is also chosen a holding time of the order of hours at 90°C to be sure that all volatile compounds have time to leave the structure.

2.2 Microstructure of biochar

At low temperatures biomass is mainly dehydrated and its structure remains unaltered. As charring intensity increases, all the organic molecules of biomass start decomposing and isolated aromatic rings begin to form. When isolated aromatic molecules with two or three rings are formed, the structure of biochar is mainly amorphous. When temperature increases further, small sheets of condensed aromatic rings stack up to form turbostratic crystallites. These are three-dimensional structures that consist of 3 to 5 stacked carbon sheets with a vertical height of about 1-2 nm and a lateral extension of 2-5 nm (these dimensions are related to the type of feedstock and to the heat treatment). When all amorphous organic carbon has been volatilized or converted into aromatic rings, the biochar can be considered as "carbonized" or "turbostratic". This happens at temperatures above 700 °C [32].
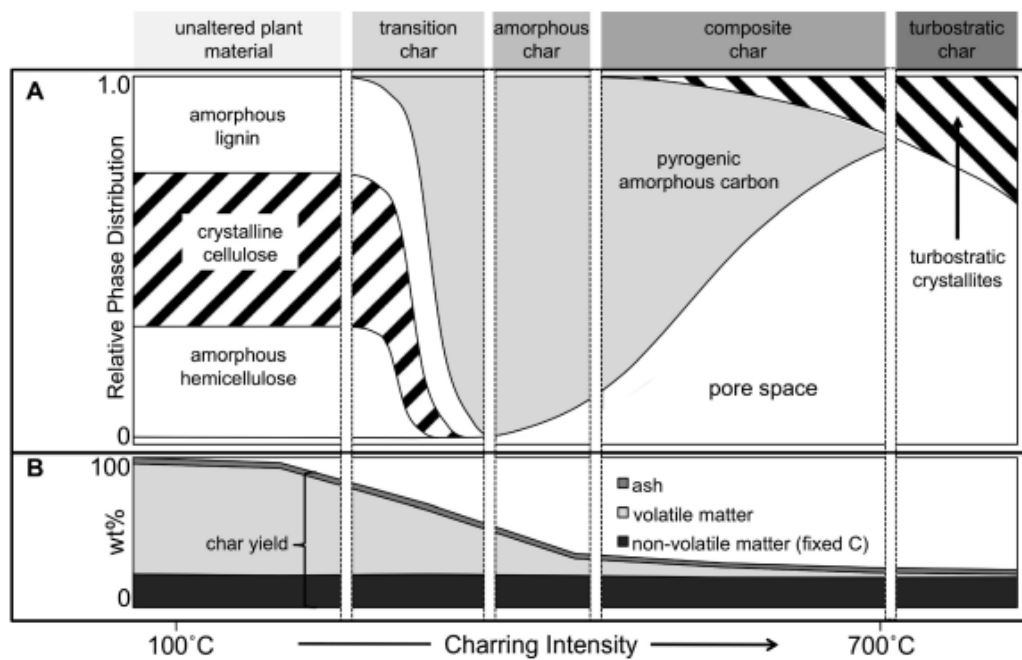
Figure 2.3 Progressive biochar structure transformation as the increasing HTT (highest treatment temperature). From ref. [34].

In the part A of figure 2.3 we can see the progressive changes in biochar structure during pyrolysis process. As already said plant materials are composed by amorphous lignin and hemicellulose and crystalline cellulose: they preserve their native structure when the temperature is below 200 °C. There are several phase transitions leading from microcrystalline cellulose to an amorphous intermediate phase towards in the end the formation of turbostratic crystallites. In the part B of figure 2.3 it is possible to see how ashes, volatile matter and fixed carbon are distributed in biochar structure as the temperature increases. Volatile matters start leaving biomass at temperatures between 150 °C and 200 °C.

The process can be described in 4 steps that are related to different categories of char [35]:

- TRANSITION CHAR: it is the char phase between 200 °C and 300 °C; the dehydration keeps going on and loss of volatile matter is promoted by the first reactions of depolymerization of biomass polymers. Cellulose is still retaining a portion of its crystallinity.

- AMORPHOUS CHAR: it is the char phase between 300 °C and 600 °C; the original biomass structure is almost totally depolymerized, and the formation of aromatic rings begins. Since the cellulose is almost completely depolymerized this phase is dominated by randomly disordered and amorphous C phase.

- COMPOSITE CHAR: it is the char phase between 600 °C and 700 °C. The dominant process in this phase is carbonization process. In this phase turbostratic crystallites begin to form and they are embedded in a low-density amorphous phase. Some spectroscopic studies pointed out that the amorphous matrix surrounding turbostratic crystallites is formed by aromatic, aliphatic and O-containing compounds that have been preserved during the process.

- TURBOSTRATIC CHAR: it is the char phase when the temperature is above 700 °C. The carbonization at higher temperatures gives a more ordered carbonaceous structure with a more ordered graphene-like sheets. The graphitic crystallites formed in this phase are denser than the original amorphous matrix (the bulk density of biochar increases as the HTT increases).

As the HTT increases, more regular spacing between the planes is formed. With the increased ordering and organization of molecules, interplanar distances also decrease. Micropores (< 2 nm in diameter) contribute the most to the surface area of biochar and they are the most responsible for the high adsorptive capacities for molecules of small dimensions [32]. We can find also mesopores (between 2 and 50 nm in diameter) and macropores (> 50 nm) though. When the use of biochar is for soil amendment or to adsorption processes, porosity is one of the most important features. In some other application, e.g. in the catalysis, surface area becomes a main parameter: the surface area of biochar generally increases with increasing HTT until it reaches the temperature at which deformation and sintering of the pores occurs and the surface area decreases. Some studies have also demonstrated that pore sizes distributed in the micropore range make the greatest contribute to total surface area [32].

2.3 Applications

Biochar has always been used as a soil conditioner in agricultural systems to improve soil fertility and recently it has been used as a tool for C sequestration. Its major utilization has been in environmental fields including besides soil improvement, also waste management, climate change mitigation and energy generation [36]. In the last few years however, interest in biochar has widely increased and a lot of recent applications have been studied and tested. Thanks to its physical and chemical properties, especially its porous structure, and with the help of physical and chemical activations to improve those properties, engineered biochar applications for sustainability were born. Among the most interesting applications we can find waste water treatment and capacitive deionization for cost-effective desalination and salt removal. The ions can be removed from water by biochar via a range of mechanisms including electrostatic interaction [1]. It may be used also as a construction material due to its low thermal conductivity, high chemical stability and low flammability. Another field of interest is catalysis. Biochar-derived materials can be used as catalysts or support for catalysts thanks to their morphology and surface functionality. In this thesis the interest is focused on sustainable energy applications in particular on energy storage and the possibility to use biochar as electrodes for supercapacitors.

2.3.1 Soil remediation and Carbon sequestration

The concept of biochar as a method for carbon sequestration is fairly new, despite a widespread use of carbonized biomass in agriculture as a soil amendment medium [37].

One of the most important issue of the twenty-first century is to reduce the rate of increase of atmospheric concentration of carbon dioxide from emissions from process industry, energy, soil cultivation exc. The rate of increase in global temperature has been 0.15 °C per decade since 1975 [38]. The carbon cycle is the movement of carbon, in its many forms, between the biosphere, atmosphere, oceans and Earth's crust. Plants absorb carbon dioxide from the atmosphere during photosynthesis and release oxygen during respiration. Animals breathe in oxygen and breath out carbon dioxide. This active carbon cycle has been balanced for millennia, but now, Earth's atmospheric CO_2 is out of balance. One of the possible solutions to mitigate the climate change risk is the carbon sequestration that implies the sequestration of CO_2 from point sources or atmosphere through natural and engineering techniques [38]. The point is to process the biomass in some form that can prevent the captured of CO_2 from returning to atmosphere [39]. To understand better this concept, we can divide energy systems in three distinct categories: carbon positive, carbon neutral and carbon negative (see figure 2.4).
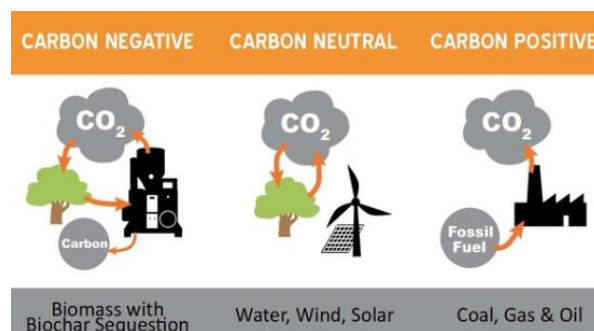

Figure 2.4 Three different carbon cycles: carbon negative, carbon neutral and carbon positive. From ref. [39].

Fossil fuels are carbon positive energy systems because they release carbon dioxide and other greenhouse gases in the atmosphere causing global warming and the increase of temperature [7]. Other sources of energy as water, wind or solar energy are carbon neutral because don't contribute to free carbon dioxide in the atmosphere. Ordinary biomass fuels can be also considered carbon neutral because the carbon captured in the biomass by photosynthesis, is returned to the atmosphere through natural processes as decomposition. They are called carbon neutral because the exchange of carbon between the fuel and the environment is balanced.

Carbon negative fuels absorb CO_2 as they grow and release less than this amount into the atmosphere when used as fuel, either through directing part of the biomass as biochar back into the soil [40]. Biochar systems are defined carbon negative because they transform the carbon within biomass into stable carbon structures within biochar that can remain sequestered in soils in a stable form for hundreds or thousands of years. CO_2 emissions in the atmosphere are drastically reduced in this way. Converting biomass into biochar through pyrolysis process leads to the production of bio-oils and syngas used as biofuels without CO_2 emissions and at the same time it generates biochar that can be buried into the soil, sequestrating C and improving soil fertility [41]. Using biomass during power generation could be the solution because biochar is a solid product and it is very easy to handle, and sequestration becomes much easier than trying to capture and storage CO_2 gas. Active carbon is transformed into inactive carbon and removed from the climate system [39].

Furthermore, biochar is very useful as a soil amendment. It brings powerful benefits to plant productivity, soil biological activity, water retention and pest management thanks to its porous structure. The climate benefits of biochar are numerous, we can list some of the most important [7, 42]:

- Soil fertility: biochar stimulates plant growth, which then consumes more CO_2 in a positive feedback effect. It reduces the need for chemical fertilizers, causing a reduction of emissions of greenhouse gases too. It can reduce the mobility of some organic and inorganic pollutants in soil. Biochar with high surface areas, oxygen-containing functional groups, and cation exchange capacity (CEC) can retain, stabilize and inactivate heavy metal elements.

- Enhanced soil microbial life: it can increase soil microbial life, because the environment becomes more favourable, resulting in more carbon storage in soil due to microbial activity.

- Reduced N_2O and CH_4 emissions: they are two of the most important greenhouse gases. Biochar has a sink effect. As already mentioned, it reduces the greenhouse gases emissions by reducing the soil organic carbon (SOC) decomposition.

- Reduced emissions from feedstocks: as written earlier, converting agricultural and forestry wastes into biochar can avoid CO_2 and CH_4 emissions otherwise generated by natural decomposition or burning of the waste.

- Energy generation: the heat generated during biochar production may be used to displace carbon positive energy from fossil fuels. Co-products of pyrolysis, such as bio-oils and syngas, may be used as biofuels. However, a net energy balance should be done to see if the energy generated by the system is more than the energy consumed. The energy is consumed in biomass cultivation, transport, handling and during pyrolysis process. Syngas, bio-oils and biochar represent the energy generate, as biofuels or in term of reduction of GHG (greenhouse gases) emission and C sequestration. When the pyrolysis requires higher HTT and longer residence time of the biomass in the reactor, more energy is required, and the net energy balance could be disadvantageous [43].

- Water treatment: biochar can adsorb water contaminants and pollutants with a high efficiency. Nowadays there are a lot of studies aiming to modify biochar to improve its properties and

achieve larger surface areas and novel structures that might lead to an improvement in functional groups, pore properties, surface active sites and catalytic degradation ability.

2.3.2 Energy storage, Supercapacitors

This is one of the most recent applications of biochar and it is the case of our interest. A group of researchers working in the Green Technologies Lab, in the Department of Chemical Engineering of the University of Toronto is studying how to use biochar to store electrical energy and to use it as electrode in supercapacitors. This is a very new application and, for this reason, is difficult to find other studies in scientific literature, apart from some recent works.

This application is part of sustainable energy applications. Renewable energies have usually the problem that their supply is intermittent (e.g. solar energy is only captured when the sun is shining, or wind turbines can work only when there is wind) [1]. For this reason, renewable energies need energy storage systems (ESSs). They are able to capture energy at any time, store it and then release it when it is necessary.

Currently, energy storage materials and devices mainly use graphitized carbon and carbon nanotubes because they have good capacity and cycle life. However, carbons produced by agricultural by-products or waste are much cheaper than carbon nanotubes and graphene [42]. The challenge in this research is to find cheaper and sustainable materials for energy storage, using waste and biomass. The group of researchers of the University of Toronto has studied in the last few years the electrical conductivity and other properties of wood-derived biochar in order to use it as electrode in supercapacitors applications. They always worked on monolithic biochar derived from monolithic pieces of wood. In this thesis, for the first time, the research is focused on studying the same properties but on pelleted biochar derived from compressed sawdust. This application is more sustainable than others because sawdust, unlike monolithic pieces of wood, is a waste of the wood industry and its compression has always been studied just to produce pellets as fuels and not for energy storage.

Using waste biomass to produce biochar is a cheap solution, readily available and a good way of combating waste disposal problems in agricultural industries.

Traditional energy storage devices, as capacitors or batteries, are considered insufficient for efficient use in transportation, commercial and residential applications [44]. The most important characteristics for energy storage devices are power density, energy density and cycle life. The power density is the amount of power (time rate of energy transfer) per unit volume. It measures how quickly the device can deliver energy. A device with a high-power density reacts very fast. Its unit is W/m^3 or W/kg (if it is defined per unit mass). The energy density is the amount of energy stored in the system per unit volume. A device with a higher energy density can power a load for longer than one with a lower energy density and the same power density and physical size. Its unit is Wh/kg or Wh/m^3.
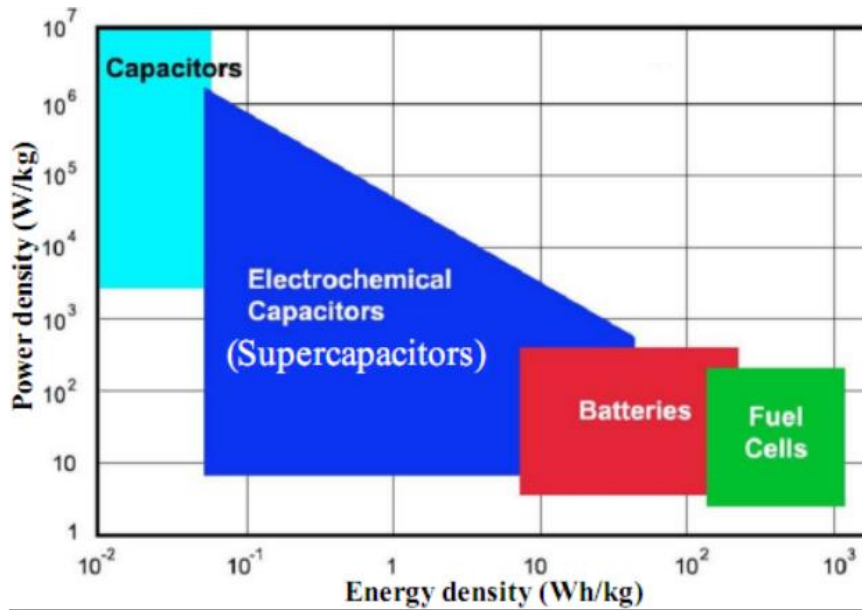
Figure 2.5 Ragone plot showing power density vs energy density of typical energy storage devices. From ref. [44].

In figure 2.5 a simplified Ragone plot is represented. It is a convenient way to compare the operational characteristics of ESSs and it plots power density as a function of energy density. Capacitors are able to provide high power densities (rates of charge and discharge), but low energy densities (the amount of charge that could be stored is low compared to the other devices) [1]. In most cases energy densities are less than 0.1 Wh/kg. The batteries show the opposite behaviour, they can store a higher amount of charge, but they suffer low power densities. To avoid both the problems, supercapacitors or electrochemical double layer capacitors (EDLCs) might be the solution, showing adequate values of energy densities and power densities. Power density is a property proportional to electrical conductivity of the material because fast rates of charges and discharges are linked to the electrons transfer rates through the device.

In Table 2.1 we can see a comparison among the typical energy storage devices. Supercapacitors can be discharged in a few seconds, but also be charged in such a short time period. Another great advantage of supercapacitors is their cycle-life: they can withstand millions of cycles thanks to their storage mechanism. Batteries and supercapacitors are constituted by two electrodes and an electrolyte. They have two different storage mechanisms: one is chemical and the other is physical. Batteries move ions from one electrode via an electrolyte to the second electrode, where they interact chemically. The electrons produced by the oxidation at the anode could be used to do electrical work as they are transferred to the cathode where they will be consumed by the reduction process. Supercapacitors store electrical charge physically, without chemical reaction take place [44]. The energy is stored in an electric double layer in an electrode-electrolyte interface of high surface area: it is a mechanism of charge separation. Because the charge is stored physically, with no phase changing or chemical reaction, the process is highly reversible, and the discharge-charge cycle can be repeated almost without limit [44]. For these reasons, the number of charge-discharge cycles that supercapacitors can undergo before failure is much higher than the batteries' one. EDLCs exhibit a very high degree of reversibility in repetitive charge-discharge cycling [45]. The main power limitations in batteries are the kinetic of reactions and mass transfer, while in supercapacitors is the electrolyte conductivity.

Table 2.1 Comparison among the characteristics of the most used electrochemical energy storage devices. Data from ref. [45].

Characteristics	Electrolytic Capacitor	Carbon Supercapacitor	Battery
Specific energy (W h kg^{-1})	< 0.1	1-10	10-100
Specific power (W kg^{-1})	> 10000	500-10000	< 1000
Discharge time	10^{-6} to 10^{-3} s	s to min	0.3-3 h
Charge time	10^{-6} to 10^{-3} s	s to min	1-5 h
Cycle-life (cycles)	Almost infinite	> 500000	About 1000
Charge/discharge efficiency (%)	~ 100	85-98	70-85
Charge stored determinants	Electrode area and dielectric	Electrode microstructure and electrolyte	Active mass and thermodynamics

Supercapacitors, compared with conventional capacitors, have specific energy of several orders of magnitude higher (hence the "super" or "ultra" prefix). They are able to store and release energy at relatively high rates because the mechanism of energy storage is simple charge-separation, as in conventional capacitors [45]. Supercapacitors show a high capacitance due to the combination of two features: an extremely small distance that separates the opposite charges and highly porous electrodes with a very high surface area. For this reason, they are typically made of highly conductive carbon materials such as graphene, carbon nanotubes or activated carbons [1]. Furthermore, a lot of supercapacitors available commercially are made by carbon materials in powder form bonded together using non-conductive binder materials, and this may be a problem. Besides, nanotubes, graphene and other materials have high costs compared to biochar, and most of the raw materials rely on fossil resources, increasing environmental pollution and unsustainability [42].

Biochar has become a popular carbon material because is a readily available, inexpensive near-pure carbon material and it can be used without the need of binders [1].

We can list some good properties of biochar, very useful for its use in supercapacitors:

- stable structure, high-temperature and corrosion resistances
- good cycle performance
- high specific surface area
- developed pore structure that can improve the electrode capacitance
- good electrical conductivity, achieving fast charge and discharge rates
- cheap material
- environmentally friendly

Most of the times the biochar used in energy storage is an "engineered biochar": it needs some physical and chemical activation methods to improve the properties that we have mentioned above [42].

The aim of this research is exploring and studying the electrical conductivity of biochar derived from compressed sawdust, without the help of any activation process.

In figure 2.6 it is possible to see how a supercapacitor works.
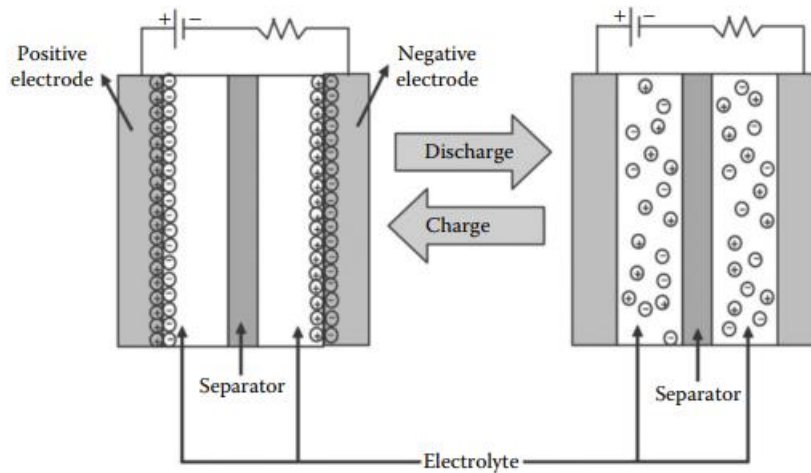
Figure 2.6 Mechanism of charge and discharge process for electric double-layer supercapacitors. From ref. [46].

The device is made by two electrodes and an electrolyte. The two electrodes are carbon porous electrodes having high surface area and they are separated by a separator that lets only ions pass through it. Electrodes are connected to a power source. Initially there is no measurable voltage between the two electrodes, but when the current flow from one electrode to the other, charge separation is naturally created at each solid-liquid interface [44]. Electric double-layer capacitance is developed at the electrode/electrolyte interface where electric charges are distributed on the surface of the electrode and oppositely charged ions are arranged in the electrolyte. Electric charges move and arrange on the electrode surfaces in order to maintain electroneutrality conditions. During the process of charging, the electrons travel from the positive electrode to the negative one through an external load [46]. Meanwhile, cations move in the electrolyte towards the negative electrode and anions move towards the positive one. In this process, energy is stored at the double-layer interface. During the process of discharging, the revers mechanism takes place. It is obvious that porosity of the electrodes surface plays a key role in the charge storage mechanism. However, not all pores are electrochemically active: only the ones having size larger than 5 Å are active. Carbon materials having the majority of pores as mesopores are considered good electrode materials. Apart from this, capacitance depends also on the surface groups attached on the carbon surface: normally surface with oxygen containing groups or with acidic functional groups show higher specific capacitance [46].

3. ELECTRICAL CONDUCTIVITY

Electrical conductivity is one of the most important features for a material candidate as electrode in energy storage devices. It affects the rates of charge and discharge of the device. The electrical properties of carbon materials are strictly related to their structure and morphology. For electrode applications, the investigation of the resistivity (and conductivity) of the material is the major concern and for this reason, the study of electrical conductivity of biochar in this thesis may be considered a preliminary study before analysing biochar performance as supercapacitor.

Electrical conductivity is the measure of a material's ability to allow the transport of an electric charge, and to conduct an electric current. Its SI unit is Siemens per metre (S/m) and it is represented by the Greek letter σ. It is the reciprocal of electrical resistivity, that describes how strongly the material opposes the flow of electric current. Resistivity is usually represented by ρ and its SI unit is the Ohm-metre (Ω·m). Resistivity and conductivity are intrinsic properties of the material, unlike resistance that depends on geometrical properties as length or area of the sample.

Electrical conductivity of monolithic biochar has been investigated in the last few years. Unlike the previous studies that were all about powdered biochar, the research at the University of Toronto has studied the electrical properties of monolithic biochar. They have tried to answer the question about what controls the conductivity of biochar, finding the electrical properties dependence on micro and macro structures of biochar [47]. Electrical conductivity was found to be highly dependent on its degree of carbonization and the bulk conductivity of biochar increased over six orders of magnitudes when its carbon content changed from 86.3 % to 93.7 %. Transmission electron microscopy and x-ray diffraction analyses revealed the presence of graphite nanocrystals, of 3 nm in dimension, and the growth in crystallinity after heat treatment at 950°C [47]. Crystallinity improves electrical conductivity of biochar.

Before the investigation of electrical conductivity of monolithic biochar, all the other researches measured the electrical conductivity of biochar particles under pressure, but this implies the destruction of biochar structure formed during carbonization. Therefore, it was difficult to link the electrical conductivity values with the structure developed during pyrolysis. Some studies show that the electrical conductivity of compressed biochar powders increases as the pressure increases, because of the better contact between particles [48]. In this study the sawdust particles are compressed before pyrolysis, and then the electrical conductivity is measured on the structure developed during carbonization.

3.1 Mechanism of electronic conduction in carbon materials

The electrons of different types of atoms have different "degree of freedom" to move. They move in their orbital around the positive nucleus of the atom and they normally stay in their shell unless they are affected by some outside force. The electrons close to the nucleus are called core electrons and they are linked to the nucleus. The outermost shell for a given atom is called the valence shell and it is important because it determines the conductivity of the atom. It contains the valence electrons, which are linked less strongly to the atom. In conductor materials such as metals, valence electrons can easily become conduction electrons, moving through the lattice.
The electronic band theory of solids describes the conductivity of conductors, semiconductors and insulators. The energy levels of atoms are divided in energy bands, separated by energy gaps. When

atoms combine to form substances and a large number of atoms are close to each other, the energy bands of individual atoms merge to a continuous band (see figure 3.1).
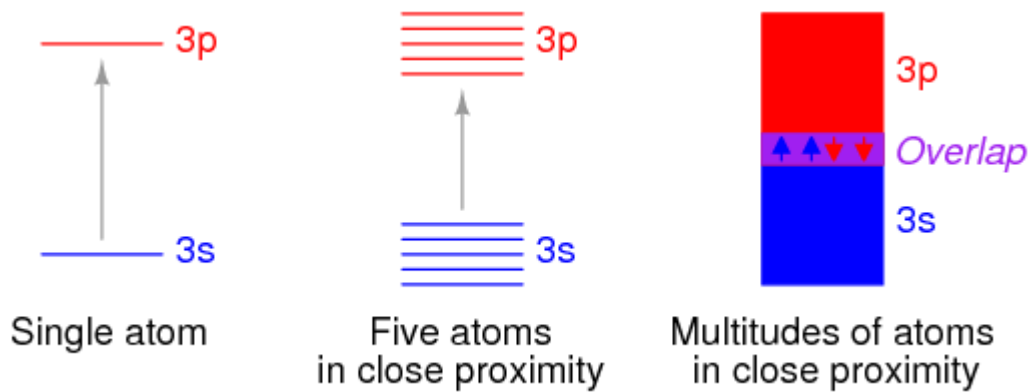

Figure 3.1 On the left: significant leap required for an electron to move to the next energy level. In the middle: shorter leap required when there are five atoms in close proximity. On the right: the single bands merge and overlap each other when there is a multitude of atoms (this is the case of a metal conductor).

The band theory of solids defines the valence band (the blue band in figure 3.1) as the highest band containing electrons and the conduction band (the red band in figure 3.1) as the next band, which is empty. In figure 3.1 they overlap each other (conductor material). Band overlap do not occur in all substances, no matter how many atoms are close to each other. In some material, a substantial gap remains between them. The band between valence and conduction band is called band gap and it determines the electrical conductivity of the material: the wider the band gap, the lower the electrical conductivity. The valence electrons are situated in the valence band and they are charge carriers.
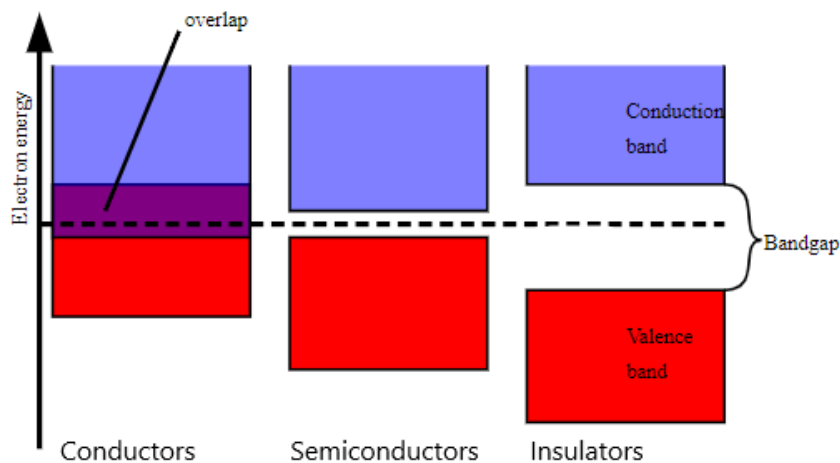
Figure 3.2 Band Model for conductors, semiconductors and insulators

As we can see in figure 3.2, in conductors, the valence band occupied by electrons overlaps with the empty conduction band. There is no band gap between valence band and conduction band and this allows electrons to move very easily. In insulators, on the contrary, the band gap is wide and only with a considerable energy consumption the gap can be overcome, and the electrons can jump from the valence band to conduction band. However, the values of electrical conductivity are very low. Even in

semiconductors, there is a band gap, but compared to insulators it is so small that even at room temperature electrons can move from the valence band to the conduction band.

Usually the typical values of electrical conductivity (at 20°C) are:

- $\sigma < 10^{-6}$ S/m (Insulators)
- $10^{-6} < \sigma < 10^{1}$ S/m (Semiconductors)
- $\sigma > 10^{1}$ S/m (Conductors)

Carbon is a chemical element with atomic number 6. The mass number is 12 for the most abundant isotope (98,93 %). It has 6 protons, 6 electrons and 6 neutrons. The core electrons are two, the valence electrons in the outermost shell are four. These four external electrons are available to form covalent chemical bonds. Carbon is versatile in its ability to form sp, sp^2, sp^3 bonds, forming different allotropes with various chemical and physical properties [49]. Carbon based materials are among the most versatile in term of their electrical conductivity since they are able to cover the whole interval of values from insulation to metallic conduction [50]. The electrical conduction takes place thanks to the sp^2 atomic hybridization: the delocalized electrons (of the π orbital) can freely move throughout the carbon structure (this is the case of the graphite). The combination of s-orbital with only two p-orbitals (p_x and p_y) creates 3 planar σ-bonds with a characteristic angle of 120° between hybrid orbitals. The additional p_z orbital is perpendicular to sp^2-hybrid orbitals and forms a π-bond. These π-bonds give rise to weak van der Waals forces between graphite layers (see figure 3.3).

Graphite has a layered and planar structure. The individual layers are called graphene. In each layer the carbon atoms are arranged in a honeycomb lattice with 0.14 nm distance between two atoms and a distance between planes of 0.34 nm (see figure 3.3). Atoms in the plane are bonded covalently: three electrons of each carbon atom are responsible for three covalent bonds, the fourth is free to migrate in the plane, making graphite electrically conductive. Bonding between layers is via van der Waals forces, that allows layers to be easily exfoliated.
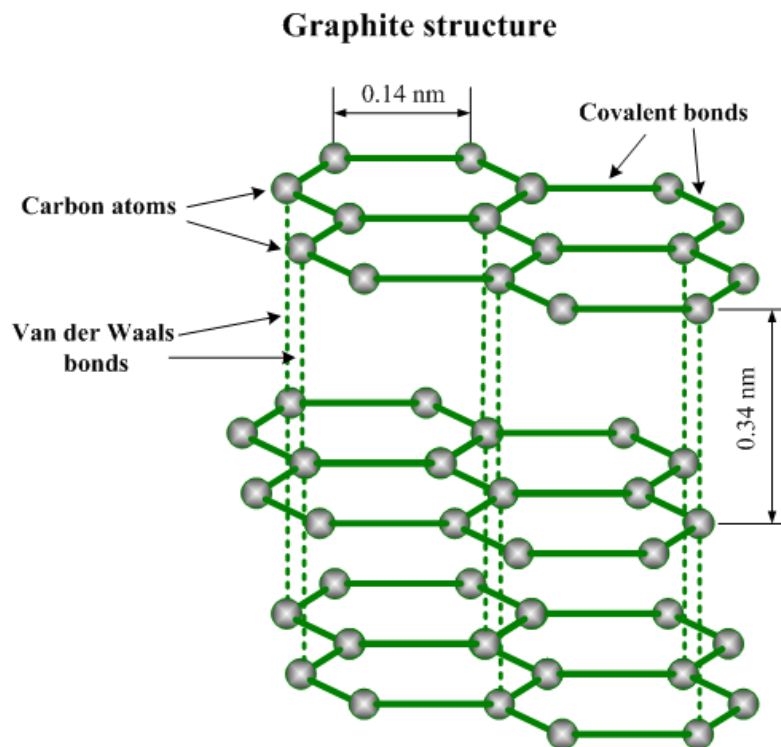
Figure 3.3 Graphite lattice.

When the sp^3 hybridization is present, there are no π electrons, and the carbon material acts as an insulator (this is the case of diamond). Every carbon atom, thanks to the four sp^3 hybrid orbitals, can bond other 4 carbon atoms with four equal bonds, with an angle of 109.5° between hybrid orbitals (see figure 3.4a). The structure is not planar, but 3D. The band gap is about 5 eV, which corresponds to an insulator. Its electrical conductivity at 20°C is about 10^{-13} S/m.

There are some recent theoretical studies that predict some metallic carbon structures constructed from fully sp^2 bonded carbons or the hybridization of a mixture of sp^2 and sp^3 carbons in a 3D network: the presence of free conductive π electrons contributes to reach a metallic electrical conductivity but, on the other hand, the presence of electron delocalization weakens the mechanical properties and the hardness of material will be lower than those of diamond [49].

Graphite and diamond are carbon allotropes: they are made only by carbon atoms, but their electrical behaviour is completely different thanks to their structure and to the way the atoms are arranged one with the other. In ordered graphite, where there is one π electron per carbon atom, the electrical conductivity is anisotropic: the values of electrical conductivity are about 2 to $3 \cdot 10^5$ S/m in the parallel direction to graphene layer (known as "basal plane"), while they are much lower in the perpendicular one, $3.3 \cdot 10^2$ S/m. Usually, the higher the average number of π electrons per carbon atom, the higher the electrical conductivity [50]. However, this is not the only factor that affects the electrical conductivity values.
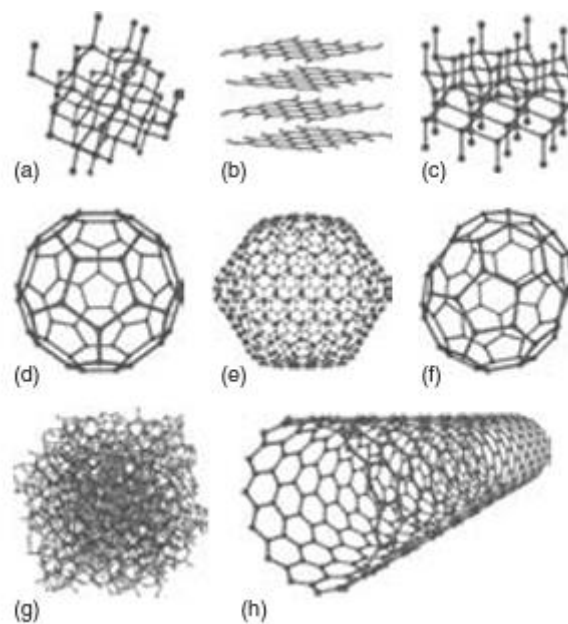
Figure 3.4 Different forms of carbon: (a) diamond, (b) graphite, (c) lonsdaleite, (d-f) fullerenes, (g) amorphous carbon, and (h) carbon nanotube. From ref. [51].

Graphene is the name given to a 2D sheet of sp^2-hybridized carbon. It can be stacked to form 3D graphite (figure 3.4 b), rolled to form 1D nanotubes (figure 3.4 h), and wrapped to form 0D fullerenes (figure 3.4 d-f). Unlike the other carbon allotropes shown in figure 3.4, fullerenes contain pentagonal and hexagonal rings. A graphene crystal is an infinite 2D layer consisting of sp^2-hybridized carbon atoms, which belongs to the hexagonal lattice [51]. It offers great electrical conductivity and it can be considered a zero-bandgap semiconductor.

Graphite is an infinite 3D crystal made of stacked layers consisting of sp^2-hybridized carbon atoms. Depending on the layers stacking, these crystals could be hexagonal or rhombohedral. In both 3D structures, the layers interact weakly through van der Waals forces and for this reason the material is more conductive in the direction parallel to the layers than in the perpendicular one [52]. The weak van der Waals forces between layers let the graphite exfoliate among layers. For this reason, diamond is stronger and harder than graphite. We can conclude that the graphite properties are anisotropic and that the presence of graphite crystals in biochar structure could improve a lot its electrical conductivity.

Most commercial carbons used today have an amorphous structure with a disordered microstructure based on that of graphite. Normally the electrical conductivity values of amorphous carbon are 1.25 to $2 \cdot 10^3$ S/m. As mentioned earlier, the process of graphitisation consists of the ordering and stacking of these layers and is achieved at very high temperatures (> 2500 °C). Between the extremes of amorphous carbon and graphite, a wide variety of carbon materials can be prepared [45]. As the temperature increases, condensation reactions begin, and localized graphitic units start growing and become aligned into "graphite-like" micro crystallites, formed by graphene sheets. The carbon precursor and pyrolysis parameters will determine the size of graphene sheets, the stacking number of graphene sheets and the orientation of crystallites [45]. The size and orientation of crystallites is fundamental to define the degree of electrical conductivity of biochar.

4. OBJECTIVES AND METHODOLOGY

As mentioned in the section 2.3, biochar has always been used as fertilizer for soils or as a fuel. Only in the last few decades interesting and renewable applications are born. Despite its structures and a lot of its properties are well known, electrical conductivity was investigated only in recent years.

The Green Technologies Lab of the University of Toronto has dedicated its research activity to the investigation of electrical conductivity of monolithic biochar and its role as electrode material for supercapacitor applications. Before that, only the electrical conductivity of biochar powders compressed was studied. For the first time they linked the electrical properties of biochar to its structure, that depends strictly on the biomass feedstock used as precursor. They have studied different monolithic wood-based biochars, finding some interesting results, that are different depending on the type of wood the biochar comes from.

The present study is the first step of a project that has the main goal to investigate the electrical conductivity of sawdust pellets biochar and their role in supercapacitor applications. Instead of starting from monolithic pieces of wood, the idea is to use the sawdust, a waste of the wood industry. This could be a way to achieve interesting results for supercapacitors application, valorising a waste and obtaining cheap and environmentally friendly materials. All the previous studies focused on the compression of sawdust are based on the idea to use sawdust pellets as fuels. In fact, the main goal of all of these previous studies, is to improve the calorific value of the pellets in order to achieve a good combustion. For this reason, we don't have a scientific literature which we can rely upon. Furthermore, there are no previous studies about the pyrolysis of compressed sawdust, so this could be the start of the study of the best pyrolysis conditions to achieve satisfying electrical conductivity results.

In all previous cases, the biomass has undergone a pyrolysis process, it has been disintegrated, and then the powders have been compressed to test electrical conductivity. In this case, the sawdust has been compressed to form pellets and then they have undergone pyrolysis process. So, the sawdust pellet may be seen as a unique structure and the main aim of this work is to understand how the sawdust pre-treatment, the compression and pyrolysis conditions can affect the final structure of biochar and its properties, especially the electrical conductivity. Moreover, the previous studies of this research team pointed out that the values of electrical conductivity could be different even if they come from the same wood species. The origin of this phenomena is because the original structure of the wood affects a lot the final properties of biochar and wood coming from different trees, grown in different conditions, can bring to different biochars. Using the compressed sawdust could help to overcome this obstacle and to achieve a structure and properties of the material that could be repeatable. In this way, it would be possible to mix together different types of sawdust from different trees and different species obtaining a homogeneous structure. While using a monolithic piece of wood means to transfer the internal defects of the wood structure to the biochar structure, making sawdust pellets could help to achieve a better control of the properties of the final structure, because we can change a lot of variables, such as the sawdust particle size or its pre-treatment conditions.

Therefore, the purpose of making sawdust pellets, pyrolyzing and studying them will be:

1- Valorising a waste, instead of producing biochar from wood pieces
2- Producing a homogeneous and more uniform material, with the possibility of mixing together different species and making the material repeatable, without depending on the original tree structure
3- Producing a dense material, denser than the original wood and this is the property expected to improve the electrical conductivity

The entire work is focused on the production and characterization of sawdust-derived biocarbon monolith. The samples will be tested in future works as supercapacitors. The experimental procedure followed is:

1- Selection of feedstock
2- Sawdust pre-treatment
3- Compression of sawdust at 100°C and pellets production
4- Pyrolysis and biochar production
5- Electrical conductivity measurements
6- Physical and chemical characterization of biochar

The first part of the work has focused the attention on the production of pellets without using binders. The main goal is to achieve a dense and compact structure without the help of binders. In the last part of the work, lignin has been added during the pellets production as a binder. We'll see how this affects the physical and electrical properties of biochar. Finding a perfect binder which can help in forming a more compact structure and at the same time does not affect the electrical conductivity could be an interesting challenge.

Since the number of parameters involved is very high, only three of them have been chosen as variables, while all the other are fixed (see Tables 4.1 and 4.2).

Tables 4.1 (on the left) and 4.2 (on the right). List of fixed parameters and variables chosen.

Fixed parameters
Type of feedstock
Sawdust particle size
Type and time of pre-treatment
Moisture content
Temperature during compression

Variables
Pressure applied during compression
Pyrolysis conditions
Percentage of added lignin in the last two sets

The work is based on 54 samples: 9 sets of 6 samples each.
The first 42 samples are pyrolyzed pellets from compressed sawdust.
Every sample of each set has been prepared in the same conditions of the other samples except for the pressure used to compress the sawdust during the pellets production.
Every set of samples is different from the other sets because of the pyrolysis conditions. Different pyrolysis conditions have been tested to see which one in term of best electrical properties could be.
The last 12 samples are biochar derived from sawdust compressed pellets obtained adding lignin as a binder. The two sets are different because of the different weight percentage of lignin added.
The main purpose of this work is to understand how the pressure applied during compression and the different pyrolysis conditions adopted to produce biocarbon monolith, affect the electrical conductivity.

In the experimental procedure of chapter 5 the pressures used for sawdust compression and the different types of pyrolysis conditions will be described. Since the number of samples is high, they will be called with a short acronym X.Y where "X" will be a number referred to pyrolysis condition while "Y" will be a number referred to the pressure adopted. For example, the sample 3.2 will be the sample that undergoes the pyrolysis conditions n.3 and that is compressed at 1000 psi (see chapter 5). For the

samples with added lignin, L10 and L20 will be added at the acronym to indicate 10 or 20 wt% of lignin added.

5. EXPERIMENTAL PROCEDURE

5.1 Selection of feedstock

Biochar physical and chemical properties are affected by the type of biomass, in this case wood, chosen. For this type of research sugar maple sawdust was used. It was provided by the Faculty of Forestry of the University of Toronto. Sugar maple is a diffuse-porous hardwood, with a density of 0,733 g/cm^3. The choice was dictated by the fact that, in previous researches about the electrical conductivity of monolithic biochar, sugar maple has shown one of the highest electrical conductivity values. The same experiments could be repeated using different type of wood sources for sawdust or mixing different types with different percentages.

The sawdust was sieved, and different particle sizes were obtained. U.S.A standard testing sieves from VWR Scientific were used. The particle size range chosen is 212 – 600 μm.

5.2 Partial removal of lignin

In order to obtain sawdust pellets, a partial removal of lignin and hemicellulose must occur to make compression easier and more efficient. Compressing the sawdust particles without a previous partial removal of lignin and hemicellulose doesn't make the particles to stick together and the pellets can not be created. Otherwise, the only way to produce a compact and uniform pellet may be the use of a very high temperature (hundreds of °C). This step is based on previous works: [53] and [54].
In ref. [53], the chemical pre-treatment adopted in this research has been used to process bulk natural wood into a high-performance structural wood. The main goal was to improve the mechanical performance of natural wood, such as strength and toughness, to use it as material for building and furniture construction. To achieve this goal, a two-step process was adopted: a partial removal of lignin and hemicellulose from the natural wood followed by hot-pressing, leading to the total collapse of cell walls and the complete densification of the natural wood with highly aligned cellulose nanofibers [53]. In this thesis the same process was chosen to make the sawdust particles more compressible and help them to stick together. As mentioned in paragraph 1.2 in fact, lignin is the one among lignocellulosic components that confers rigidity to cell walls and resistance to compression. Its removal is a crucial step in this work since one of the main goals is to achieve a denser material than normal wood and to ensure a better contact between particles. Furthermore, lignin and hemicellulose act as cementing agents: the effect of pressure and temperature during the pellets production may determine the release of lignin from cellular structures to act as a glue among sawdust particles, resulting in an increase of pellets density.
In previous works, other pre-treatments have been adopted to enhance mechanical properties of natural wood: steam, heat, ammonia, cold-rolling, followed by densification, lead to higher densities. However,

they confer lack of dimensional stability, particularly in response to humid environments, and wood treated in these ways can expand and weaken [53].
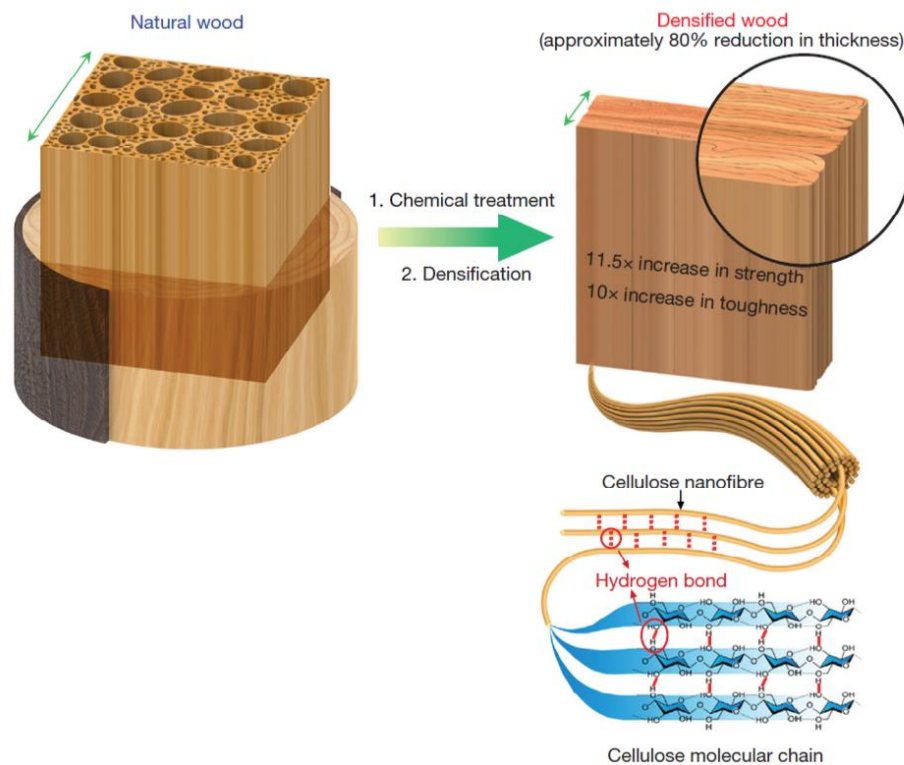
Figure 5.1 Schematic of two-step approach to transform bulk natural wood into densified wood. From ref. [53].

In figure 5.1 a representation of the two-step process is shown. The first step is a chemical treatment in a boiling aqueous mixture of NaOH (sodium hydroxide) and Na_2SO_3 (sodium sulphite) to partially remove lignin and hemicellulose from the wood structure. The second step is a mechanical hot-compression at 100 °C which leads to a reduction in thickness of about 80 %. Most of the densified wood consists of well aligned cellulose nanofibers, which greatly enhance hydrogen bonds formation among neighbouring nanofibers [53]. The chemical treatment leads to substantial reduction of lignin and hemicellulose content, but only modest reduction in cellulose content, largely owing to the different stabilities of these three components in the NaOH/ Na_2SO_3 solution. Thank to the partial removal of lignin and hemicellulose from the wood cell walls, the wood becomes more porous and less rigid.

The same chemical treatment has been used in ref. [54]. The main goal was to achieve a super-flexible wood to obtain flexible porous membranes for electronic, energy storage device, sensor applications. The research has been done on balsa wood (see figure 5.2).
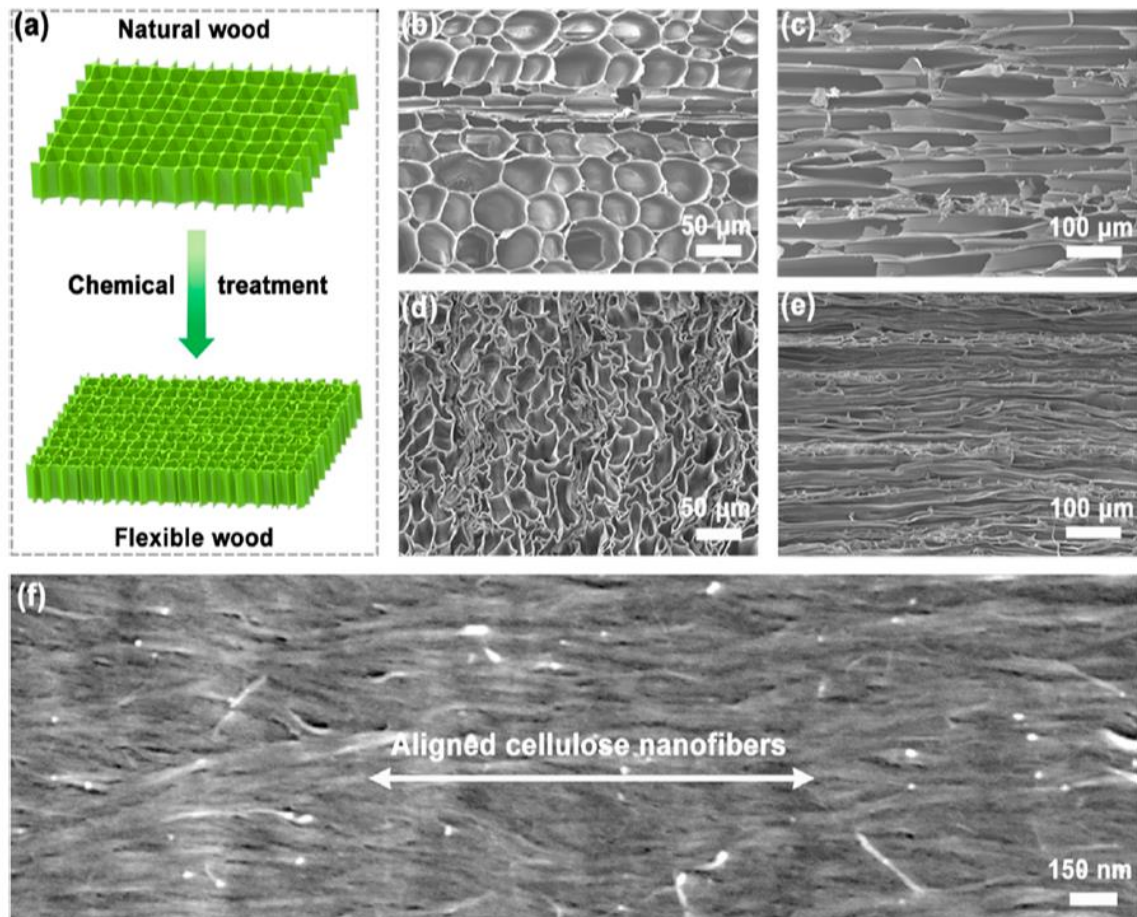
Figure 5.2 (a) Structural characterization of natural balsa wood and flexible balsa wood after the chemical treatment. (b,c) SEM images of natural wood; (b) cross-sectional image showing hexagonal fiber cells; (c) longitudinal image that shows elongated cells; (d,e) cross-sectional and longitudinal SEM images of flexible wood; (f) magnified SEM image showing aligned cellulose nanofibers in flexible wood. From ref. [54].

The figure 5.2 shows the change in structure of balsa wood after the alkali pre-treatment. Balsa is a hardwood as sugar maple. The morphology and microstructure of balsa wood has been characterized in ref. [54] by scanning electron microscopy (SEM) before and after chemical treatment. Natural balsa wood has a unique 3D porous structure with irregular hexagonal cells of 30-50 μm in diameter along the tree-growth direction (see figure 5.2 b and c). After chemical treatment these 3D porous channels are preserved but they have irregular shapes and shrunken diameters (see figure 5.2d, 5.4e), [54]. The figure 5.2f shows the aligned cellulose nanofibers after chemical treatment. Their alignment is perfectly preserved and numerous nanopores between them are generated due to the partial removal of lignin and hemicellulose [54]. In the wood structure the lignin fills the space between cellulose and hemicellulose and its partial removal leads to the formation of nanopores between aligned cellulose nanofibers.
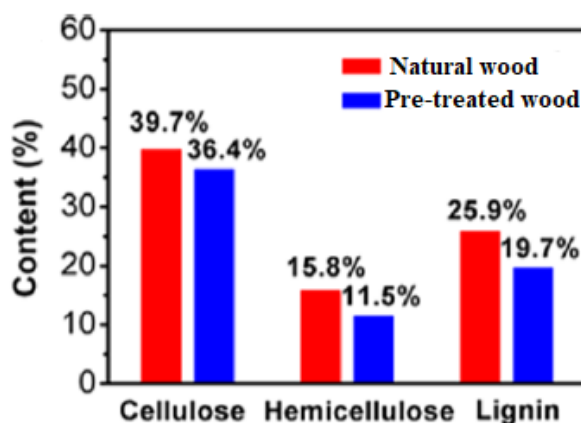
Figure 5.3 Cellulose, hemicellulose and lignin content evolution from natural wood to chemical treated wood, after 1-hour pre-treatment. From ref. [54].
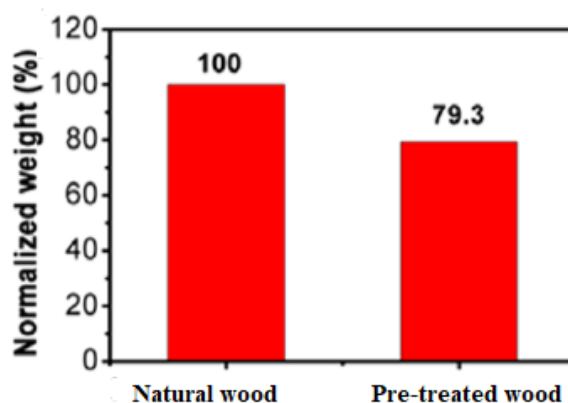
Figure 5.4 Weight loss of wood samples before and after 1-hour pre-treatment. From ref. [54].

In figure 5.3 it is possible to see the content of the three lignocellulosic components in the wood before and after the chemical treatment of the ref. [54]. Lignin is the component removed in highest percentage, followed by hemicellulose. Cellulose is also removed but in lower quantity compared to the other two. The figure 5.4 shows the difference in total weight of balsa wood sample. The wood underwent a total weight loss of 20.7 % [54].

The role of NaOH is to selectively degrade lignin and hemicellulose, while having little effects on cellulose components. The lignin is removed in larger quantity than hemicellulose because of the presence of Na_2SO_3. The increase of sulphite groups SO_3^{2-} into the lignin side chains by means of sulfonation enables the lignin to be dissolved quickly in alkaline solution [54,55]. The interaction between the NaOH and Na_2SO_3 solution with cellulose, hemicellulose and lignin can swell the cell walls, making them softer for feasible bending, folding or compressing [54]. The ref. [54] highlights the differences between alkali treatment and other treatments using water or HCl. In these latter there is absence of colour change of the solution after the treatment. We will see in the next chapter how the solution changes its colour after the chemical treatment thank to the release of lignin and hemicellulose.

5.2.1 Sawdust pre-treatment

Sawdust pre-treatment is the first step of the experimental procedure adopted. The sawdust underwent a pre-treatment in a boiling aqueous solution of mixed 2.5 M NaOH and 0.4 M Na_2SO_3 for two hours, followed by immersion in boiling deionized water several times to remove chemicals. For every immersion, new deionized water was used, and the sawdust was immersed many times until the colour of water do not change by visual inspection. The volume ratio of NaOH solution and Na_2SO_3 solution is 1:1. Normally 20-30 gr of sawdust were immersed in 400 mL of boiling solution. A magnetic stirrer was used to stir the solution during the pre-treatment and the immersions in deionized water, to improve the surface area available for solid-liquid contact.
From the figure 5.5 (on the left) it is possible to see the solution after the chemical pre-treatment. It became dark brown thank to the release of lignin.

After each immersion, to separate the sawdust from the liquid solution, a glass fiber filter and a vacuum pump were used. The filters used are Whatman glass fiber filter 934 AH of 9 cm of diameter. The filter was placed on a perforated plate connected to a vacuum pump which helped the liquid passing through the membrane (see figure 5.5, on the right).
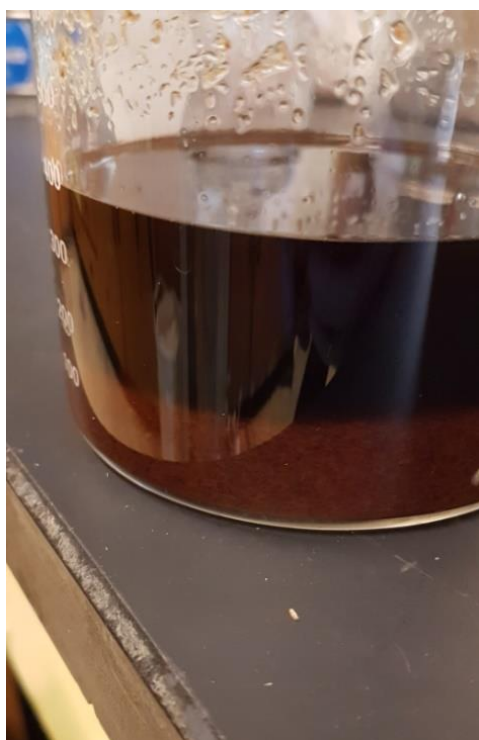
Figure 5.5 Sawdust pre-treatment. On the left: sawdust after the chemical pre-treatment in a boiling aqueous solution of mixed 2,5 NaOH and 0,4 M Na_2SO_3 for two hours. On the right: solid-liquid separation with a filter, perforated plate and vacuum pump.

After that, the sawdust underwent several washings with deionized water, until the post-washing water electrical conductivity is about or less $15 - 20$ μS/cm. The reference is the electrical conductivity of deionized water, 8 μS/cm. If the electrical conductivity is close to 8 μS/cm, the chemicals are almost completely removed from the sawdust.

In figure 5.6 we can see the changing in colour of sawdust thank to the immersion in boiling deionized water. After the chemical pre-treatment, the sawdust particles were still covered with the chemicals and with lignin's residues which conferred them a dark brown colour.

Figure 5.6 Changing in colour of the sawdust during the immersion in boiling deionized water. On the left: sawdust after the alkali pre-treatment. In the middle: sawdust after some immersion in boiling deionized water. On the right: sawdust at the end of the pre-treatment process.

The sawdust was weighed before and after the pre-treatment and the mass loss percentage basing on dry mass, was about 35 – 40 %. The choice of the time of pre-treatment was based on the ref. [53]: the pre-treatment time chosen was about 7 hours, but the work has been done on big pieces of wood. In our case, the particles were very small, with a high surface area available for solid-liquid contact. For this reason, a shorter period was chosen. By changing the boiling times, pre-treated sawdust with different degrees of lignin removal can be obtained. In this work, the pre-treatment time was fixed as 2 hours, but it could be a variable to be optimized in the process for future works.

5.2.2 TGA analysis

The thermogravimetric analysis (TGA) was done on a sample of sugar maple sawdust in order to have a preliminary idea of volatilization and decomposition of wood components before and after the chemical pre-treatment.

TGA is a technique in which the mass of a substance is monitored as a function of temperature or time while the sample is subjected to a controlled temperature program in a controlled atmosphere. A thermocouple placed 2 mm above the sample monitors the temperature and a balance monitors and records the weight every increase of 0.1°C. As the temperature increases, the sample's weight may increase or decrease, depending on the type of reactions that occur. The curve, that the instrument releases, shows on x-axis time or temperature and on the y-axis the weight or the weight percentage remained. The TGA was performed in a TA Instruments Inc. TGA Q500 Evolved Gas Analysis (EGA) furnace.

Approximately 10 mg of maple sugar sawdust were settled on a platinum plate and then placed in the furnace chamber of the instrument. Before loading the sample, the platinum plate was cleaned from remains of previous analysis thank to a flame that burnt the residues. After the calibration, the sample was loaded, and the furnace was moved up. An argon flow rate of 90 ml/min was provided to ensure an inert atmosphere, avoiding the sample combustion. The purpose was to simulate the decomposition during pyrolysis and an oxygen-free environment is required. To ensure a perfect sealing of the furnace chamber, avoiding the presence of oxygen inside, it is recommended to grease the ring on the border between the furnace and the external environment.

The heating methodology chosen for TGA analysis was a ramp program:

- 5 °C/min from room temperature (~ 22 °C) up to 1000 °C.

The heating rate was low enough to show qualitatively the thermal decomposition reactions of maple sugar sawdust.
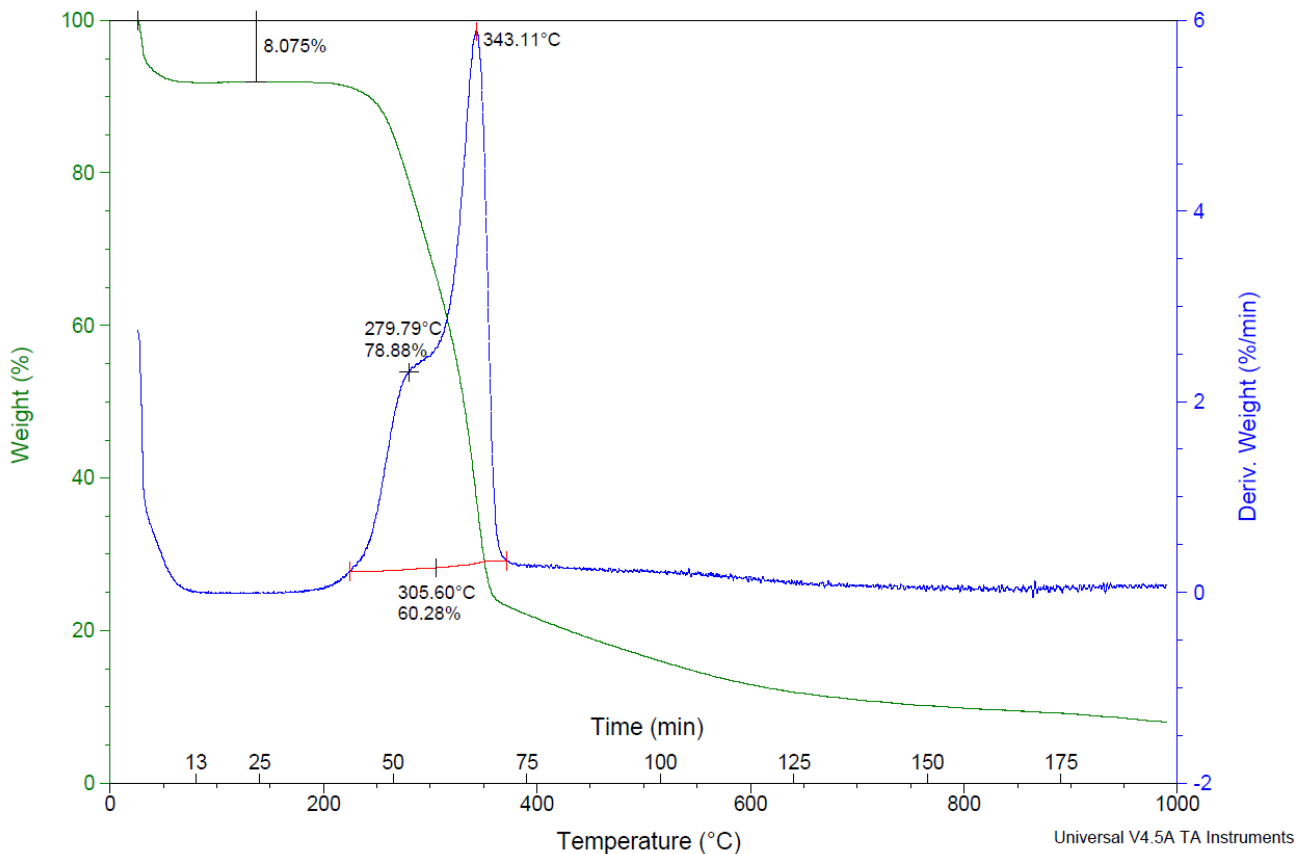
Figure 5.7 Thermogravimetric analysis (TGA) of sugar maple sawdust sample. The green curve is the TGA curve: weight % as a function of temperature (from 20 °C up to 1000 °C). The blue curve is the first derivative of the green curve, DTG curve.

The figure 5.7 shows the thermal decomposition of sugar maple sawdust. The green curve is the thermogravimetric spectra of the sample: it plots the weight percentage compared to the initial weight of the sample as a function of temperature and time (there are two x-axis). The blue curve is the DTG curve: differential thermogravimetric spectra. It is the first derivative with respect to time of the TGA curve. It represents dm/dt and it plots the rate of change of mass (% wt/min) as a function of temperature or time. The software used to manipulate the curves is TA Universal Analysis. The curves were smoothed, and the smoothing region width chosen was 0.5 min. Compared to the TGA curve, it is easier to distinguish the different type of decomposition that occur since they are represented as peaks. The height of the peaks in DTG curve is an indicator of the reactivity of the sample. The higher the peaks, the more reactive the sample. A smaller peak indicates more thermal stability. The area under DTG curve gives the amount of decomposed material. The point where the peak starts shows the degradation temperature of the component, while the point where the peak ends indicate the temperature at which the component is lost. The highest point in the peak represents the highest mass loss rate with respect to temperature. This curve is very useful especially for the materials that exhibit multistep decomposition behaviour, such as woody biomass.

TGA analysis were performed before and after the chemical pre-treatment to see how the peaks change because of the partial removal of lignin and hemicellulose. In the chapter 6 all the results will be reported and discussed.

5.2.3 Sawdust analysis

The content of lignin and cellulose of the feedstock untreated and treated has been calculated to have more information about how much lignin has been removed during the pre-treatment.

The Klason method was adopted for the determination of lignin content, while for the determination of cellulose content, the procedure of ref. [56] was adopted.

With the Klason method it is possible to determine the content of acid-insoluble lignin. Some of the lignin dissolved in acid solution during the test and it is not included in the test results. In hardwoods, the content of soluble lignin is about 3 to 5% (wt%). Two samples (treated and untreated sawdust) of 2 gr were prepared. The test specimens were placed in a beaker with 40 mL of 72% (wt%) sulfuric acid solution. The solution has boiled for 4 hours, maintaining constant volume by frequent addition of hot water. To allow the insoluble material (lignin) to settle, the beakers were kept in an inclined position. The lignin was then transferred to a filter. The lignin was washed free of acid with hot water. The filtering crucibles with lignin was dried in an oven at 105°C to constant weight and then cooled in a desiccator and weighed. To calculate the lignin content in the test specimen the ratio between the weight of lignin and the oven-dry weight of test specimen was performed.

$$Lignin, \% = \frac{A}{W} \cdot 100 \qquad (5.1)$$

(A is the weight of lignin and W is the oven-dry weight of the test specimen)

To calculate the cellulose content, 1 gr of sawdust was placed in a beaker with 50 cc. of water and 5 cc. of 10% (wt%) NaOH solution. It was placed in a boiling water-bath for 5 minutes and the solution is poured on to a piece of cloth and wash many times with water. The sawdust is then transferred from the cloth to the beaker with 50 cc. of water and 5 cc. of 10% (wt%) HCl solution. The beaker was placed again in a boiling water-bath for 5 minutes and the sawdust was filtered and washed as before. The extraction of sugars, starch, and hemicelluloses was completed by a second alkali and acid treatment carried out in exactly the same manner as the first [56]. Then the sawdust was placed in a beaker with 50 cc. of water and 5 cc. of sodium hypochlorite solution. The mixture stayed for 20 minutes in a cool place away from bright sunlight. The sawdust was then filtered, washed, transferred to the beaker and chlorinated a second time for 20 minutes. It was next filtered, well washed with cold water, then with 50 cc. of 2% of hydrogen peroxide, and then with boiling water. Finally, the residual cellulose was filtered (with a cotton cloth), and dried. Cellulose content is calculated through the eq. 5.1, where A is the weight of the cellulose.

Both the experiment for the calculation of lignin and cellulose content were repeated three times.

5.3 Sawdust compression

The second step of the experimental procedure adopted in this work is the compression of the sawdust to produce pellets. However, after the chemical pre-treatment and before the compression, it is necessary to determine the right moisture content of the sawdust. The moisture content is a fixed parameter and it is the same for each sample of this work. In literature it is possible to find many works about the densification of wood residues or sawdust to produce fuels. The main goal of these works is to increase the pellets density to facilitate storage, handling and transportation. Moreover, a denser pellet has a high-energy content per unit volume and a longer burning time. In this work the main goal is the same but for a different reason. The purpose is to increase the density of the pellets because a better contact between particles is expected, and this could increase the electrical conductivity of the material. In ref. [55] and [57] it was pointed out that the optimum moisture content to produce pellets or logs, keeping constant all the other conditions, is in the neighbourhood of 8%.
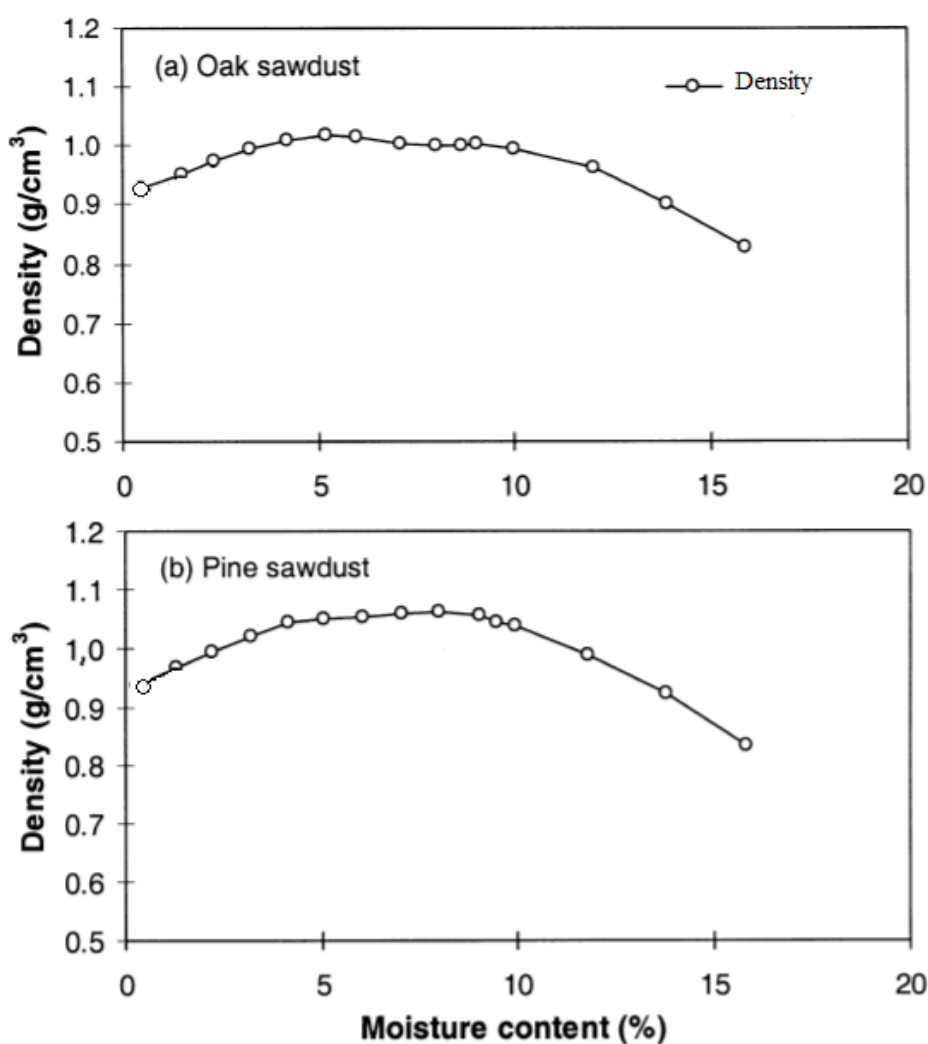
Figure 5.8 Density vs moisture content of logs made by oak sawdust (a) and pine sawdust (b). From ref. [55].

In figure 5.8 the density of logs from oak sawdust and pine sawdust of ref. [55] has been plotted as a function of the sawdust moisture content (MC). All the other variables as pressure and temperature have been kept constant. It is possible to see that in both of cases, the highest density is reached when the MC is close to 8 %. A higher moisture content would make the pellet expand after the compression, the vaporization of surplus water would tear it into pieces. The moisture content is an important parameter which has a great influence on lignin plasticisation process, during the compression [58]. On the other hand, when the moisture content is too low, the pellet is too dry, and it tends to adsorb moisture from the air and expand significantly [55]. Moreover, the lignin plasticisation process is less efficient, and the particles do not stick together.

For this work a MC in the range of 8-8.5 % was chosen. To achieve the right MC, the first thing was to calculate the moisture content of the sawdust after the pre-treatment. The use of the vacuum pump helped removing water from sawdust particles, but the MC was still 40 – 50 %. A sample of sawdust was put in an oven at 110 °C and its weight was monitored until it remained stable: it meant that all the moisture had left the particles.
The moisture content was then calculated:

$$\% \, MC_{sawdust} = \left(\frac{wt_{in} - wt_{fin}}{wt_{in}} \right) \cdot 100 \tag{5.2}$$

When the moisture content of the sawdust is well-known, the quantity of water that must be removed in order to achieve a MC of 8.5 % can be calculated. The total mass of the sawdust and the percentage of weight loss to remove water are known, so it is possible to calculate the final weight that the sawdust should have. The weight was monitored until it reached the right value.

5.3.1 Compression at 100°C

The pellets production consists in a "high-temperature" compression. The temperature adopted during the compression is 100°C, according to the ref. [53]. The mechanical hot-pressing involves the combination of temperature and pressure. The pressure causes the total collapse of the cell walls and the consequent release of lignin from the cell walls, while the temperature helps the lignin plasticization process. The heat causes plasticization of the lignin and, in consequence, the separation of the fibres. Upon cooling down, the lignin hardens again and forms a glassy crust on the surface of the fibres, acting as a glue as mentioned earlier. For this reason, a partial, not total, removal of lignin is required. A total lignin removal would lead to wood that can be easily crushed during hot-pressing, probably owing to the absence of lignin as a binder [53]. Thank to the combination of pressure and temperature, lignin moves from the inner cell walls layers to the fibre surface. The result is a higher degree of adhesion among the fibres. Moreover, pressing at high forces and temperatures for long periods can create water-resistant bonds. In fact, the pellets produced in this work do not adsorb moisture easily. Their dimensions have been measured after some days since the compression, after leaving them in the lab, with a temperature of 21-23°C and a humidity range of 25 – 35% and they were within the error bars. Obviously, the fact that the pellets did not undergo expansion was proved only for these conditions.

Figure 5.9 Set-up for sawdust compression to produce pellets.

In figure 5.9 the set-up for sawdust compression is shown. It is mainly composed by two components: a Carver mechanical manual press and a heatable pellet press die set for cylindrical shape samples. The latter is from Zhengzhou TCH Instrument Co. and it is a simple piston and mold system with the possibility to heat up at a certain temperature the chamber where the pellet is produced (see figure 5.10). The maximum temperature reached by the mold is 300°C and the temperature rise rate is about 5-10°C/min. It has a PLC controller to control the temperature and make the actual temperature of the mold the same of the given set-point.

Figure 5.10 On the left: all components of heatable pellet press die set. On the right: cross section of the piston-and-mold system that shows how the components are arranged together during the compression, the one on the left is showing the sample preparation process and the one on the right the pellet release process. The white cylinder is the compressed sample.

The sample shape is cylindrical, and the diameter is 20 mm. The die material is alloy tool steel Cr12MoV. The heating die was put between the two plates of the manual press in order to apply a well-known pressure. Two pads were put at the top and at the bottom of the die to prevent the contact between the die material and the press plates.

Here the detailed procedure followed to produce a single pellet:

1) Assemble the die
2) Put the heating die in the manual press
3) Adjust the temperature to required value with the thermostat
4) Wait for the temperature to reach the setpoint
5) Install the sample in the cavity and wait for 5 minutes to heat up the material before the compression
6) Apply pressure and keep it for 60 seconds of holding time
7) Release pressure
8) Take out the die from the manual press
9) Remove the sample gently
10) Clean the die after each time with a dust-free paper to avoid that the residues affect the following tests. It is recommended to not use chemical reagents to clean and soak.

In this work the temperature during compression has been fixed at 100°C for all the samples.
Temperature, pressure and holding time are important parameters in the phase of compression. Since the press is manual and keeping the pressure for minutes would cause uncertain values and fluctuations and in ref. [57] it was pointed out that the temperature is more influent than time on the degree of compression, a short holding time was chosen. Moreover, in ref. [55] it was highlighted that when the holding time was longer than 20 seconds, the effect on pellets density diminished significantly. The choice in this work has been to wait for 5 minutes after installing the sawdust in the die cavity, to heat up the material and increase its temperature to help the plasticization of lignin. Wood has a very low thermal conductivity, so it takes a long time to heat up, especially for the particles that are not in contact with the metal walls. After that, the pressure has been applied and a holding time of 60 seconds was chosen.
As mentioned earlier, each set contains six samples, produced at different pressures.
The maximum pressure reached by the manual press is 3000 psi.
The six pressures chosen are:

1) 500 psi (3.45 MPa)
2) 1000 psi (6.89 MPa)
3) 1500 psi (10.34 MPa)
4) 2000 psi (13.79 MPa)
5) 2500 psi (17.24 MPa)
6) 3000 psi (20.68 MPa)

The numbers in the list above are the terms "Y" of the samples' acronym that we mentioned in chapter 4.
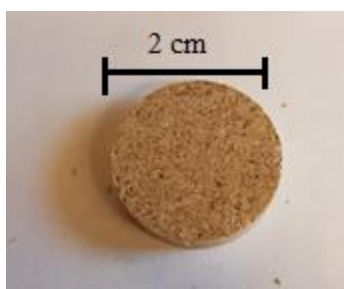
Figure 5.11 Sawdust pellet produced through the procedure described above.

The two sets of pellets with added lignin are produced following the same procedure described above, adding a certain amount of powder lignin and mixing it with the pre-treated sawdust before the compression. The added lignin is a pure lignin extracted from sawdust from different sources. The amount added are 10 and 20 % of the total weight. From a visual inspection we can see that the lignin is not perfectly distributed in the pellet structure (see figure 5.12). In this case the partial removal of lignin is still important because lignin confers rigidity to the cell walls of the sawdust particles and the purpose is to make them more compressible. Lignin is added as a binder: its presence among particles, outside the cell walls may create a denser and more compact structure, thanks to its plasticization.
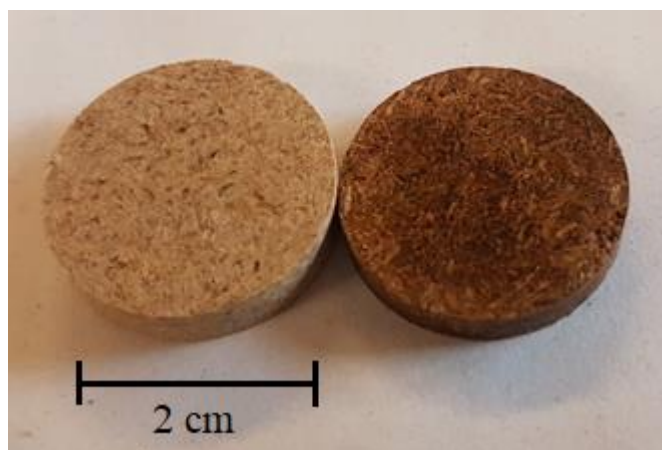
Figure 5.12 On the left: pellet made by compressed sawdust. On the right: pellet made by compressed sawdust with 20 % (wt%) of added lignin.

In figure 5.12 it is possible to see the difference between the two types of pellets: the lignin confers a dark brown colour. We can also notice that the colour is not uniform: lignin is more concentrated in some areas compared to others. The purpose of this test is to make a comparison in term of structure and electrical conductivity between pellets produced with and without binders. The choice of the binder is not easy, it should be a material that, after pyrolysis, is able to conduct electricity. In this case the binder comes from the same type of biomass, wood, but in future works it would be interesting testing other materials as binder and trying to improve pellets physical and electrical properties.

5.3.2 Pellets density

After the compression the pellets are weighed and their dimensions (diameter and thickness) are measured. The volume and the bulk density are calculated. These parameters are important because we can see how the density changes as the applied pressure increases and we can compare mass, diameter, thickness, volume and density before and after the pyrolysis process.

The volume is:

$$V = \pi \cdot \frac{D^2}{4} \cdot t \quad (cm^3) \tag{5.3}$$

where D is the pellet diameter, and t is its thickness.

The bulk density is calculated as:

$$d = \frac{m}{V} \qquad (\frac{g}{cm^3}) \tag{5.4}$$

where m is the pellet mass, and V its volume.

5.4 Production of biochar

The third step of the experimental procedure is the production of biochar. All the samples underwent a pyrolysis process but with different conditions. We'll see how the different pyrolysis conditions affect the physical and electrical properties of the final biochar.
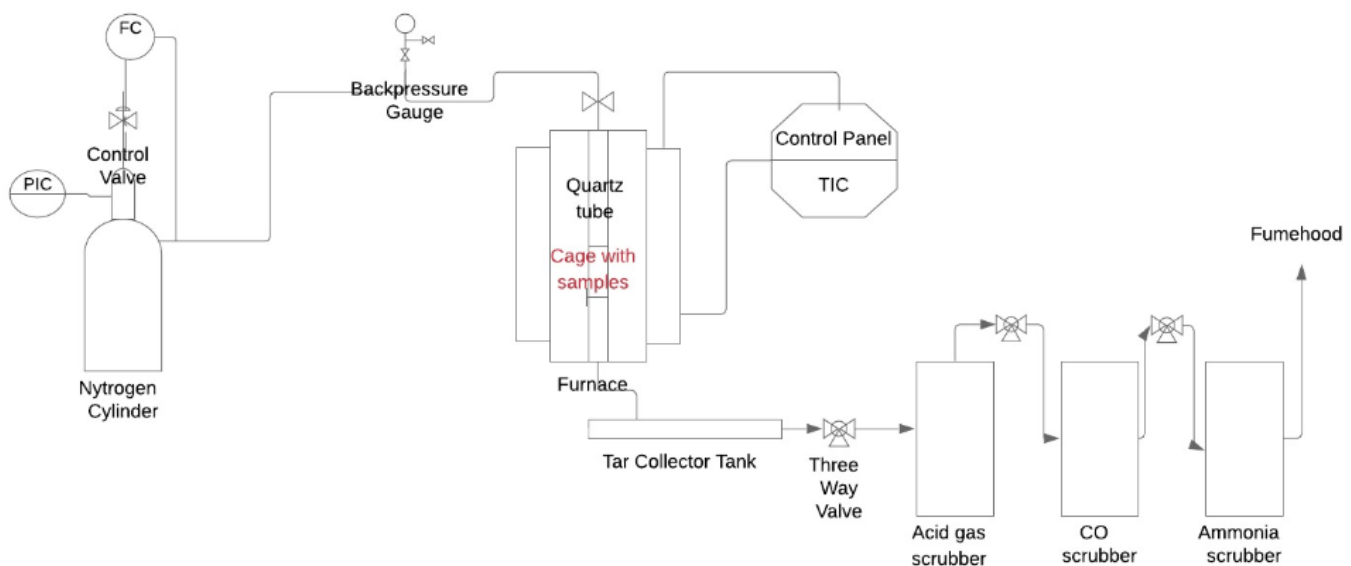
Figure 5.13 Schematic illustration of pyrolysis plant.

In figure 5.13 a schematic illustration of pyrolysis process plant is shown. On the left it is possible to see the nitrogen cylinder: as already said, a flow of inert gas is required to ensure an oxygen-free environment to avoid the combustion of the sample. The cylinder has a pressure regulator, that works as indicator and pressure controller. It is possible to open manually a valve to set the nitrogen pressure (20 psi). On the line that brings the nitrogen in the reactor there is a mass flow controller and an indicator. The mass flow rate of nitrogen is 400 ml/min. Before the reactor there is a backpressure gauge with the function of monitoring the backpressure. There is an inlet nitrogen flow and an outlet exhaust gas flow in the process. When something wrong happens, for example when a valve downstream of the process is close, the gas tends to accumulate in the system and the backpressure will increase. Moreover, the outlet flow of gas products is collected at the bottom of the reactor: a backpressure is necessary as driving force. It is very important to monitor this value and be sure that it is always 10 psi.

The reactor is a vertical quartz tube of 900 mm length, inserted in a Carbolite TZF 12/75 furnace heated up electrically (see figure 5.14). The internal diameter is 68 mm, while the external is 72 mm. The furnace is connected to the control panel equipped with an indicator and temperature controller. It can heat up to 1200°C. The pyrolysis conditions are put manually through the control panel, that brings the temperature at the desired set-point through a certain heating rate, keeping it constant for a certain holding time, if it is required. The furnace is jacketed to ensure operator's safety. The samples are put in a cage made by a mesh steel (see figure 5.15), which is placed in the quartz tube. As we can see in figure 5.14, at the top and at the bottom of the quartz tube, there is glass wool to ensure a good insulation and to avoid the heat dispersion. While the pyrolysis takes place, as said in the first part of the introduction, aside from biochar, also tar and a mixture of gases are produced. Since the interest is focused on biochar, slow pyrolysis conditions were adopted in this work to maximize its yield. In figure 5.13 and 5.14 it is possible to see that at the bottom of the reactor there is the tar collector tank: the tar is collected, and after pyrolysis it is placed in an appropriate container for the disposal. The outlet flow of exhaust gases passes through a plastic tube and is led to three different scrubbers to remove the pollutants through a process of gas-liquid absorption. Before each scrubber there is a manual three-way valve. The first scrubber is made by an alkali solution of KOH 1 M and it has the function to remove the acid gases. The second scrubber is the CO scrubber and the last one is a solution of sulfuric acid to remove the ammonia produced during the process.
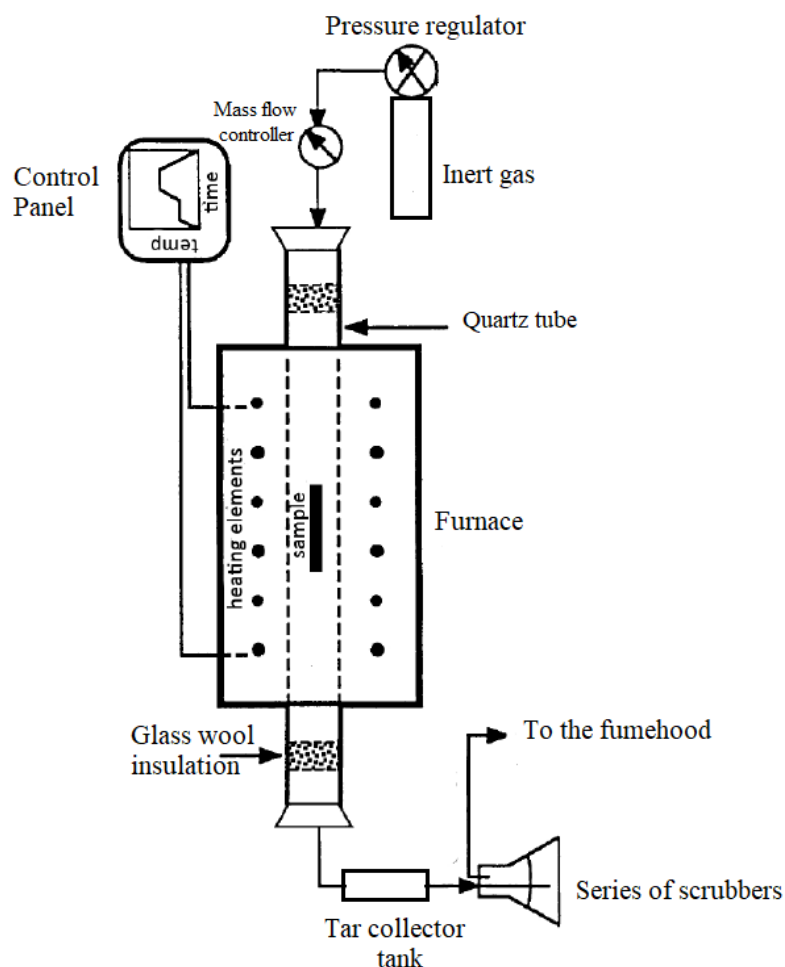
Figure 5.14 Pyrolysis reactor configuration. Adapted from ref. [58].

Before starting each pyrolysis all the set-up connections were well-cleaned with ethanol and a thin layer of sealing paste was applied to ensure the airtightness. At the end of the process, samples were cooled down under nitrogen flow (400 ml/min) to avoid absorption of moisture or undesired combustions. The samples can be taken out of the reactor when the furnace temperature reaches 70°C.

In figure 5.15 a picture of the steel mesh cage is reported. Since in this case we had 6 samples that must undergo the same pyrolysis process, the pellets were put in the cage placing a layer of steel mesh between one another. The last layer at the top was fixed on both sides through a folded piece of steel mesh. This configuration was adopted to make sure they were not in contact, so their pyrolysis could not affect each other, and each sample had its surface area free to release pyrolysis products.
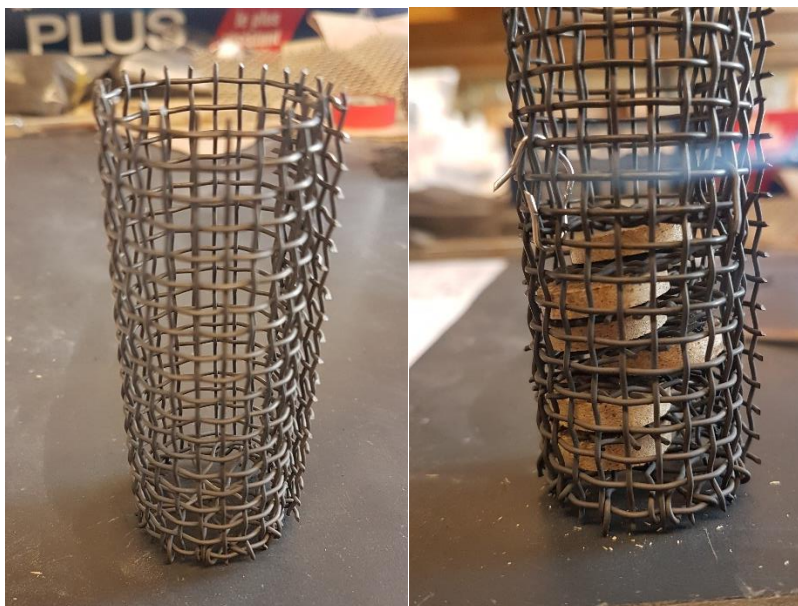
Figure 5.15 On the left: empty steel mesh cage. On the right: samples ready to undergo pyrolysis process. Between one sample and the following one there is a thin layer of steel mesh to prevent their contact.

The small cage represented in figure 5.15 was placed in a bigger one and then placed in the quartz tube. Before starting pyrolysis, it is very important to make sure that all connections are well-sealed to prevent the oxygen from entering the reactor. The last step is to check that the nitrogen pressure and flow rate, the backpressure and the pyrolysis parameters are set on the right values. All the three-way valves must be close to the atmosphere because the outlet gas flow must pass through the scrubbers and then collected by the fume hood.

5.4.1 Pyrolysis conditions

Since there are no available works about pyrolysis of monolithic biochar from compressed sawdust, different pyrolysis conditions were tested in this work. One of the purposes of this thesis is to compare their consequences on the final biochar properties.

As already said, the production of biochar samples is focused on the control of the following parameters:

- Highest treatment temperature (HTT).

In this work the HTT used are 1000°C and 1200°C. As mentioned before, at 700-800°C most of the organic content is lost. After the initial water loss, hemicellulose, cellulose and lignin undergo decomposition. As the HTT increases, the aliphatic chains turn into aromatic groups, and a possible microstructure graphitization can occur.

- Heating rate (HR).

Low heating rate were always adopted since biochar is the product we are interested in. The standard pyrolysis conditions adopted by other researchers in the Green Lab were based on very low values (less than 1°C/min) to obtain a biochar structure without cracks. However, since this work is on sawdust particles compressed together and not on biochar derived from trunk tree pieces, in this work higher heating rates were tested. Moreover, the dimension of the samples was very small, so the moisture and pyrolysis products could leave the structure easier.

- Holding time (HT).

This is an important parameter, especially when the HTT is high. We will see in the next chapters that increasing the holding time is more efficient on electrical properties than decreasing the heating rate. A long holding time (hours instead of minutes) at 1000°C or 1200°C helps the cyclization and cross-linking of polymers during their decomposition, resulting in a higher possibility to obtain a more ordered microstructure.

In this work 6 different pyrolysis conditions were tested. Here they will be listed and numbered:
(the numbers in the list below are the terms "X" of the samples' acronym that we mentioned in chapter 4).

1) It is the typical slow pyrolysis process adopted in the Green Lab. It is a six-stage thermal schedule from the ref. [57] to produce crack-free monolithic biochar from sugar maple hardwood.

Table 5.1 Heating schedule used for the pyrolysis condition n.1. From ref. [57].

Temperature range (°C)	Hold Temperature (°C)	Ramp rate (HR) (°C/min)	Holding time (HT) (min)
25-90	90	0.83	180
90-200	200	0.25	6
200-400	400	0.13	6
400-600	600	0.33	6
600-800	800	0.33	6
800-1000	1000 (HTT)	0.33	6

The table 5.1 shows the pyrolysis parameters always adopted by the researchers of the Green Technology Lab. It is a slow pyrolysis since the heating rates are always lower than 1°C/min. The sample is held at 90°C for 3 hours: this ensures a proper dehydration of cellulose and a slow free water

removal. If it is heated up too quickly, the water evaporates, and the vapours pressure could cause the structure break. This can lead to the formation of cracks in biochar structure. We can notice that the lowest heating rate (0.13 °C/min) is adopted in the range between 200 and 400°C. This is the range in which most of the decomposition reactions take place. The low heating rate has been chosen in ref. [57] to avoid the formation of cracks and to give the sample the right time to release the products.

In this work faster heating rate were tested, 1 and 2 °C/min. This choice was dictated by the fact that in this case it was more difficult obtaining a biochar with cracks since the moisture had more pathways to leave the samples because of the interparticle spaces. Moreover, wood has a very low thermal conductivity, and this slows down the heating of the internal part of the sample. The external part decomposes more quickly than the internal one and the shrinkage caused by dehydration, decomposition and carbonization is different. The surface undergoes a great pressure, and this can cause the break of the structure. This pyrolysis condition is appropriate for big pieces of wood.

In our case, samples are very small: 2 cm of diameter and 0.3-0.5 mm of thickness. For this reason, others "faster" pyrolysis were tested.

2) It is the same process but the holding time at 1000°C is set at 60 minutes.

Table 5.2 Heating schedule used for the pyrolysis condition n.2.

Temperature range (°C)	Hold Temperature (°C)	Ramp rate (HR) (°C/min)	Holding time (HT) (min)
25-90	90	0.83	180
90-200	200	0.25	6
200-400	400	0.13	6
400-600	600	0.33	6
600-800	800	0.33	6
800-1000	1000 (HTT)	0.33	60

We can compare the physical and electrical properties of biochars from conditions n.1 and n.2 knowing that all the parameters are the same, except the holding time. We will see the difference between a holding time at 1000°C of 6 and 60 minutes.

As mentioned earlier, since the samples are small, and they are made of particles stuck together, the risk to obtain a biochar with cracks is very low compared to that derived from wood pieces. The heating rate was increased (2 and 1 °C/min were tested) and it was kept constant for all the pyrolysis process and the holding time at 90°C was decreased.

3) The heating schedule n.3 has a faster heating rate: 2 °C/min. The HTT is still 1000 °C and the holding time is still 60 minutes.

Table 5.3 Heating schedule used for the pyrolysis condition n.3.

Temperature range (°C)	Hold Temperature (°C)	Ramp rate (HR) (°C/min)	Holding time (HT) (min)
25-90	90	2	60
90-1000	1000 (HTT)	2	60

4) The heating schedule n.4 is the same of n.3 apart from the ramp rate, 1°C/min ramp rate was tested.

Table 5.4 Heating schedule used for the pyrolysis condition n.4.

Temperature range (°C)	Hold Temperature (°C)	Ramp rate (HR) (°C/min)	Holding time (HT) (min)
25-90	90	1	60
90-1000	1000 (HTT)	1	60

5) The heating schedule n.5 is the same of n.4 apart from the holding time that was increased until 6 hours.

Table 5.5 Heating schedule used for the pyrolysis condition n.5.

Temperature range (°C)	Hold Temperature (°C)	Ramp rate (HR) (°C/min)	Holding time (HT) (min)
25-90	90	1	60
90-1000	1000 (HTT)	1	360

6) The heating schedule n.6 is the same of n.5 until 1000°C and then a further step until 1200°C for 60 minutes was added.

Table 5.6 Heating schedule used for the pyrolysis condition n.6.

Temperature range (°C)	Hold Temperature (°C)	Ramp rate (HR) (°C/min)	Holding time (HT) (min)
25-90	90	1	60
90-1000	1000	1	360
1000-1200	1200 (HTT)	1	60

Each heating schedule was tested on one set of pellets, apart from the last one which was tested twice, to have more samples for the following characterization.
The last two sets of pellets with added lignin were tested with the heating schedule n.4.

5.4.2 Biochar physical properties

A comparison of physical and geometric properties of pellets before and after pyrolysis was made. After pyrolysis the samples were weighed, and the dimensions were measured. The char yield and carbon yield were calculated. Char yield is the remaining mass obtained at the end of pyrolysis.

$$Char\ yield\ (\%) = \frac{m_{biochar}}{m_{sawdust\ pellet}} \cdot 100 \tag{5.5}$$

In eq. (5.5) $m_{biochar}$ is the mass of the biochar produced by pyrolysis and $m_{sawdust\ pellet}$ is the mass of the pellets before pyrolysis.

The carbon yield is the same ratio of the char yield but referred to the mass of carbon retained after pyrolysis.

$$Carbon\ yield\ (\%) = \frac{mass\ of\ C_{biochar}}{mass\ of\ C_{sawdust\ pellet}} \cdot 100 \tag{5.6}$$

To calculate the carbon-yield an assumption has been made: the carbon content of sawdust pellet was assumed as 50% of the total mass, while the carbon content of the final biochar was provided by elemental analysis (see paragraph 5.6.1).

The thickness and diameter were measured after pyrolysis to calculate the axial and radial shrinkage.

$$Axial\ shrinkage\ (\%) = \frac{(t_{sawdust\ pellet} - t_{biochar})}{t_{sawdust\ pellet}} \cdot 100 \tag{5.7}$$

$$Radial\ shrinkage\ (\%) = \frac{(D_{sawdust\ pellet} - D_{biochar})}{D_{sawdust\ pellet}} \cdot 100 \tag{5.8}$$

The volume and density of biochar after pyrolysis were calculated respectively through the eq. (5.3) and (5.4). In figure 5.16 it is possible to notice how the samples change with pyrolysis. The shrinkage is axial and radial. The samples after pyrolysis are lighter, their volume and density are lower.

Figure 5.16 Example of sample before and after pyrolysis. The shrinkage is axial and radial.

The density of biochar can be measured in two ways: in terms of either bulk density, which includes structural and pore volume, or particle density (also known as skeletal or true density), which includes only the volume occupied by solid molecules [59]. Bulk density is measured by adding a known amount of sample mass into a container of known volume [59]. Biochar particle density is not affected by compaction, unlike the bulk density and it generally increases with pyrolysis temperature as the solid carbon condenses into dense aromatic ring structures. After pyrolysis the bulk density was calculated, while the skeletal density was used for skeletal conductivity calculation.

5.5 Electrical conductivity measurements

The measurements of the biochar electrical resistivity were based on the two-probe method. Two different set-ups were used. Two-probe method is the simplest method of measuring resistivity as shown in figure 5.17. A voltage-drop V across the sample and current I through the sample are measured.
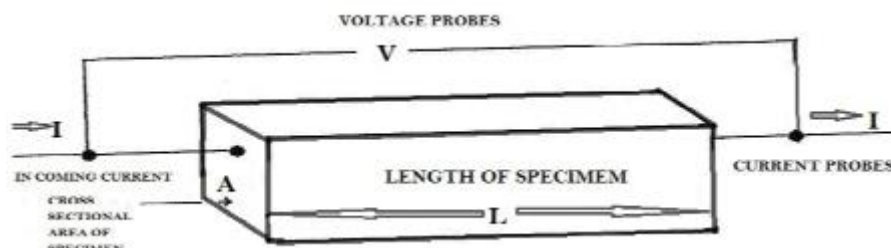
Figure 5.17 Electrical resistivity measurement by two-probe method. From ref. [59]

In the first set-up used in this work, the samples were placed between two electrodes made of tin foil. The tin foils were settled on two pieces of plexiglass. Since the samples surface is not smooth, a certain pressure was applied during the measurements to ensure a proper contact between samples and tin foil. The pressure was applied using a copper weight of 230 g placed on the top of the uppermost plexiglass plate. The electrical resistance of the sample was detected by a Hewlett Packard 34401A DC multimeter (see figure 5.18).
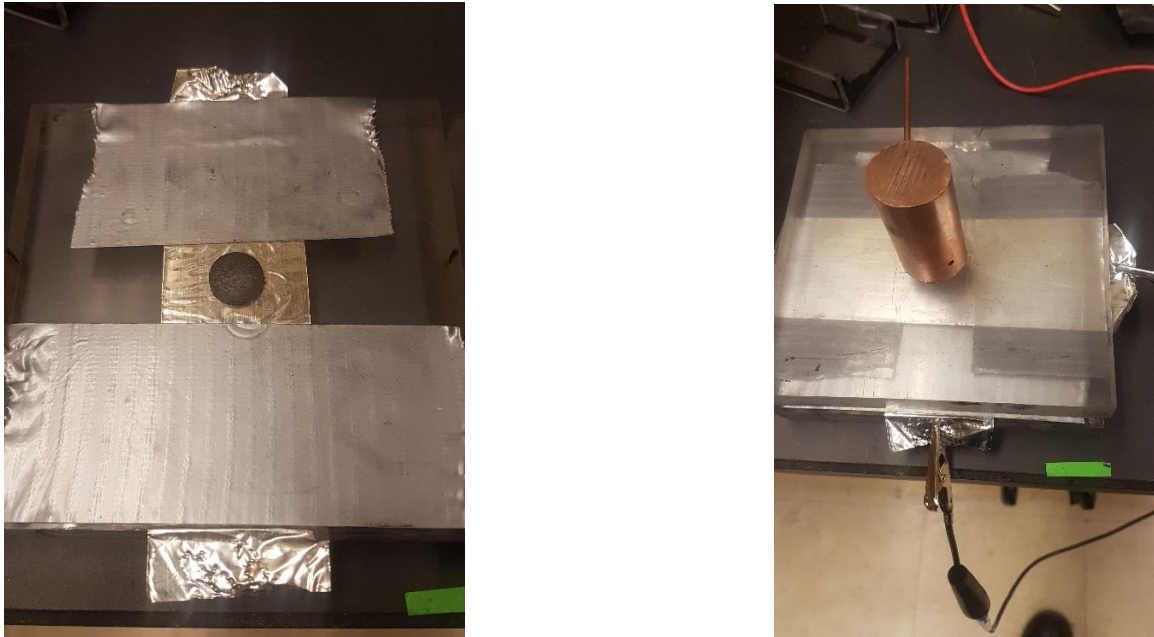
Figure 5.18 First set-up two-probe method used to measure electrical conductivity. On the left: sample placed on tin foil. On the right: sample between the two tin foil electrodes fixed on two pieces of plexiglass. A copper weight is placed at the top of the set-up to apply pressure. Two points of the tin foil are connected to the multimeter.

In this set-up the multimeter detected the resistance of the sample. The resistivity was calculated knowing the geometric properties of the samples (area and thickness) through the second Ohm's law:

$$\rho = R \cdot \frac{A}{t} \quad (\Omega \cdot m) \tag{5.9}$$

Where R is the resistance detected by the multimeter, A is the area of the sample and t its thickness.

The second set-up used in this work is still a two-probe method. The samples were still placed between two tin foil electrodes. Two molds of plexiglass were filled with clay and the tin foils were placed on the clay. The clay is a soft material and ensured a better contact between the sample and the tin foil. The tin foil could adapt its shape on the surface of the sample (see figure 5.19). Two devices were used: a Hewlett Packard 34401A multimeter was used to detect the voltage drop across the sample and a Hewlett Packard E3612A DC Power supply was used to supply a 500-mA direct current. A copper weight of 230 g was applied at the top of the set-up to apply pressure and improve the contact between the sample and the electrodes. In the previous set-up we only knew the resistance of the sample; in this case we know voltage drop and current across the sample and we can calculate the resistance with the first Ohm's law:

$$R = \frac{V}{I} \quad (\Omega) \tag{5.10}$$

Where V is the voltage drop and I is the current. Once the resistance is calculated, the resistivity ρ is calculated through eq. 5.9. Since this set-up needed two different devices, the uncertainty on the measurements could be higher than the one made with the first set-up.
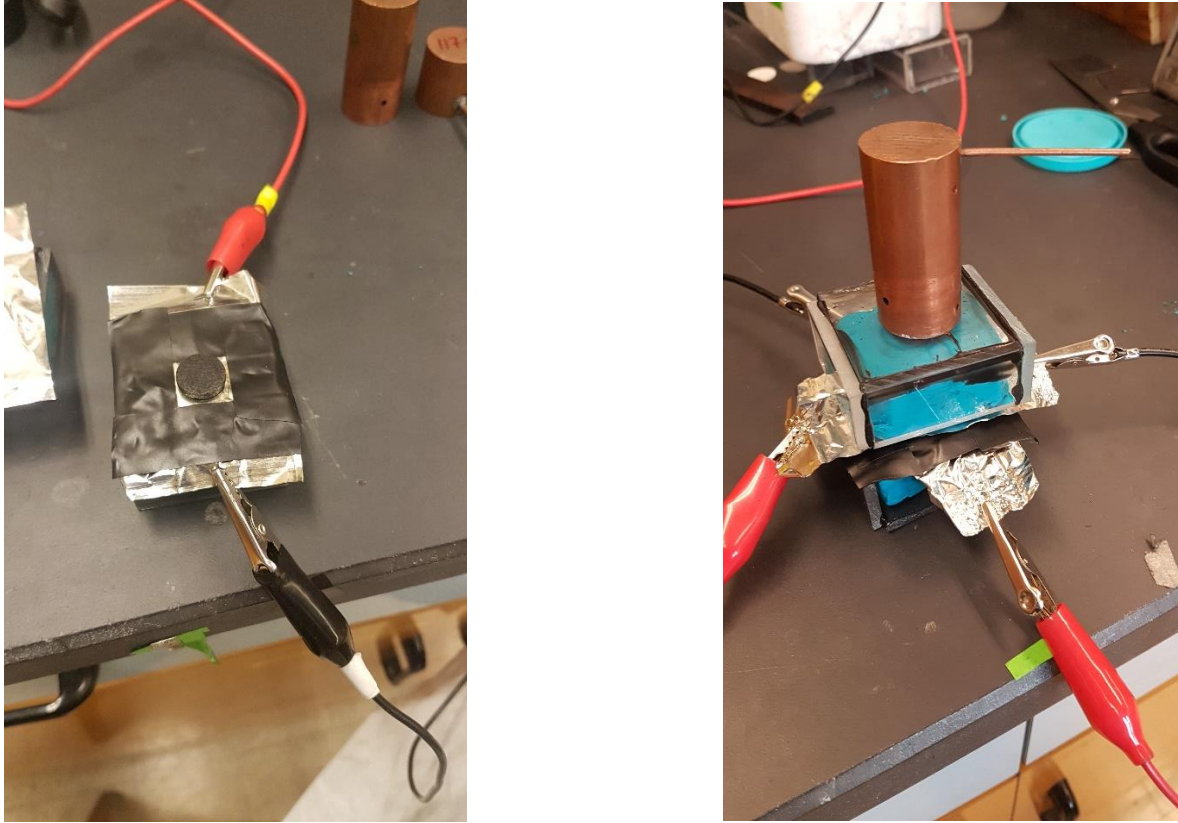
Figure 5.19 Second set-up two-probe method used to measure electrical conductivity. On the left: sample placed on the tin foil. On the right: sample between the two tin foil electrodes placed on clay. A copper weight is placed at the top of the set-up to apply pressure. Two points of the tin foil are connected to the multimeter and two points are connected to device that supplies current.

After calculating the resistivity, the conductivity was calculated:

$$\sigma = \frac{1}{\rho} \quad \left(\frac{S}{m}\right) \tag{5.11}$$

This can be defined as "bulk conductivity", it is the measure of the conductivity of the entire structure (biochar and air), since the material is porous. To relate the value of electrical conductivity to only the solid part made of biocarbon, without considering the pores, since the carbon structure is the only responsible for electrical conductivity, a new conductivity is defined. It is called "skeletal conductivity". It is the conductivity related to the skeletal (or particle) density.

First, the volume fraction was calculated. It is the fraction of the solid biocarbon volume compared to the total volume. It is calculated as the ratio between the sample density (already known) and the density of amorphous biocarbon (1.8 g/cm³). We assume that the biochar structure is almost completely amorphous since the HTTs were 1000 °C or 1200 °C. These temperatures are not high enough to obtain

a complete ordered and crystalline structure. XRD analysis will confirm this hypothesis since there could be few graphite micro-crystals but they are very small.

$$Volume\ fraction\ of\ carbon = \frac{density\ sample}{1.8} \qquad (5.12)$$

Once the volume fraction was known, the "effective area" of the sample was calculated: it is the area that contributes effectively to the electrical conductivity. A sort of correction to the area of the sample was introduced.

$$Effective\ area = A \cdot Volume\ fraction \qquad (cm^2) \qquad (5.13)$$

The resistivity was calculated again, through the eq. (5.9), with the effective area. Though the eq. (5.11) the skeletal conductivity was calculated. In the next chapter the trends of bulk and skeletal conductivity of the samples will be shown.

For each sample 5 measurements were made with each set-up. The measurements were repeated increasing the weight at the top of set-up (see chapter 6).

Those equations are based on the assumption that:

bulk conductivity = volume fraction of carbon * skeletal conductivity of carbon + volume fraction of void*conductivity of air (=0).

Bulk conductivity = (1-volume fraction of void) * skeletal conductivity of carbon

Therefore, the skeletal conductivity is calculated as follows:

Skeletal conductivity of carbon = bulk conductivity of biochar/volume fraction of carbon

Where the volume fraction is (1- volume fraction of void)

5.6 Characterization of biochar

The last part of this work was dedicated to the investigation of the structural and physical properties of the obtained biochar. The purpose was to explain the electrical conductivity trend of the sets of pellets. Only the most interesting samples in terms of electrical conductivity were analysed. The samples were crushed to obtained powders to be used for elemental analysis, X-Ray diffractometry and RAMAN spectroscopy.

5.6.1 Elemental analysis

The elemental analysis was conducted in a Flash 2000 CHN Analyzer in the Analytical Laboratory for Environmental Science Research and Training of the Department of Chemistry of the University of Toronto. The device measures the thermal conductivity of the products released after combustion and reduction of the samples (CO_2, H_2O, N_2), to measure the levels of carbon, hydrogen and nitrogen. For CHN determinations, the elemental analyser operates according to the dynamic flash combustion of the sample. Samples were oven dried and stored in a desiccator prior to be weighed in a tin capsule (1 mg) and introduced into the combustion reactor together with a proper amount of oxygen. After combustion, the resultant gases are carried by a helium flow to a layer filled with copper, then swept through a Gas Chromatography column that separates the combustion gases. Then they are detected by a thermal conductivity detector (TCD). A complete report is automatically generated by Thermo Scientific Eager Xperience data handling software and is displayed at the end of the analysis. The description of the device is taken from ref. [60]. Elemental analysis was performed on the sets that underwent heating schedule n.5 and n.6. Since the analysis were conducted outside the Green Lab, the values have been taken only once, but usually this analysis is repeated 3 times to reduce the uncertainty on the values. Elemental analysis was performed because we are interested in the carbon content of the samples, that shows the degree of carbonization reached during the pyrolysis.

5.6.2 X-Ray Diffractometry (XRD)

The X-Ray diffractometry (XRD) was conducted in a Rigaku Miniflex 600 device on powder ground and sieved to reach a size < 50 μm. The system is equipped with a 2.0 kW Cu X-ray tube, NaI scintillation detector, graphite monochromator and an automatic 6-position rotation system. Scans were carried out over the 2ϑ range of 10-50°. The amount of sample used was 1-2 mg, enough to cover XRD grid. XRD analyses biochar to detect {002} and {100} peaks of graphite crystals [47] and the width of the peaks gives information about the size of the graphite micro-crystals in biochar structure.
This analysis is used to quantify the crystallography of the biocarbon, that is linked to degree of graphitization developed during pyrolysis.

5.6.3 Raman spectroscopy

The Raman spectra were obtained through a Renishaw Ramanscope InVia H43662. It used a green laser beam with an excitation wavelength equal to 514.5 nm and a power of 4 mW. The Raman spectroscopy is a useful tool to study the hybridization of the carbon in the biochar samples because the Raman spectrum is particularly sensitive to the microstructure of carbon. Two Raman bands of the biochar spectrum are called D and G bands. Their intensities provide information about the disorder (sp^3 carbon) and order (sp^2 carbon) in a carbon structure [61]. A D/G peak height ratio of ~1% represents high crystallinity.

6. RESULTS AND DISCUSSION

6.1 Sawdust pre-treatment

6.1.1 TGA analysis before and after the pre-treatment

TGA analysis was performed on the sawdust before and after the pre-treatment. In figure 6.1 TGA and DTG curves are shown. The devolatilization process starts at 70-80 °C. This is the first step and involves the free water loss contained in the sample. The moisture content of the analysed sample was about 8 % in weight. The mass remains constant until 200 °C, then hemicellulose and cellulose start to decompose and in the range between 200 °C and 400 °C almost the 70 % in weight of the mass is lost. The decomposition of lignin is slower and involves a wider range of temperatures, from 300 °C to 700-800 °C: the green line in fact keeps on decreasing above 400 °C, but slower than before, the slope of the curve is less steep. The char yield at the end of the process, when the temperature is 1000 °C, is about 10 % of the initial weight (see figure 6.1).

From the DTG curve of figure 6.1 we can observe that the temperature of the first peak is about 280 °C and it represents the decomposition of hemicellulose. Normally it decomposes in the range between 250 °C and 300 °C, as mentioned in section 1.3.1.

The second peak is higher, it is at 343 °C and represents the decomposition of cellulose. It is in accord to what said earlier: the temperature range should be 300 – 450 °C. With TA Universal Analysis software, it is also possible to integrate the peak and see how much the amount of materials is decomposed. The hemicellulose and cellulose's content is about 60% (even if in the range 200-400°C a part of lignin started its degradation too).
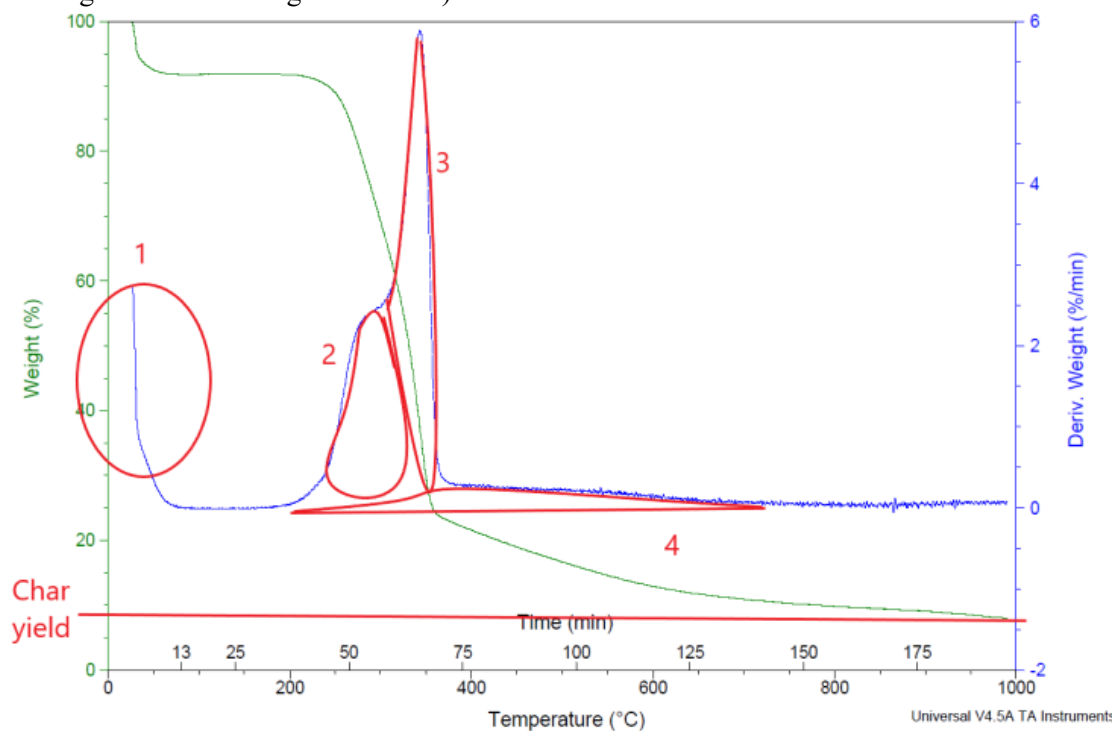
Figure 6.1 TGA and DTG curves of figure 5.7. The char yield is shown on the y-axis on the left. The highlighted regions correspond to (1) moisture loss, (2) decomposition of hemicellulose, (3) decomposition of cellulose, (4) wider range of decomposition of lignin.

We will see later that the char yield of the pelleted biochar is higher than the one shown in the figure 6.1. The value obtained with TGA analysis is lower than that of the pyrolysis with the furnace because different heating rates were adopted: lower heating rates lead to an increase of the char yield. Another cause may be the compression of the sawdust before pyrolysis. The compression leads to a more uniform structure and the components are less free to leave the structure compared to the case in which the particles are simply put on the platinum pan. In the latter, the sawdust particles have a higher surface area, that means better heat adsorption. Moreover, the char yield calculated after pyrolysis process, will be more reliable because sometime, at the end of the ramp temperature during TGA analysis, the low amount of material left on the pan could be blown down by the argon flow. Furthermore, among lignocellulosic components, lignin is the most responsible for the char yield. We will see that the char yield of the biochar from pellets with added lignin is much higher than the others.

To highlight the different thermal decomposition of treated sawdust compared to that of figure 6.1, TGA analysis on a sample of pre-treated sawdust has been done. Following the same procedure, a sample of sawdust after 2-hour pre-treatment has been placed on a platinum pan. The heating methodology chosen is the same: 5 °C/min from room temperature (~ 22 °C) up to 1000 °C.
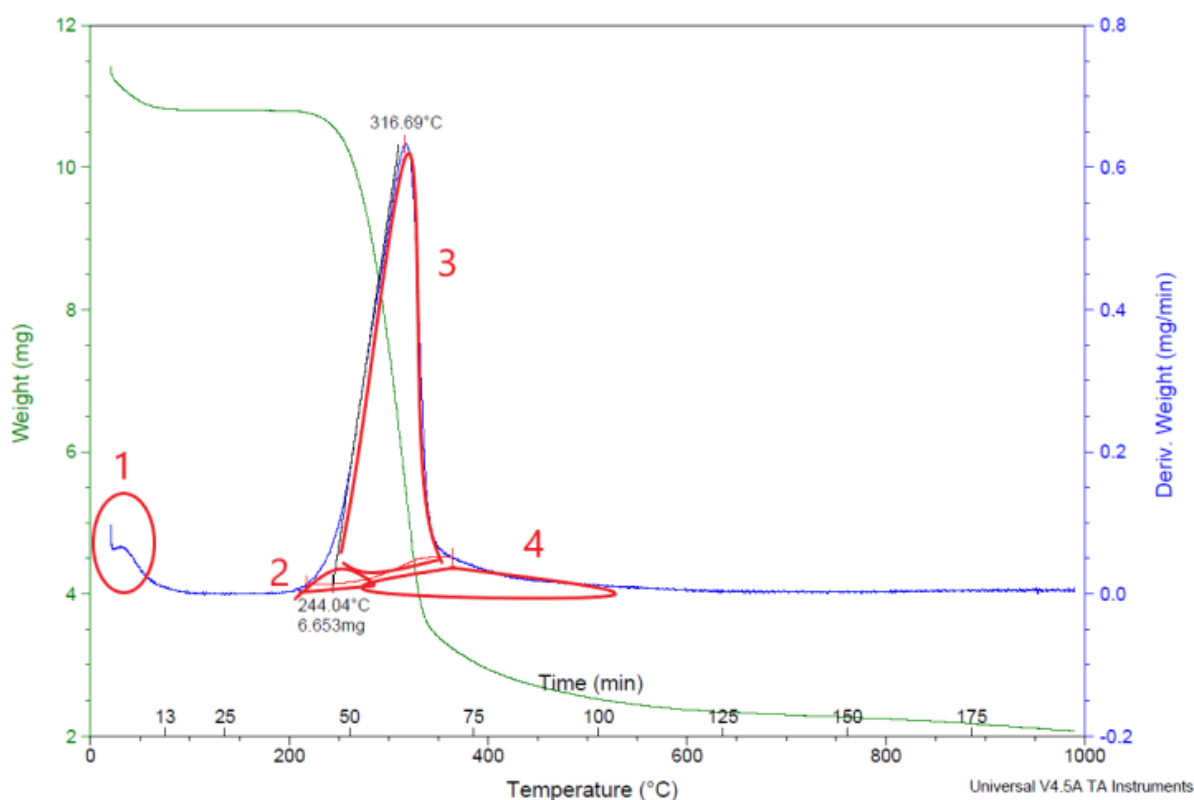
Figure 6.2 TGA analysis of a 2-hour pre-treated sawdust sample. The green line is the TGA curve and the blue line is the DTG curve, differential thermogravimetric spectra. The highlighted regions correspond to (1) moisture loss, decomposition of (2) hemicellulose, (3) cellulose and (4) lignin.

In figure 6.2 it is possible to notice the absence of the hemicellulose peak. The chemical pre-treatment has removed a certain amount of hemicellulose and lignin and maybe, the actual hemicellulose content is not enough to give rise to a distinct peak, but its decomposition is overlapping with that of cellulose. The region of lignin decomposition is smaller than the previous one and the range of decomposition is between 300 and 700-800°C. After 700°C the green line is still decreasing but it is almost flat. The cellulose peak is very similar to the one in figure 6.1: the shape of the peak is the same, but the highest point is reached at a lower temperature than the previous. Here the cellulose peak is at 317°C. It is still

in the typical range of cellulose decomposition (300-450°C) but the value is lower. This could be another consequence of the partial removal of hemicellulose: the two decomposition steps are overlapping each other, and the peak temperature is a value in the middle of the two peaks of figure 6.1.

6.1.2 Removal of lignin

The amount of cellulose and acid insoluble lignin (AIL) in the untreated and treated sawdust is shown in table 6.1.

Table 6.1 Results of analysis on untreated and treated sawdust

	Cellulose [wt%]	Acid insoluble lignin [wt%]	Ash [wt%]
Feedstock untreated	37.9±0.6	31.4±0.8	1.05±0.6
Feedstock treated	53.1±1.8	13.7±1.3	0.79±0.01

Normally the content of soluble lignin in hardwoods as sugar maple is about 3 to 5% (wt%).
According to the figure 6.1 we can say that the moisture content of the feedstock was about 8%, the total content of cellulose and hemicellulose was about 60% (the cellulose was almost 38% of the total weight), the lignin content is a slightly higher than 32% if we consider also the soluble lignin and the ashes are 1% (wt%).
The amount of lignin in the sawdust decreased from 31% (wt%) in the untreated sawdust to 14% (wt%) in the treated one. The 2-hour pre-treatment have removed more than the 50% of the lignin contained in the original feedstock.
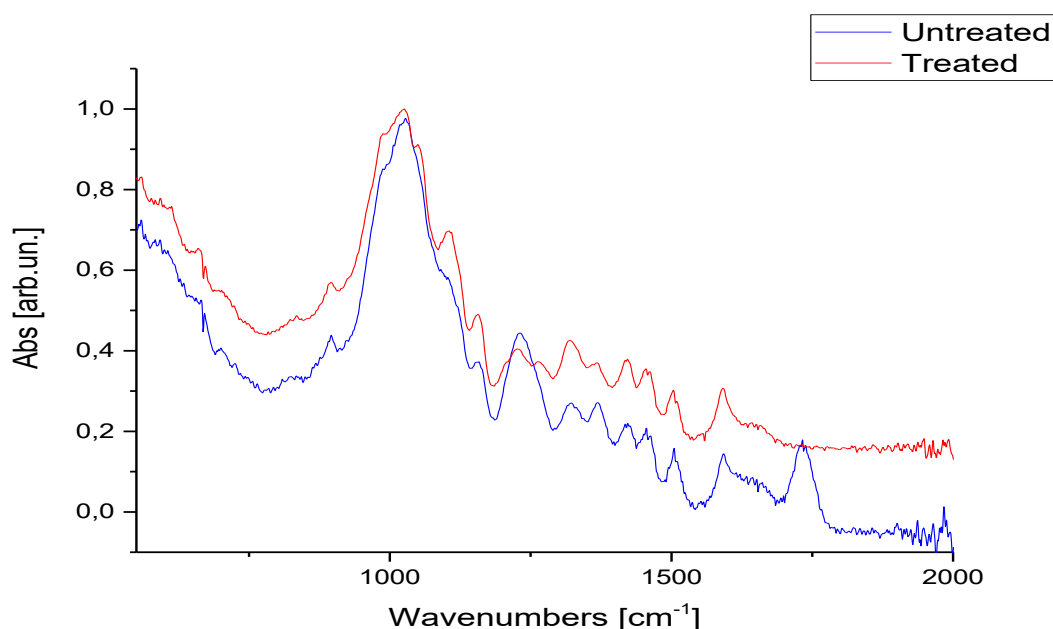
Figure 6.3 IR spectra of untreated and treated sawdust. The blue curve is the spectra of untreated sawdust, the red one is the spectra of treated sawdust.

Figure 6.3 gives the IR spectra of untreated and treated sawdust. The two spectra are very similar, apart from the peak at 1729 cm^{-1}. This signal represents the stretching of the bond C=C, typical functional

group of the aromatic rings in the lignin structure. Looking at the red spectra we can notice that the peak is completely disappeared: this is another proof of the fact that the pre-treatment had removed a large quantity of lignin from the original feedstock.

6.2 Pellets properties

Table 6.2 is an example of mass, dimensions and density values of one set of samples.

Table 6.2 Mass, thickness, volume and density values of one set of pellets. The diameter is 2 cm for each pellet, since is the same of the mould cavity.

Pressure (psi)	Mass (g)	Thickness (cm)	Volume (cm^3)	Density (g/cm^3)
500	1.471	0.520	1.634	0.90
1000	1.435	0.435	1.367	1.05
1500	1.433	0.400	1.257	1.14
2000	1.444	0.385	1.209	1.19
2500	1.453	0.375	1.178	1.23
3000	1.449	0.365	1.147	1.26

From table 6.2 it is possible to compare thickness, volume and density of pellets produced at different pressures, since the masses are very similar to each other. As the pressure increases, the thickness decreases. Since the diameter is constant, the volume is decreasing, and the density is increasing.

Seven sets of pellets were made from treated sawdust. The density results were plotted as a function of the pressure applied during the pellets production in figure 6.4.
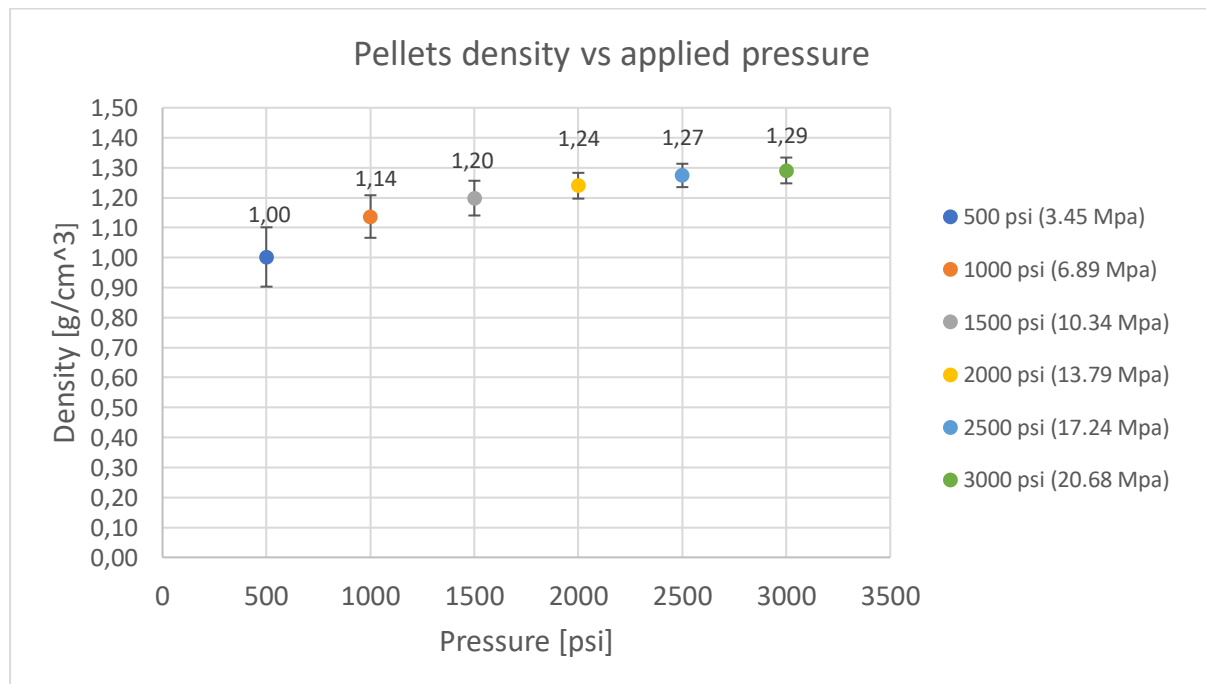
Figure 6.4 Density of pellets made from treated sawdust plotted as function of pressure applied during the compression. The densities shown in the graph are an arithmetic mean based on 7 values and the error bar is the standard deviation.

Figure 6.4 shows how the density of the pellets made from treated sawdust changes as the applied pressure increases. As expected, the density increases as the pressure increases, from 1.00 to 1.29 g/cm^3. Even at the lowest pressure (500 psi or 3.45 MPa), the resulting density is much higher than that of dry sugar maple wood ($\approx$ 0.7 g/cm^3). The values of figure 6.3 are an arithmetic mean based on the densities of the seven sets. Standard deviation has been calculated and it is possible to notice that it is higher when the pressures are lower. Applying higher pressure makes the density value more repeatable. Even though the step increase in the applied pressure is always the same (500 psi), the increase in density tends to decrease as the pressure increases. The increase in density is attributed to the elimination of void between and within sawdust particles. Increasing the pressure, the density would achieve an asymptote and approach a constant.

Figure 6.5 shows the increase of density with pressure of two sets of pellets made with treated sawdust and added lignin (10% and 20%).
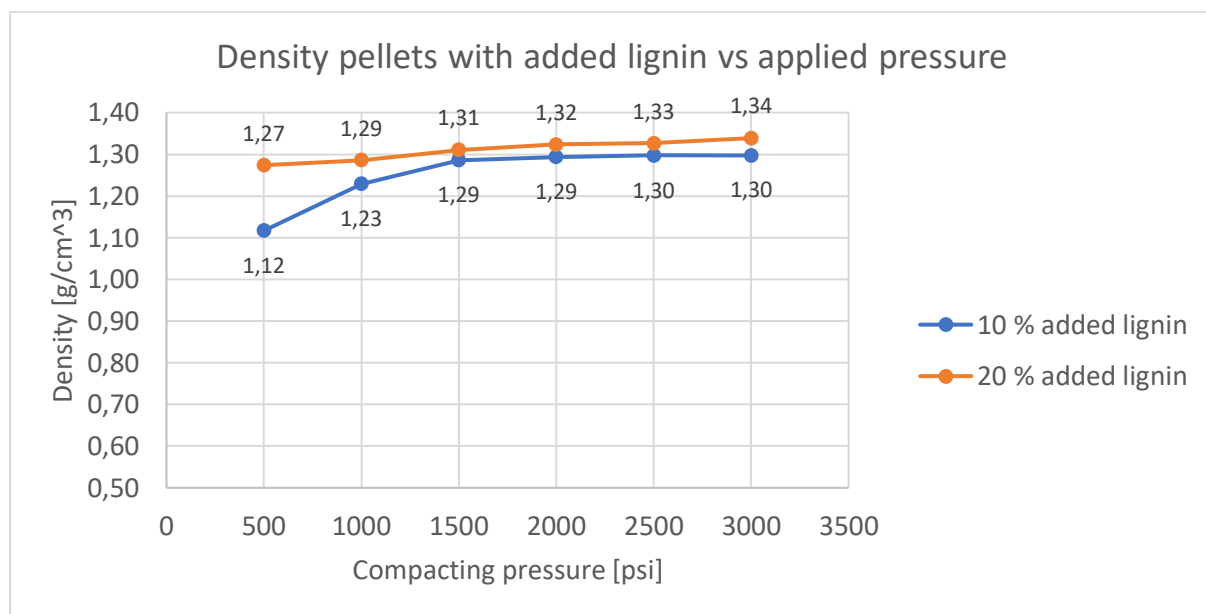
Figure 6.5 Density of pellets with added lignin plotted as a function of the pressure applied during the compression. The blue curve is for the set of samples with 10 % (of the total weight) of added lignin. The orange curve is for the set of samples with 20 % of added lignin.

The density trend of figure 6.5 is very similar to that of the figure 6.4. Density increases as the applied pressure increases. However, the values in this case are higher than those of figure 6.4, especially those obtained at lowest pressures. The density obtained now at 500 psi has the same value of the pellet density at 2500 psi in the case without added lignin. Comparing figure 6.4 (case with 0% of added lignin) and figure 6.5 (10% and 20% of added lignin), we can notice that the range of values increases from 1.00-1.29 to 1.12-1.34 g/cm^3. The difference in density increasing the pressure are less evident than the case of figure 6.4. Moreover, the densities of the samples with 20% of added lignin are higher than those with 10% of added lignin. In pellets made from treated sawdust, the added lignin may act as smaller particles. Smaller particles can make a pellet denser. The added lignin may act as a binder when biochar monolith is formed during pyrolysis at higher temperature.

To better understand the importance of the partial removal of lignin on the compression and therefore on the final pellet density, see the figure 6.6. It shows the dependence of briquettes density from oak sawdust (hardwood as sugar maple) from compacting pressure by various temperatures. It is taken from ref. [62] in which the optimal conditions for valuation of sawdust by briquetting were studied. The moisture content (10 %) and the particle size were very close to those adopted in this work. If we focus on the curve of the densities at 100 °C, the same temperature adopted in this work, we can notice that the maximum density obtained is close to 0.9 g/cm^3 and it is reached applying 191 MPa. In this work a density of 1.3 g/cm^3 has been obtained in the same conditions, applying 20.68 MPa. This comparison is very useful to highlight how much the lignin removal is a key point in this research. It makes the density improve a lot, without applying very high pressures, that would be uneconomic in the point of view of production technology.
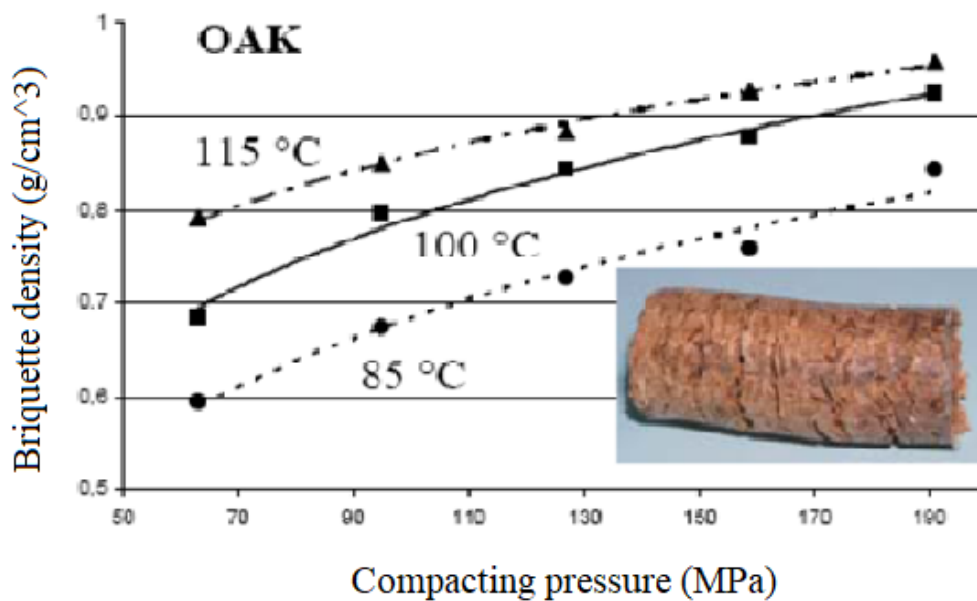
Figure 6.6 Dependence of briquettes density from oak sawdust from compacting pressure by various temperatures. From ref. [62].

6.3 Biochar properties and their dependence on pyrolysis conditions

After each pyrolysis, mass, thickness and diameter of the samples were measured and volume, density, axial and radial shrinkage were calculated.
The most important values will be reported and discussed.

6.3.1 General trend of char yield and density decrease

Pyrolysis condition n.1:

Table 6.3 Biochar characteristics of set n.1.

Pressure (psi)	Char Yield (%)	Axial shrinkage (%)	Radial shrinkage (%)	Volume loss (%)
500	27%	28%	26%	60%
1000	28%	29%	26%	61%
1500	28%	29%	26%	61%
2000	27%	31%	26%	62%
2500	27%	34%	26%	64%
3000	27%	32%	27%	63%

From table 6.3 we can notice that the values don't change a lot as the pressure applied during the pellets production increases. The char yield is the same of that of monolithic biochar from wood pieces. In ref. [33] and [63] we can find the same values of char yield. They are works conducted in the Green Technologies Lab previously: the char yield of monolithic biochar is always in the range 26-29%. In particular in ref. [63] we can find the char yield values of biochar from sugar maple obtained with the same pyrolysis conditions: its value is 26.4%. The char yield depends on the type of feedstock (when the source is wood the value is basically the same) and on pyrolysis conditions. Looking at the table we can notice that the axial shrinkage is slightly higher than the radial shrinkage: this leads to the hypothesis that there could be a preferential orientation in the structure. The reduction of the structure is anisotropic. This is an interesting result since in the case of monolithic biochar from wood pieces, the axial shrinkage is significantly lower than that in the cross section of the sample [63]. A possible explanation is that the application of pressure during pellets production, leads to a preferential orientation of the fibers, oriented along the radial direction (perpendicular to the direction of applied pressure): during the carbonization, cellulose and hemicellulose decompose and release products by shrinking the cell walls. The data show that increasing the applied pressure, the axial shrinkage increases slightly.
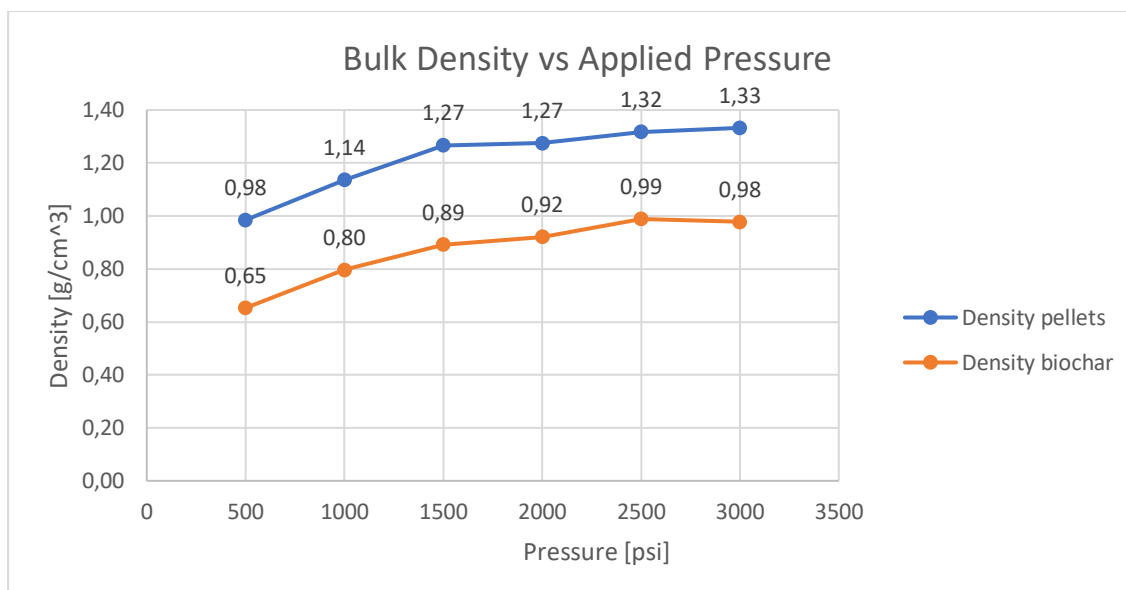
Figure 6.7 Comparison between pellets density and biochar density for set n.1.

In figure 6.7 the densities of pellets and biochar are shown. We can notice that the trend is maintained after pyrolysis. The bulk density of biochar is lower than its precursor because the mass loss prevails over the shrinkage: the mass decreases more than the volume. The density after pyrolysis is about the 70% of the initial pellet density. However, the values of biochar bulk density are higher than those of the biochar obtained from wood pieces. In ref. [63] the biochar density from sugar maple obtained at the same pyrolysis conditions was 0.552 g/cm³.

6.3.2 Effect of holding time at HTT

To study the effect of holding time at the HTT of 1000°C, we can compare the sets n.1 and n.2. Set n.1 was produced with a holding time of 6 minutes while set n.2 with 1 hour.

Table 6.4 Biochar characteristics of set n.2

Pressure (psi)	Char Yield (%)	Axial shrinkage (%)	Radial shrinkage (%)	Volume loss (%)
500	27%	29%	25%	60%
1000	28%	26%	25%	58%
1500	28%	30%	25%	61%
2000	28%	29%	25%	60%
2500	27%	28%	25%	60%
3000	27%	29%	26%	61%

Comparing tables 6.3 and 6.4 we can notice that the values are almost the same. There is no evidence of the effect of the holding time at 1000°C on the char yield and on the shrinkages. We can say that the axial and radial shrinkages seem to be slightly lower when the holding time is longer. The char yields are the same for all the samples (without added lignin).
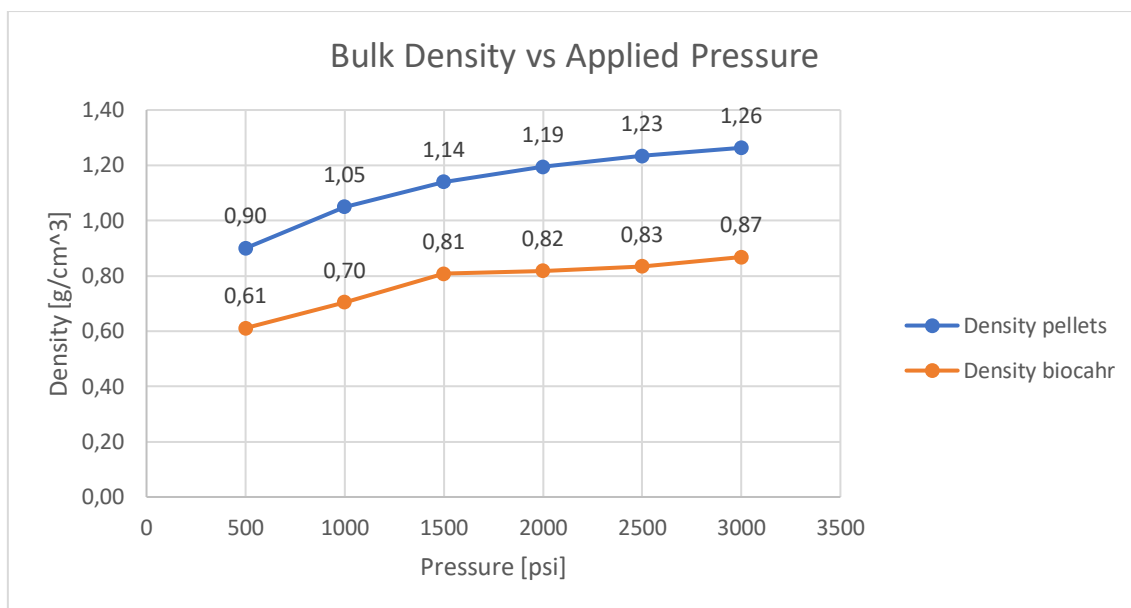
Figure 6.8 Comparison between pellets density and biochar density for set n.2.

Looking at the figure 6.8 we can notice that there is a decrease in density when the pellets were pyrolyzed. The density of the biochar is, on average, about the 68% of the values of the initial density of the pellets.

6.3.3 Effect of heating rate

A comparison among pyrolysis conditions n.2, 3 and 4 has been done to study the effect of the heating rate on biochar properties. The radial shrinkage has not been reported since the values are the same for the three conditions and they are equal to those of table 6.4.

Table 6.5 Comparison of axial shrinkage between pyrolysis conditions n.2, 4 and 3

	n.2: slow pyrolysis + 1 hr @1000°C	n.4: 1°C/min + 1 hr @1000°C	n.3: 2°C/min + 1 hr @1000°C
Pressure (psi)	Axial shrinkage (%)	Axial shrinkage (%)	Axial shrinkage (%)
500	29%	23%	27%
1000	26%	23%	26%
1500	30%	26%	27%
2000	29%	24%	23%
2500	28%	24%	25%
3000	29%	24%	23%

From table 6.5 we can notice that in the case of slow pyrolysis the axial shrinkage is slightly higher than in the cases in which a higher heating rate has been chosen. Since the holding time at the HTT is the same, we can say that the heating rate could affect the shrinkage.

6.3.4 Effect of HTT

Increasing the HTT, the dependence showed in section 6.3.3 changes: in fact, keeping constant the heating rate at 1°C/min but increasing the HTT from 1000 to 1200°C, the axial shrinkage increases again, and it is higher than the radial one. In table 6.6 axial and radial shrinkage of the pyrolysis conditions n.5 and 6 are shown. The heating rate is 1°C/min and the holding time is 6 hours at 1000°C and one hour at 1200°C. In this case the axial shrinkage is higher than the radial one. We can notice that the radial shrinkage is not affected by the increase of HTT as the axial shrinkage.

Table 6.6 Axial and radial shrinkage of samples under pyrolysis conditions n.5 and n.6

Pressure (psi)	n.5: 1°C/min + 6 hr @1000°C		n.6: 1°C/min + 6 hr @1000°C + 1 hr @1200°C	
	Axial shrinkage (%)	Radial shrinkage (%)	Axial shrinkage (%)	Radial shrinkage (%)
500	16%	25%	31%	25%
1000	23%	26%	30%	25%
1500	25%	26%	32%	25%
2000	24%	26%	30%	26%
2500	24%	26%	31%	25%
3000	24%	27%	33%	25%

In figure 6.9 the densities of pellets and biochar of set n.6 are shown. As we can see the trend is the same and it is like that of figure 6.7 and 6.8. The different pyrolysis conditions don't affect the density of biochar since the char yield and the volume loss are almost the same.
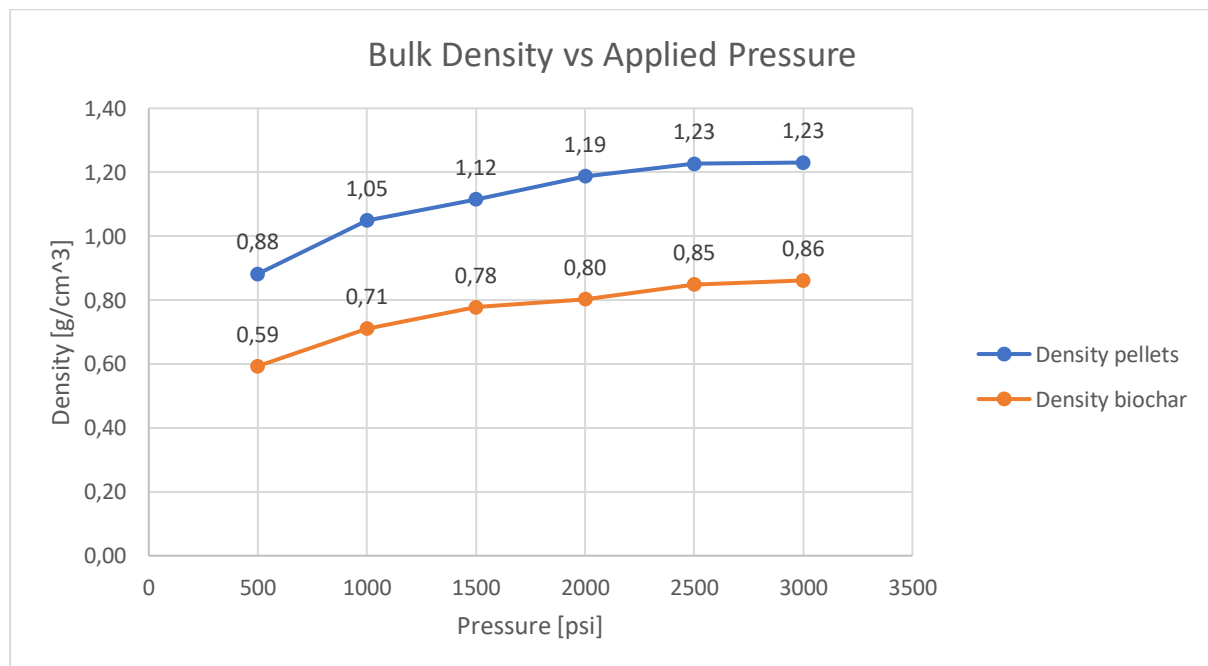
Figure 6.9 Comparison between pellets density and biochar density for set n.6.

The carbon yield was calculated for the set n. 5 and 6. Assuming that the carbon content of the feedstock was 50% (wt%) and knowing from elemental analysis (see tables 6.10 and 6.11) the carbon content of the biochar, the carbon yield was calculated. It represents how much carbon of the original sawdust was preserved in the final biochar structure. The values are very similar to each other and they do not depend

on the pressure applied. For the set n.5 the average was 48.8 % while for the set n.6 was 49.8 %. Half of the carbon was preserved in the biochar structure.

6.3.5 Effect of added lignin

For the samples produced adding lignin the values are slightly different.

Table 6.7 Biochar characteristics of set of samples with 20% added lignin with pyrolysis condition n.5.

Pressure (psi)	Char Yield (%)	Axial shrinkage (%)	Radial shrinkage (%)	Volume loss (%)
500	29%	36%	26%	65%
1000	29%	33%	26%	63%
1500	29%	33%	26%	63%
2000	29%	35%	26%	64%
2500	30%	32%	26%	63%
3000	29%	33%	26%	63%

As we can see from table 6.7, the char yield is higher than in previous cases: among lignocellulosic components, lignin is the most responsible for the char yield because its decomposition, compared to those of cellulose and hemicellulose, leaves a larger amount of residue at the end of pyrolysis as we saw in figure 1.13, ref. [23, 10]. The radial shrinkage is the same, but the addition of lignin leads to higher values of axial shrinkage. Since the volume loss is the same of that of sample without lignin, but the char yield is higher, the difference between the density before and after pyrolysis is less huge than before. The density after pyrolysis is about 80% of the pellets' density (see figure 6.10). Adding lignin made both sawdust and biochar monoliths denser. This effect is particular significant for samples made under lower pressures. A likely reason is the finer particle size of added lignin that made the pellets more compact.
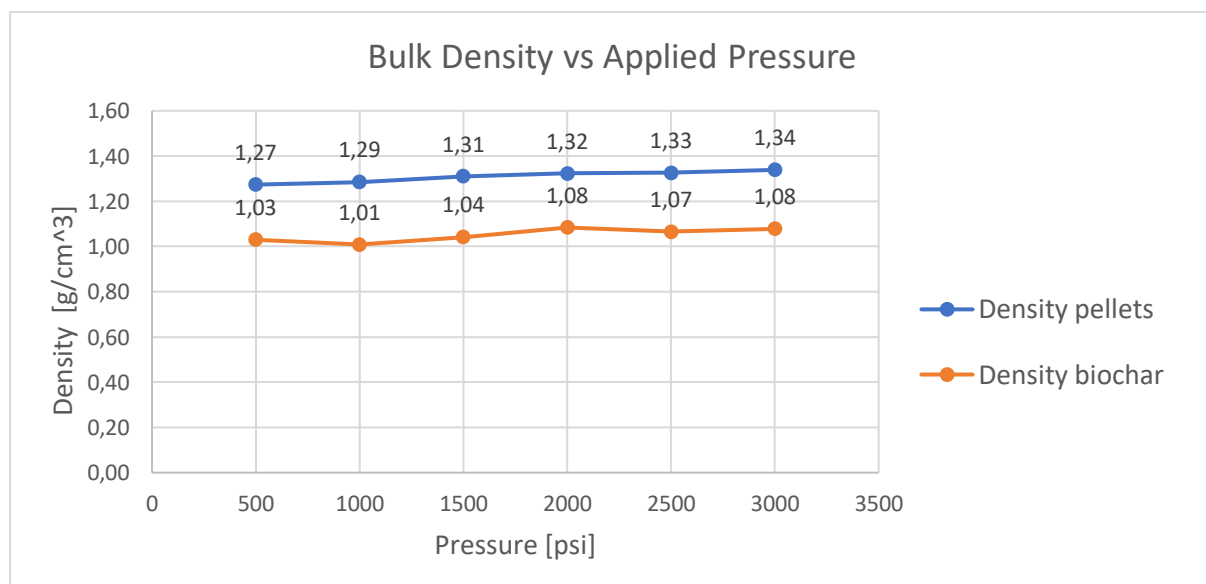
Figure 6.10 Comparison between pellets density and biochar density for samples with 20% added lignin (pyrolysis conditions n.5).

6.4 Electrical conductivity

Now electrical conductivity results will be discussed. Only the most interesting results will be shown. We will se the effects of holding time, heating rate, HTT and pressure on the electrical conductivity of biochar samples. The electrical conductivity will be plotted as a function of sample density, not pressure, since the density is a property of the material.

As mentioned earlier, the electrical conductivity could be reported as bulk or skeletal. Bulk conductivity is the conductivity that takes into account the fact the biochar structure is made up by solid biocarbon and void (air), while the skeletal conductivity represents the conductivity of the volume fraction of biocarbon in the structure.
In figure 6.11 the bulk conductivity of set n.1 plotted as a function of bulk density of biochar is reported as example. In this section all the values reported will be values of skeletal conductivity, which represents the effective electrical conductivity of the material.
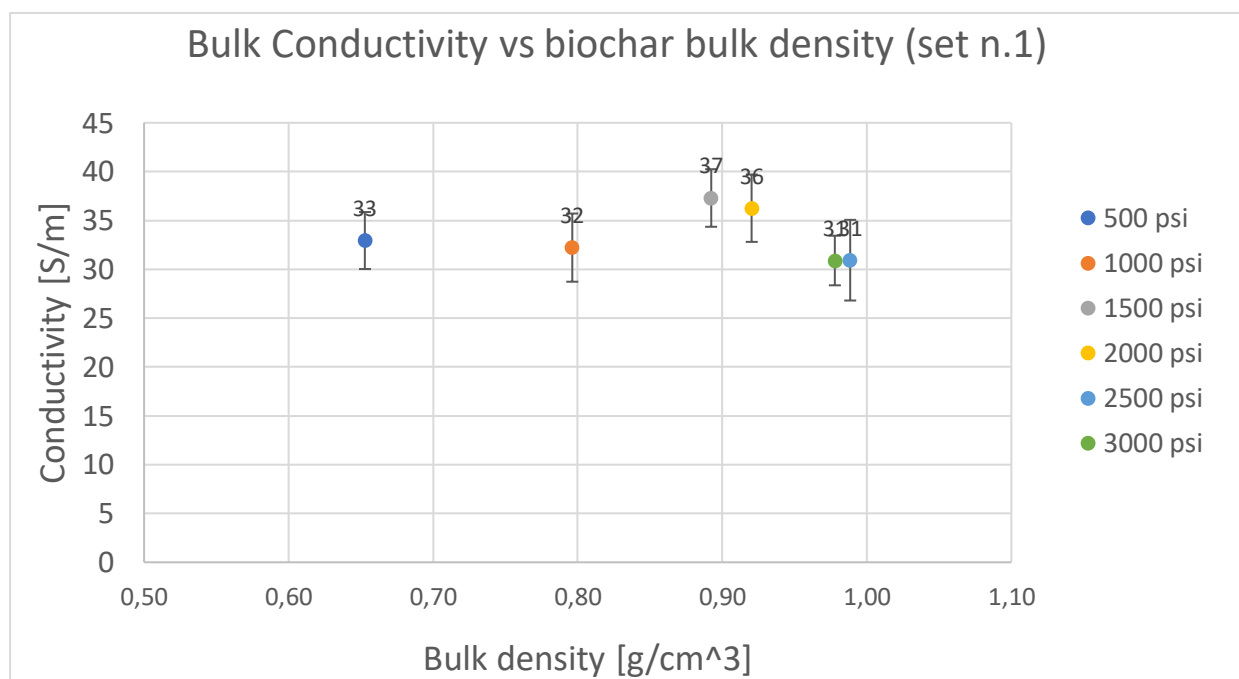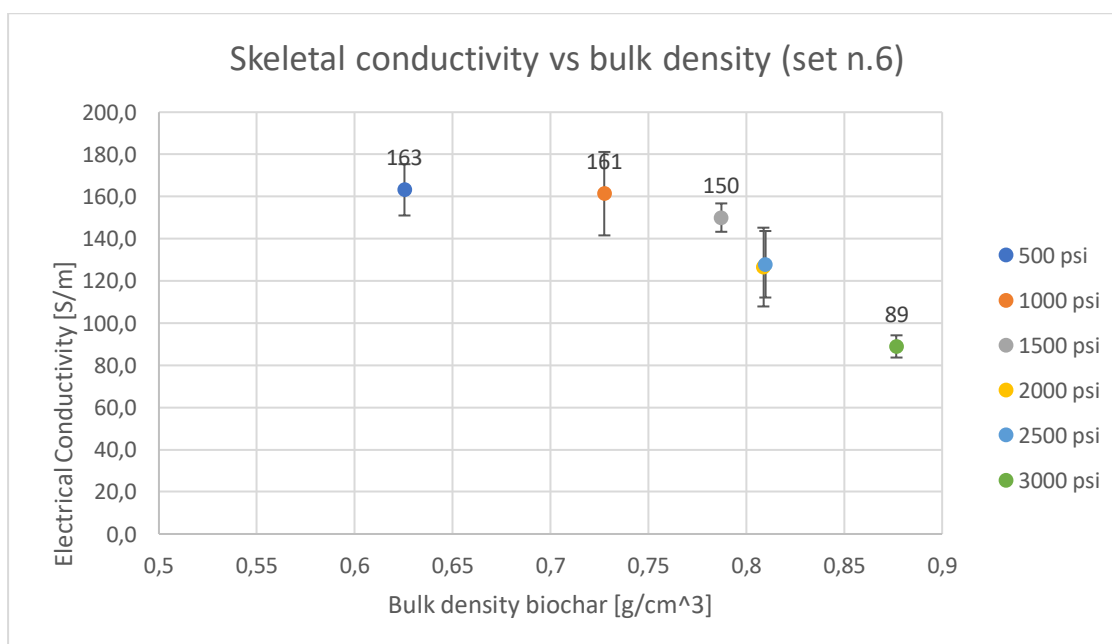

Figure 6.11 Bulk conductivity of set n.1 plotted as a function of bulk density of biochar. Different colours are referred to different pressures applied during the compression.

Given the uncertainty in the measurements, the dependence of bulk conductivity on bulk density is weak. If skeletal conductivity is a constant, bulk conductivity should increase with density, as void fraction decreases when density increases. This result, however, suggests that the skeletal conductivity of biochar particles is not a constant and there may be a decrease in skeletal conductivity with the increase in applied pressure. This is consistent with the results that follow.

6.4.1 Effect of holding time at HTT

To study the effect of holding time on the electrical conductivity, a comparison between set n.1 and 2 and between n.4 and 5 will be done. In figures 6.12-6.15 the skeletal conductivity is plotted as a function of the bulk density of the samples. The values are an arithmetic means based on 5 measurements and they are referred to the first two-point method set-up. A copper weight of 230 gr is applied during the measurements, it corresponds to about 12,8 kPa.

Set n.1 is obtained with the slow pyrolysis schedule adopted by the researchers of the Green Technologies Lab while set n.2 is obtained with the same heating schedule adding a holding time of one hour at 1000 °C.
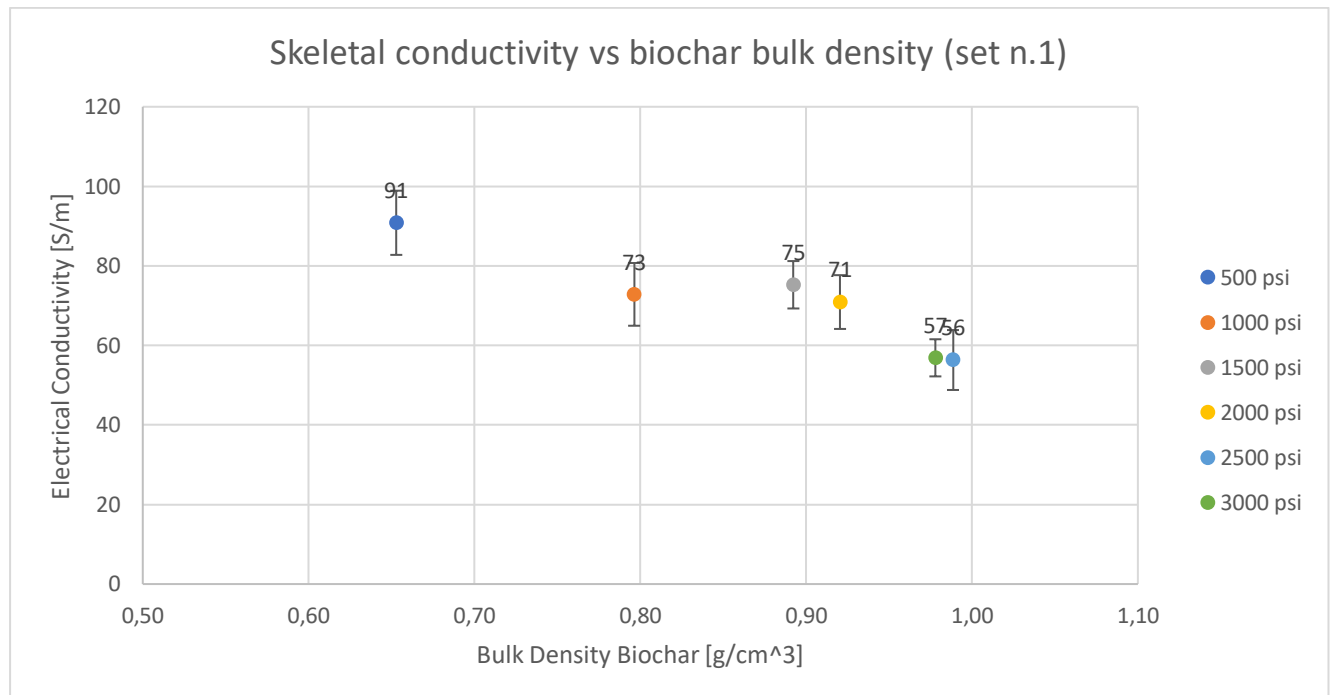
Figure 6.12 Skeletal conductivity of set n.1 plotted as a function of bulk density of biochar. Different colours are referred to different pressures applied during the compression.

As we can see from figure 6.12, the values of electrical conductivity are already in the range of values belonged to conductor materials. We can compare the values of electrical conductivity with the values obtained from sugar maple wood (monolithic pieces) that underwent the same pyrolysis conditions. The values come from some works of a student who works in the Green Technologies Lab. The electrical conductivity in the axial direction was about 1233 S/m, more than ten times higher. Biochar from monolithic pieces of wood is more conductive than that obtained by compressed sawdust.
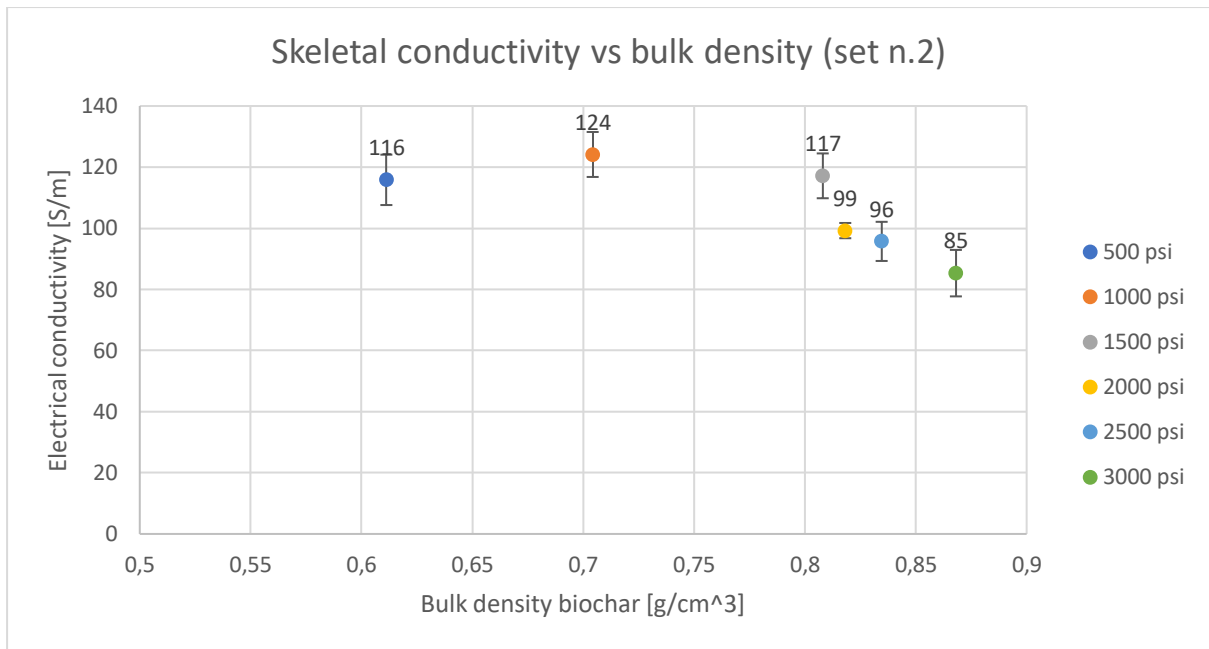
Figure 6.13 Skeletal conductivity of set n.2 plotted as a function of bulk density of biochar. Different colours are referred to different pressures applied during the compression.

If we compare figure 6.12 and 6.13 we can observe that the trend is the same: as the applied pressure (and bulk density) increases, the electrical conductivity decreases. All the values (85-124 S/m) of figure 6.13 are higher than those (56-91 S/m) of figure 6.12 because of the longer holding time. Increasing the holding time from 6 to 60 minutes at 1000 °C allows carbon atoms to form more ordered graphitic structure that is conductive.

Now, we compare holding time of 1 hour (set n.4) and 6 hours (set n.5) at 1000°C, but the heating rate is 1°C/min (faster than the previous comparison).
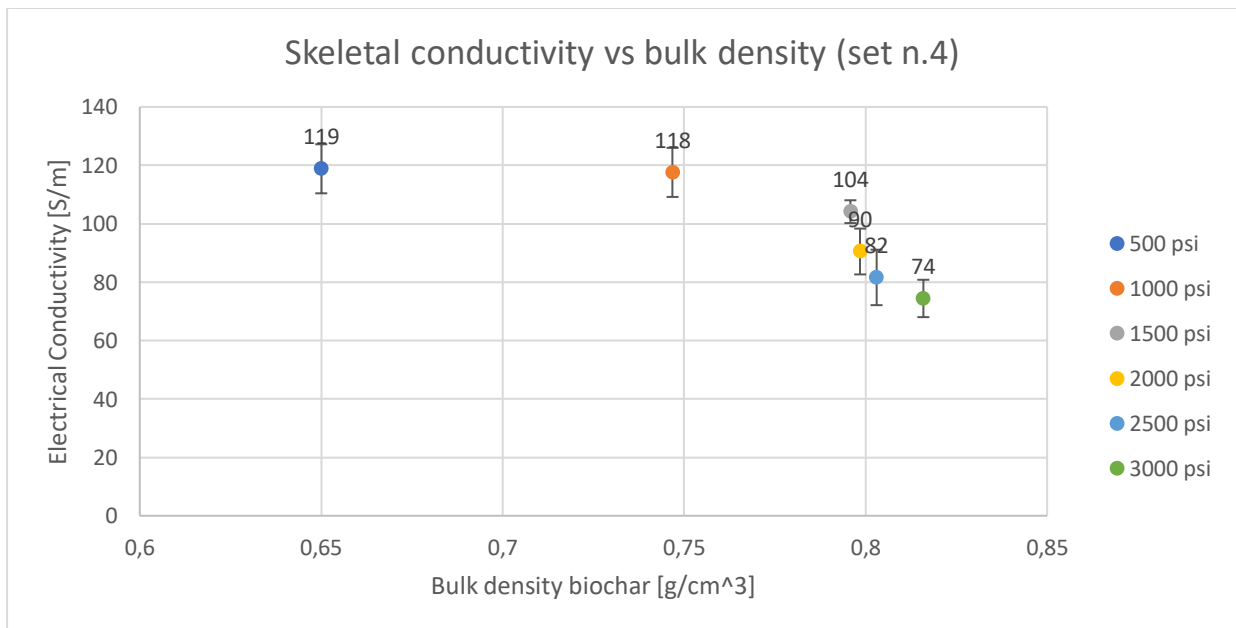
Figure 6.14 Skeletal conductivity of set n.4 plotted as a function of bulk density of biochar. Different colours are referred to different pressures applied during the compression.
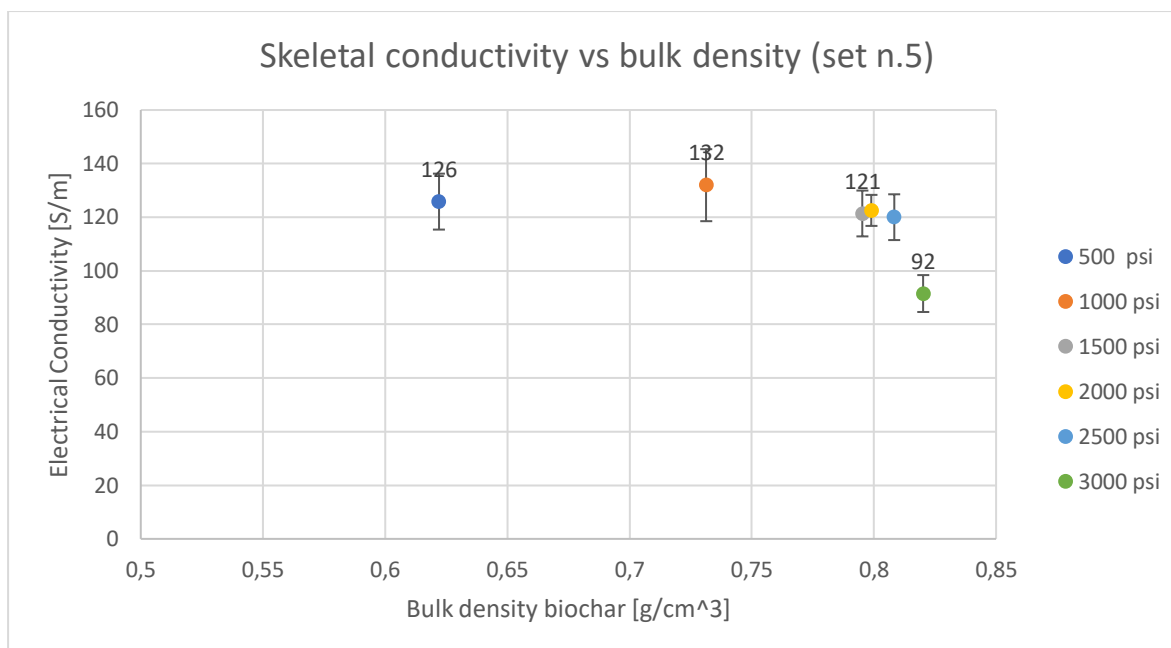
Figure 6.15 Skeletal conductivity of set n.5 plotted as a function of bulk density of biochar. Different colours are referred to different pressures applied during the compression.

Comparing the figures 6.14 and 6.15 we can observe again that the skeletal conductivity increases with holding time at HTT, from 74-119 to 92-132 S/m. The effect of the holding time is more visible in the comparison between 6 minutes and 1 hour than in the one between 1 hour and 6 hours.

6.4.2 Effect of heating rate

To study the effect of the heating rate, we can compare the electrical conductivity values of the set n.2, 3 and 4. The samples of these sets underwent a pyrolysis with the same HTT (1000 °C) and the same holding time (1 hour) but different heating rate. Set n.2 was produced following the heating schedule n.2 with different ramp rates (but always less than 1°C/min). Set n.4 was produced with a heating rate of 1°C/min and set n.3 with 2°C/min.

Let's focus on figures 6.13, 6.14 and 6.16: set n.2, 4 and 3 respectively. The ranges of skeletal conductivity values were 85-124, 74-104 S/m; there seems a decreasing trend with the heating rate. When heating rate increases from a condition of slow pyrolysis to a condition of conventional pyrolysis, biochar products are produced in a shorter period of time and had less time for carbon atoms to organize in a more ordered and conductive structure.
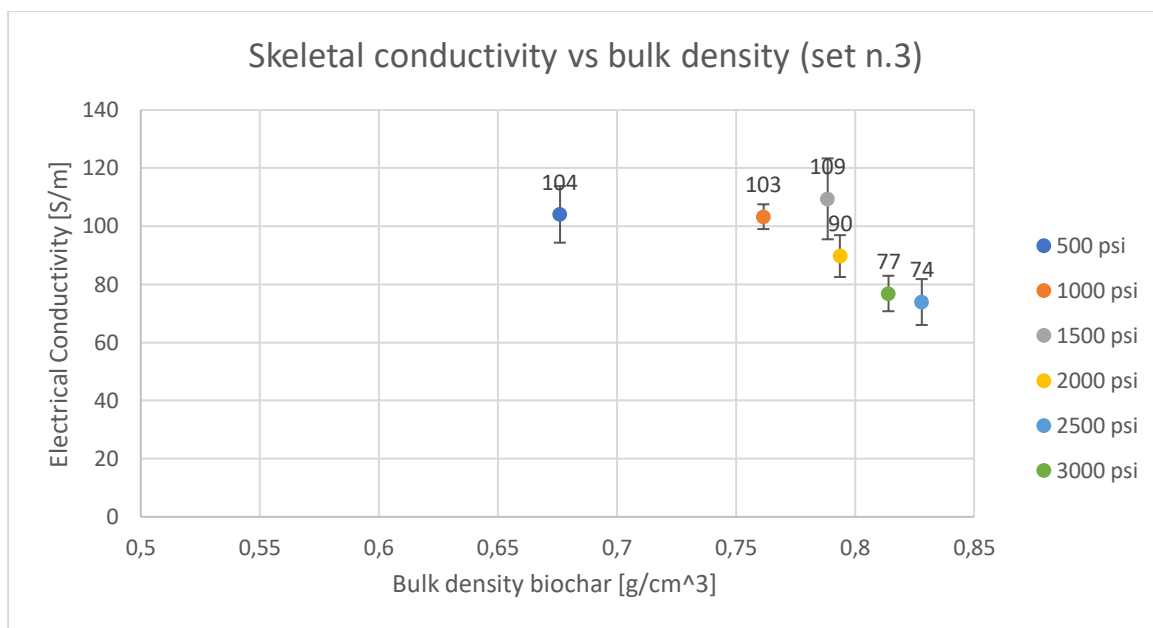
Figure 6.16 Skeletal conductivity of set n.3 plotted as a function of bulk density of biochar. Different colours are referred to different pressures applied during the compression.

6.4.3 Effect of HTT

Now we analyse the most important parameter: as we mentioned earlier, the HTT is the most responsible for the process of carbonization and graphitization. To highlight the effect of the highest treatment temperature, we will compare the set n.5 and 6. Set n.5 underwent a pyrolysis with 1°C/min of heating rate and 6 hours at 1000°C, while set n.6 underwent the same pyrolysis with the addition of an hour of holding time at 1200°C.

Figure 6.17 Skeletal conductivity of set n.6 plotted as a function of bulk density of biochar. Different colours are referred to different pressures applied during the compression.

If we compare the figures 6.15 and 6.17 we can notice that a higher HTT brings to a better electrical conductivity. The range of skeletal conductivity values of samples treated at 1200°C is 89-163 S/m, compared to 92-132 S/m for samples at 1000°C. Increasing the final treatment temperature helps to develop the turbostratic structure, that is more ordered and conductive. We will see in the next section that XRD analysis show that in these samples very small crystallites are present.

The highest skeletal conductivity value obtained at the lowest pressure from this set of samples treated at 1200°C was 163 ± 6 S/m. Another set (n.6bis) underwent the same pyrolysis conditions until 1200°C: the highest value was still obtained at the lowest pressure and it was 176 ± 5 S/m.

The skeletal conductivity measured along the axial direction in monolithic sugar maple wood derived biochar pyrolyzed with an HTT of 1250°C is about 1763 S/m [value taken from another student's work that still have to be published]. It is one order of magnitude higher than the most conductive sawdust-derived biochar monolith. This gap suggests that the connection between individual particles in sawdust-derived biochar monolith may be weak and there may be substantial contact resistance between those particles.

6.4.4 Effect of added lignin

As indicated earlier, adding lignin to the treated sawdust made the pellets and biochar monoliths denser.

Table 6.8 shows skeletal conductivity values of sawdust-derived biochar produced under the same pyrolysis condition (heating schedule n.4) without and with 10 and 20 wt% of lignin. From Table 6.7 the effect of the addition of lignin is clear: increasing the amount of lignin added makes skeletal conductivity lower. This can be explained by the fact that among lignocellulosic components, lignin is the most amorphous. Cellulose has an ordered structure and its presence favours the formation of graphite crystallites, while the presence of lignin confers to biochar a more amorphous and less conductive structure. Consequently, in the treated-sawdust added-lignin-derived biochar monolith, there are two biochar particles – sawdust-derived and lignin-derived particles. The sawdust-derived particles are larger in size and more conductive than the lignin-derived. When small lignin-derived can make the monolith dense and improve particle contact, they can lower the conductivity. It is interesting that the first 10% lignin has a smaller effect on conductivity than the second 20%. This may be due to fact that adding small amount of lignin makes the biochar denser and therefore a tighter packing of biochar particles in the monolith.

Table 6.8 Electrical conductivity values for the same pyrolysis heating schedule (n.4) for three different sets: without lignin and with the addition of 10% and 20% (wt%) of lignin.

Pressure applied	No added lignin [S/m]	10% (wt%) of lignin [S/m]	20% (wt%) of lignin [S/m]
500 psi	118.8 ± 4.2	115.9 ± 7.5	52.2 ± 2.1
1000 psi	117.6 ± 4.5	99.5 ± 7.6	87.9 ± 4.1
1500 psi	104.1 ± 1.9	84.2 ± 7.8	70.6 ± 2.8
2000 psi	90.5 ± 3.9	88.5 ± 7.9	65.8 ± 1.5
2500 psi	81.6 ± 4.8	79.0 ± 3.8	67.5 ± 3.0
3000 psi	74.4 ± 3.2	75.1 ± 4.0	67.0 ± 2.2

6.4.5 Effect of pressure applied during the measurements

Since the samples do not have a smooth surface, it is difficult to make a good contact between the surface and the tin foil, current collector. In all the previous measurements a weight has been placed on the superior plate of the set-up to improve the contact. The measurements have been repeated with both the set-ups using heavier weights. Apart from 230 gr weight, 347 gr and 460 gr have been used.

In general, increasing the pressure during the measurements leads to an increase of the electrical conductivity, because the contact resistance between the sample and the tin foil is reduced.

However, the conductivity should increase until a certain value, and then starts decreasing because when the applied pressure is too high, it could cause cracks inside the structure and decrease the electrical conductivity. Weights heavier than 460 gr have not been used, because the samples are very fragile, and we noticed that after applying pressure during the measurements, they started disintegrating, leaving some powder residues on the set-up.

We tried also to apply the pressure during the measurements with the Carver mechanical press used for the pellets production: however, at pressures lower than 500 psi the sample was completely disintegrated. The presence of contact resistance will result in under-estimation of conductivity of biochar.

In table 6.9 the electrical conductivity values (measured with the second two-point set-up) of the set n.6 (the most conductive set) are shown. Increasing the pressure applied during the measurements, the electrical conductivity increases.

The work conducted in the Green Technologies Lab of ref. [47], shows that electrical conductivity depends on the effective contact between carbon particles. The closer the particles after expulsion of air from the pores, lesser the void space. The compression may further eliminate the empty space in the internal structure of the biochar, increasing the electrical conductivity. This behaviour was demonstrated for biochar from monolithic pieces of wood. In our case, the increase of pressure may cause the same situation, but at a certain point the structure breaks.

Table 6.9 Electrical conductivity values of set n.6 with different applied pressures during the measurements.

Pressure applied during compression	Bulk density of biochar (g/cm^3)	Electrical conductivity (230 gr ≈ 12.8 kPa)	Electrical conductivity (347 gr ≈ 19.6 kPa)	Electrical conductivity (460 gr ≈ 25.5 kPa)
500 psi	0.625	197.9 ± 5.7	221.8 ± 7.8	264.8 ± 5.4
1000 psi	0.727	173.7 ± 9.4	215.7 ± 10.9	216.4 ± 12.2
1500 psi	0.787	183.4 ± 7.0	200.3 ± 7.5	195.9 ± 1.1
2000 psi	0.809	161.7 ± 7.7	170.7 ± 5.3	185.3 ± 4.3
2500 psi	0.810	168.0 ± 8.4	157.4 ± 9.2	182.7 ± 11.6
3000 psi	0.877	115.2 ± 6.6	118.5 ± 7.1	135.8 ± 6.2

Moreover, we can notice that the values of electrical conductivity obtained in the same conditions (230 gr) with the second two-point set-up are slightly higher compared to the other set-up. All the measurements have been repeated with both the set-up: the trend of the conductivity as a function of the pressure during the compression and the comparisons among different sets are the same, but all the values and the standard deviations are slightly higher. This could be related to the fact that the second set-up relied on two devices: one to supply current and another one to measure the voltage drop. The uncertainty of two devices cause an uncertainty on the final value higher than the first set-up.

6.4.6 Effect of pressure applied during the compression

An interesting observation is the decrease of the electrical conductivity (both bulk and skeletal) of all set of samples with the pressure applied during the pellets' production. As expected, high pressure did result in high bulk density. But, a higher bulk density didn't lead to a higher bulk conductivity. The nine sets of samples have shown the same trend despite changing pyrolysis conditions and adding lignin. In each set the most conductive sample is the one produced at the lowest pressure and the least conductive is the one produced at the highest pressure. In some cases, the least conductive showed an electrical conductivity almost the half of the most conductive. In figure 6.18 the typical trend of the conductivity as a function of pressure is shown.
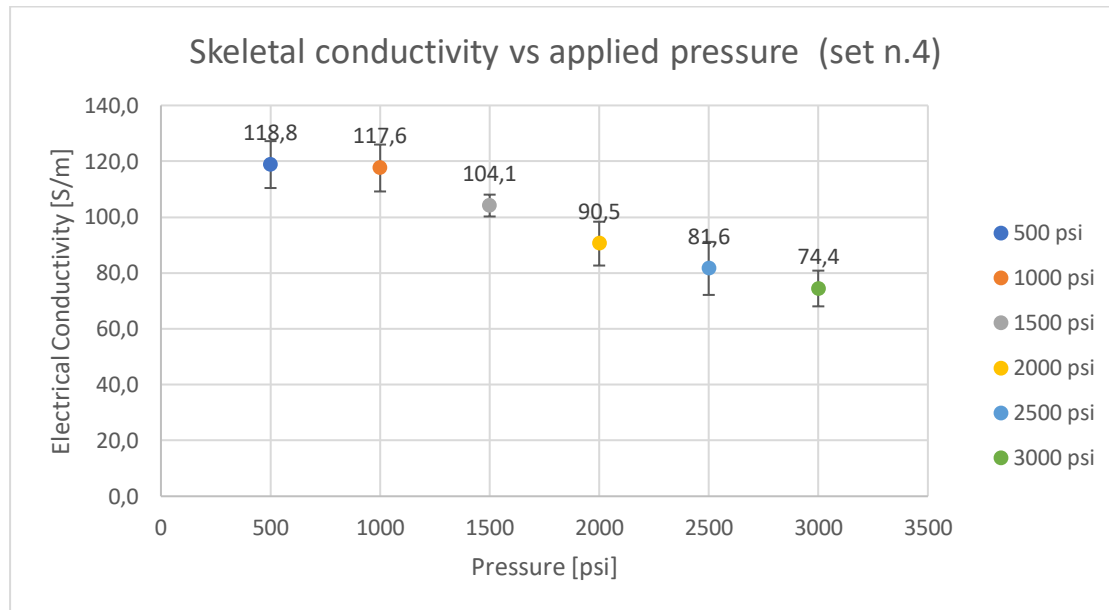
Figure 6.18 Example of dependence of electrical conductivity on applied pressure during pellets' production (set n.4).

The behaviour shown in figure 6.18 is not the one expected. Increasing the compression on sawdust particles should improve the contact among particles, reduce contact resistance and make the biochar monolith more conductive.

Some hypotheses have been formulated to explain this phenomenon. What can be the cause?

1) Degree of carbonization: increasing the pressure during the pellets' production could hinder a good process of carbonization because the volatile products have more difficulties in leaving the structure. We'll see that elemental analysis has denied this hypothesis.
2) Degree of graphitization: increasing the pressure during the pellets' production could hinder the process of graphitization, because sawdust particles are compressed, and this could hinder the development of graphite nano-crystallites in the structure of biochar. We'll see that XRD analysis and Raman spectroscopy have denied this hypothesis.
3) Presence of microcracks in the structure: applying pressure during the pellets' production could induce the formation of cracks in wood particles and therefore in biochar particles. It has been reported that cracks in biochar lower conductivity [1]. Moreover, during pyrolysis, moisture, vapours and gases may have more difficulties in leaving a denser sawdust pellet structure due less pathways available. This could increase the pressure inside the structure and cause the formation of cracks, defects that make the structure less continuous or connected.

4) Presence of moisture: the pellets produced at lower pressures are less dense and this could favour the adsorption of moisture from the environment. The pellets produced at higher pressures are denser and less porous, with a lower possibility of adsorbing moisture. The presence of moisture inside the structure could have the function of "linking" the pyrolyzed particles, favouring the current passing through the sample. We'll see that also this hypothesis has been denied.

5) Contact resistance among particles: increasing the pressure during the pellets' production could make the contact resistance among particles higher. This could explain lower values of electrical conductivity shown by the samples produced at higher pressures. We'll see that also this hypothesis has been denied: from previous works about measuring the electrical conductivity of biochar compressed powders, we'll see that increasing the pressure makes the conductivity increase.

The set n.6, the most conductive, has been placed in the oven at 110°C for 3 hours. The samples have been weighed and electrical conductivity has been measured again. The percentage of mass loss between the mass before and after drying was about 1.3%: the samples did not absorb moisture from the environment. The electrical conductivity values after drying were very similar to the previous values: some values showed a decrease in conductivity of about 1.2% and other samples showed an increase. We cannot explain the electrical conductivity behaviour of the samples with the absorption of the moisture from the environment.

In ref. [64] a study of the electrical conductivity under compression of nanostructured carbon powders is reported. The apparent electrical conductivity of a powder increases as it is compacted due to a greater contact between its components: crystals, particles and grains [64]. In figure 6.19 the apparent electrical conductivity of different carbonaceous powders was measured at different degrees of compaction and in all cases, the conductivity increases with the applied pressure as a result of an apparent density rise.
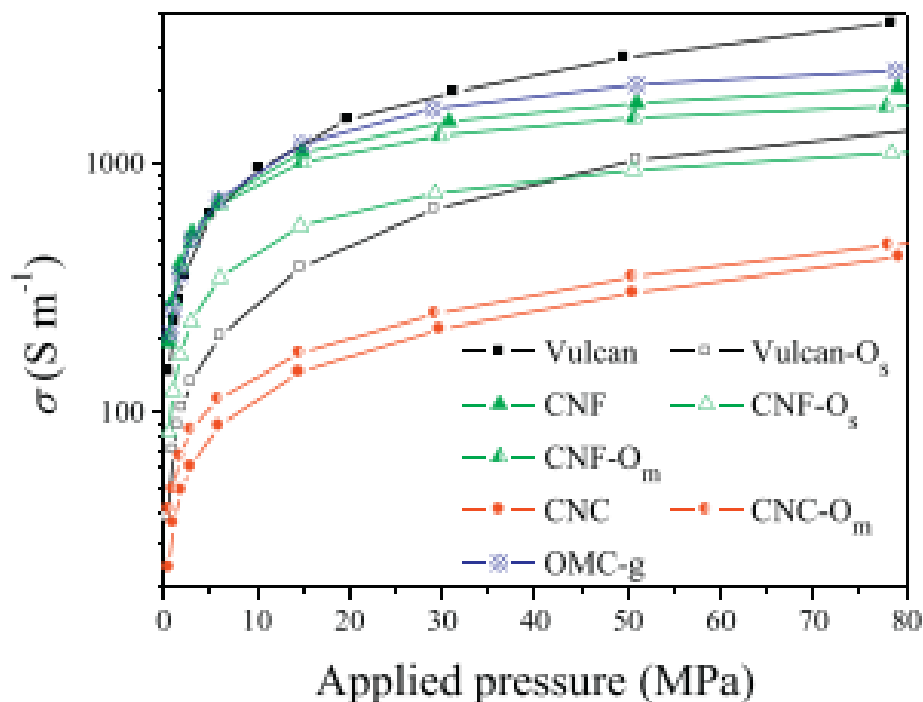
Figure 6.19 Variation of apparent electrical conductivity with applied pressure during the measurements (on powders sample). From ref. [64].

Although the works are completely different, literature shows that electrical conductivity should increase as the particle contact and the density increase. Since the sawdust is compressed before the pyrolysis process, the presence of microcracks could be a possible explanation for this intriguing observation.

6.5 Characterization

In this section the characterization analyses results will be shown and discussed. Furthermore, a deeper explanation of the previous hypotheses will be reported. The characterization of biochar has been done only on the most conductive and the most interesting samples.

6.5.1 Chemical composition

Elemental analysis has been conducted on the last two sets: set n.5 and 6. They are the most conductive samples. The C, H, N content of the twelve biochar samples are presented in table 6.10 and 6.11.

We don't have an uncertainty on the values since the measurements have been taken only once. We cannot consider these values very precise, but we have some information about the degree of carbonization we are interested in.

Table 6.10 Elemental analysis results of biochar samples of set n.5 (pyrolysis conditions: HR: 1°C/min, HTT: 1000°C and holding time: 6 hours)

Sample	%C	%H	%N	H/C	O/C
5.1	92.86	0.14	0.98	$1.51 \cdot 10^{-3}$	0.065
5.2	92.68	0.15	0.97	$1.62 \cdot 10^{-3}$	0.067
5.3	93.38	0.12	0.86	$1.29 \cdot 10^{-3}$	0.060
5.4	88.66	0.08	0.90	$9.02 \cdot 10^{-4}$	0.117
5.5	96.71	0.08	0.87	$8.27 \cdot 10^{-4}$	0.024
5.6	93.06	0.13	0.78	$1.40 \cdot 10^{-3}$	0.065

Table 6.11 Elemental analysis results of biochar samples of set n.6 (pyrolysis conditions: HR: 1°C/min, 6 hours @1000°C, HTT:1200°C, holding time: 1 hour)

Sample	%C	%H	%N	H/C	O/C
6.1	94.39	0.00	0.62	-	0.053
6.2	95.17	0.00	0.54	-	0.045
6.3	94.89	0.00	0.56	-	0.048
6.4	94.54	0.04	0.57	$4.2 \cdot 10^{-4}$	0.051
6.5	94.54	0.00	0.61	-	0.051
6.6	98.09	0.00	0.71	-	0.012

Comparing the tables 6.10 and 6.11 we can notice that the increase of the HTT causes an increment of the carbon content. This is explained by the gradual evaporation and decomposition of heteroatoms from the structure. Increasing the temperature, biomass loses functional groups and C, H, O, N and other elements, progressively aromatises and then polycondenses into a polyaromatic network [65]. When hydrogen, nitrogen and oxygen leave the biochar's matrix, the carbon content and the degree of carbonization increase and the ratios H/C and O/C decrease reaching the zero. The H/C and O/C ratios are used as indicators for the degree of condensation, with high values suggesting a large portion of uncarbonized C [65]. The fact that the set n.6 has a higher degree of carbonization than the set n.5 explains the higher electrical conductivity values of set n.6. Beside its carbon content, another indicator of the degree of carbonization is the ratio H/C: low values of this ratio indicate a high degree of unsaturation (number of bonds C=C) and aromaticity. In set n.6 the ratio is always zero since hydrogen has not been found in the samples through elemental analysis.

The percentage of oxygen has been calculated as the complement to 100 of the other percentages. It's not an exact calculation since small amount of S from the pre-treatment and other elements may be present. However, the O/C ratios provide information about biochar stability and degree of aromatization. The aromatic compounds, with minor oxygen percentage, are more stable. Biochar-C stability increases with the decreasing atomic O/C ratios of biochar [66]. Due to its predominantly aromatic structure, biochar is widely recognized as a relatively stable form of C with long mean residence time ranging from hundreds to thousands of years [66].

Comparing the samples inside a single set, it is not possible to find a relationship between the pressure applied during the compression and the degree of carbonization. The carbon content and the H/C ratios are very similar among the samples of the same set and do not increase or decrease with the pressure applied during the pellets' production. For this reason, the degree of carbonization cannot be the explanation for the observed conductivity decrease with pressure applied or bulk density. The degree

of carbonization depends on the pyrolysis conditions, especially on the HTT, but it is not linked to the pressure applied and the pellets' density.

6.5.2 XRD analysis results

Four samples have been chosen for XRD analysis: the most conductive sample of set n.5 (5.2) and 3 samples of the set n.6 (6.1, 6.3 and 6.6). Since the XRD patterns of the sample have a lot of noise, they will not be reported here. The X-ray diffraction pattern is a plot of the intensity of x-rays scattered at different angles by a sample. The pattern shows the X-ray intensity as a function of the angle 2theta that describes the position of the detector with respect to the sample. The two main peaks in the $2\vartheta = 20\text{-}30°$ and $2\vartheta = 40\text{-}50°$ regions refer to the graphite crystallographic directions {002} and {100}: they are respectively the perpendicular and parallel direction to the graphitic planes [63]. Broad peaks are typical of amorphous carbon structures, while narrow peaks are related to a development of a partial ordered structure with the formation of graphite nanometric crystallites.

Since we would like to use XRD analysis to see if there are some differences in the microstructure of samples produced at different pressures, we calculated the crystal size through the Scherrer equation. The Scherrer equation, in X-ray diffraction and crystallography, is a formula that relates crystallites in a solid to the broadening of a peak in a diffraction pattern.

$$\tau = \frac{K\lambda}{\beta \cos\vartheta} \tag{6.1}$$

Where:

τ is the mean size of the ordered (crystalline) domains;

K is a dimensionless shape factor, with a value close to unity. It has a typical value of about 0.9;

λ is the X-ray wavelength;

β is the line broadening at half the maximum intensity (FWHM);

ϑ is the Bragg angle, half of the 2ϑ mentioned earlier.

Table 6.12 Calculation of crystal size from XRD analysis results.

Sample	2theta (deg)	Theta (rad)	FWHM (deg)	FWHM (rad)	τ (crystal size), Å
5.2 [002]	22.2	0.193	6.231	0.109	13.0
5.2 [100]	42.9	0.374	6.700	0.117	12.7
6.1 [002]	21.7	0.189	6.954	0.121	11.6
6.1 [100]	43.0	0.375	5.600	0.098	15.2
6.3 [002]	22.6	0.197	5.401	0.094	15.0
6.3 [100]	43.7	0.381	4.900	0.085	17.5
6.6 [002]	21.5	0.188	7.214	0.126	11.2
6.6 [100]	43.0	0.375	7.450	0.130	11.5

From table 6.12 we can observe that the crystal size of the samples is in the range 1.1 – 1.7 nm, the same crystal size found in monolithic biocarbon obtained at the same temperatures [33]. Even in this case there is no relationship between the pressure applied during pellets' production and the crystal size. For this reason, a different degree of graphitization is not the explanation of the electrical behaviour of the samples. The crystal sizes are very similar to each other. The biggest crystal size belongs to the sample 6.3. The set n.6 underwent a pyrolysis with an HTT of 1200°C and the sample 6.3 was produced at 1500 psi, an intermediate pressure. The samples produced at lower and higher pressure present a smaller crystal size. The crystal sizes are so close to each other that we can not define a trend of sizes as a function of the applied pressure.

6.5.3 Raman spectroscopy results

All the samples of the sets n.5 and 6 underwent Raman spectroscopy. The obtained results confirmed XRD analysis. The main features of the Raman spectra of carbons are the so-called G and D peaks, which lie around 1560 and 1360 cm^{-1} respectively [67]. These bands are present in all poly-aromatic hydrocarbons. The G peak is due to the bond stretching of all pairs of sp^2 atoms in both rings and chains. The D peak is due to the breathing modes of sp^2 atoms in rings [67]. The D band characterizes the disorder in sp^2 carbon materials.
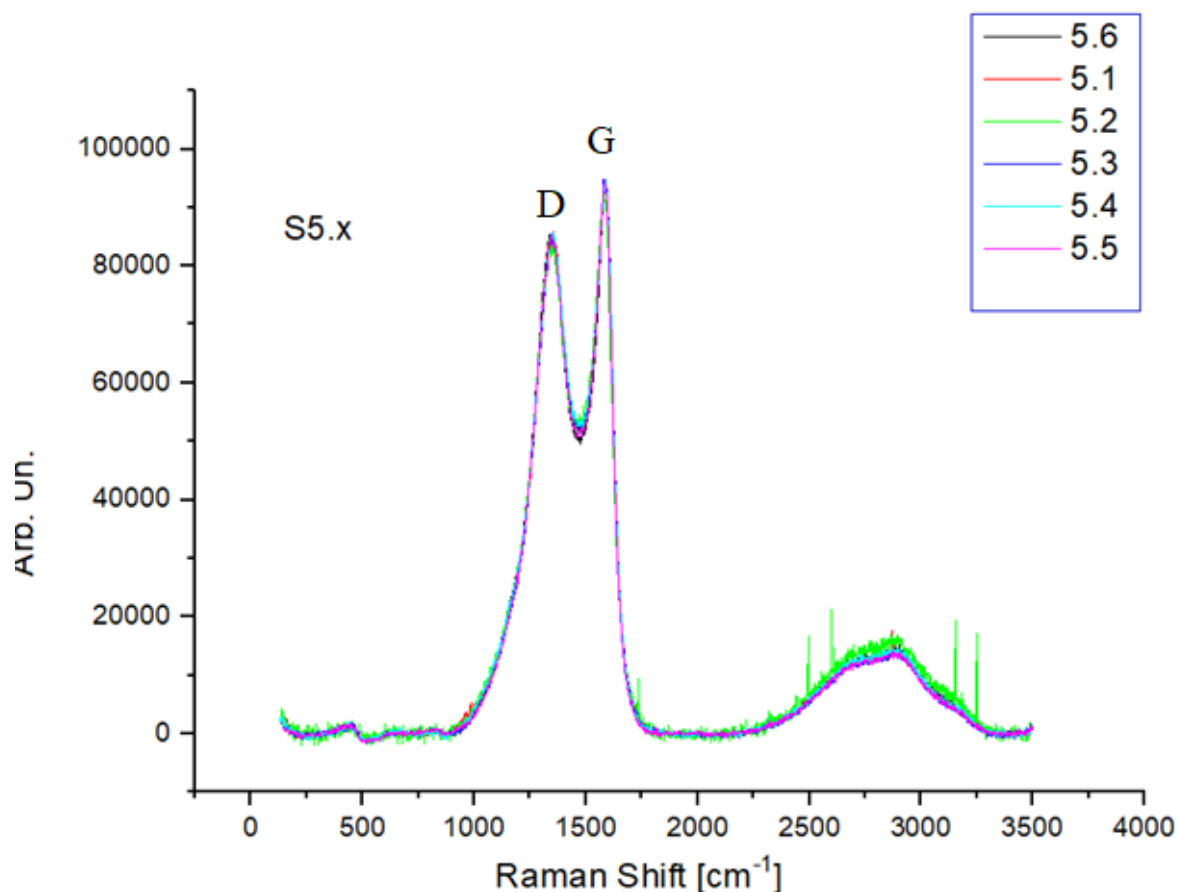
Figure 6.20 Raman spectra of set of samples n.5
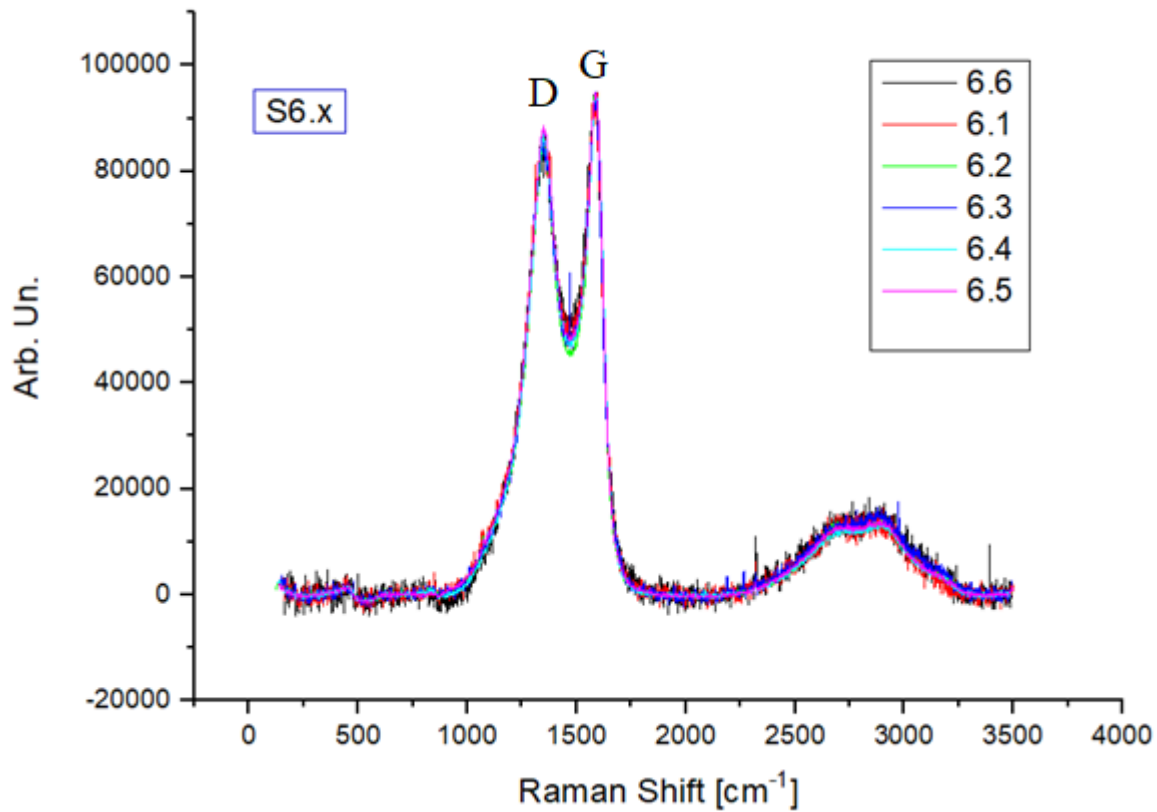
Figure 6.21 Raman spectra of set of sample n.6

Looking at figures 6.20 and 6.21 we can notice that samples from set n.5 and 6 seem to be quite similar to each other with a worst signal/noise ratio for set n.6. A very slight narrowing of D peak width and a small lowering of inter-components between peak D and G is observed in set n.6 compared to set n.5. This means that increasing the HTT, the structure is slightly more ordered. However, no evident trend as a function of the sample production pressure is observed, both in set n.5 and 6. There are no differences in the degree of graphitization among the samples of the two sets, as we noticed from XRD analysis. We can observe in fact, that all the curves belonging to the same set overlap each other.

7. Conclusions

Biochar is among the materials of the future. It is a sustainable, cheap and readily available material that can be produced from countless feedstocks. It is suitable for various applications including climate mitigation and soil amendment, wastewater treatment, air decontamination, biogas production, controlling emissions and it can be used in many sectors such as metallurgy, cosmetics, energy production ecc. In this work the application of interest is the energy storage: can we use the biochar as electrode material for supercapacitor applications? Since we need to store the energy coming from renewable sources, supercapacitors could be a good solution in terms of energy density, power density and cycle life. Biochar can substitute other more expensive and non-sustainable materials used in this field.

The feedstock used in this research is wood, in particular sawdust from sugar maple wood. All the previous studies about biochar produced from wood, with the aim of finding a material for electrodes, focused their attention on biochar from monolithic pieces of wood. Previous works conducted at the University of Toronto found out that monolithic biochar is a good conductor (conductivity with an order of magnitude of 10^3 S/m) and an excellent electrode material for supercapacitor. In this work, the main aim is to study the feasibility in terms of production and characterization of sawdust-derived biochar monolith. Sawdust is a waste and biochar from sawdust could be a very inexpensive material. The application of pressure during the production of pellets makes the biochar material denser than wood-derived biochar, helping achieve a greater energy density.

The study consists of partial lignin removal pre-treatment, sawdust compression, pyrolysis and characterization of the obtained biochar. In particular, we are interested in the electrical conductivity of the biochar (that is a required property for a supercapacitor electrode) and its dependence on the pyrolysis conditions and the pressure applied during the pellets' production. Moreover, the work studies the effectiveness of adding a binder (lignin) to treated sawdust particles in improving physical and electrical properties of sawdust-derived biochar monolith.

The main conclusions can be summed up as follows:

The partial removal of lignin is a key point in this research since it helps the particles stick together during the compression, increasing the pellets' density. Lignin confers rigidity to the cell walls and its removal makes the sawdust more compressible.

Increasing the pressure applied during the sawdust pellets production at 100°C leads to an increasing in density achieving values of 1.2-1.3 g/cm^3, much higher compared to the feedstock's density (0.733 g/cm^3).

The pyrolysis conditions affect the final physical and electrical properties of the biochar: the increase of the HTT improves the electrical conductivity. The holding time and heating rate chosen plays an important role on the electrical conductivity, but less effectively than the HTT. In particular, increasing the holding time at HTT is more effective than decreasing the heating rate to HTT. The most conductive samples belonged to the set n.6, pyrolyzed until 1200°C with a holding time of one hour. The highest electrical conductivity value measured is 176.2 ± 4.6 S/m.

The electrical conductivity of the monolithic biochar from compressed sawdust is much lower than that of the monolithic biochar from the same type of wood monolith: the values are one order of magnitude inferior. This could be explained by the fact the wood-derived biochar monolith has a continuous solid

structure preserved from its precursor-wood monolith, while the sawdust-derived biochar monolith is likely made of individual biochar particles loosely connected.

The most intriguing results is the dependence of the electrical conductivity on the pressure applied during the pellets' production. Every set of samples showed the same trend: the most conductive sample is the one produced at the lowest pressure (3.45 MPa) and the least conductive is the one produced at the highest pressure (20.48 MPa). Higher pressure resulted in higher density of both sawdust pellets and biochar monoliths, as well as lower bulk and skeletal electrical conductivity of biochar decrease. A yet-to-confirm mechanism is the possible formation of microcracks induced by the increased pressure.

The carbon content and degree of carbonization is higher for the samples pyrolyzed at higher temperatures, as already mentioned in the literature, but there is no link between the degree of carbonization and the pressure applied. XRD and Raman spectroscopy analyses show that the samples pyrolyzed at 1200°C show a slightly more ordered structure. The crystal sizes are in the range 1.1-1.7 nm, consistent with literature values. No dependence of the degree of graphitization on the applied pressure is found.

The samples with added lignin show an increment in the char yield, a higher density and lower electrical conductivity. The decrease in conductivity after first 10% lignin addition is much smaller than that after second 20% lignin addition. Added lignin has smaller particle size and makes the pellets and biochar monoliths denser. However, biochar particles derived from lignin are more amorphous and less conductive than those from treated sawdust which contains mainly cellulose and hemicellulose.

8. Future outlooks

Since there are no previous studies about the use of compressed sawdust to produce biochar, a lot of future works may be conducted.

First of all, the same work could be repeated changing the variables and fixed parameters. i.e. changing the pyrolysis conditions such as increasing the HTT to increase the crystal sizes and the electrical conductivity, changing the sawdust particle size, trying to mix together sawdust from different feedstocks or increasing the temperature adopted during the sawdust compression. Changing the time pre-treatment and increasing the content of lignin removed may be another solution to increase the electrical conductivity.

An interesting measurement could be the measure of the electrical conductivity along the radial direction of the pellets: since the particles' fibers may be oriented more along the radial direction, there could be fewer contact points and the samples could be more conductive. However, the thickness of the pellets produced in this work are very low, and after pyrolysis it reached 0.2-0.3 cm. The solution may be creating a new set-up to measure the conductivity along the radial direction or producing thicker samples.

An interesting challenge may be the use of some binders: they should act as glue among the sawdust particles, even after the pyrolysis, creating more pathways available for the current. The choice of the right binder is not easy: it should carbonize leaving a high carbon content and it must be a conductive material.

Moreover, the dependence of the electrical conductivity on the applied pressure has to be studied and explained more deeply. A deeper investigation of the samples' structure, for example with SEM images, may provide very important information about the orientation of the fibers in the biochar structure. The problem of studying the samples through SEM is that the surface is not smooth and the samples are very fragile: it is difficult cutting them and leaving smooth surfaces available for the analysis. They are made of particles stuck together and cutting them means disintegrating the structure.

In this work, a preliminary investigation of the physical and electrical properties of the samples has been done. The samples have showed a good conductivity, although it is not as high as the biochar from monolithic pieces of wood. In future works, students in the Green Technologies Lab will work on the samples of this work and test them as supercapacitors. Electrical conductivity is only one of the required properties; they need to charge and discharge themselves very quickly and store the energy.

Moreover, if the use of compressed sawdust will not reveal successful, the same procedure of partial removal of lignin and compression may be repeated on monolithic pieces of wood. In this way, a denser material will be obtained, preserving the tree structure features and maybe developing a more ordered structure due to the removal of lignin.

LIST OF FIGURES

LIST OF TABLES

Bibliography

[1] Ngan A., Jia C.Q., Tong S., (2019), *Production, characterization and alternative applications of biochar,* In: Fang Z., Smith R.L., Tian X., Production of Materials from Sustainable Biomass Resources, Springer Singapore

[2] Lehmann J., Joseph S., (2015), *Biochar for environmental management: an introduction,* In: Lehman J., Joseph S., Biochar for Environmental Management: Science, Technology and Implementation, Second Edition, Oxon and New York: Routledge, 1-11

[3] Maroušek, J., Vochozka, M., Plachý, J., (2017), *Glory and misery of biochar*, Clean Technologies and Environmental Policy, 19**:**311-317

[4] Parliament of Australia, The basics of biochar, Tallberg A., 2009

[5] Bezerra J., Turnhout E., Vasquez I.M., Francischinelli Ritti T., Arts B., Kuyper T.W., (2016), *The promises of the Amazonian soil: shifts in discourses of Terra Preta and biochar*, Journal of Environmental Policy & Planning, DOI: 10.1080/1523908X.2016.1269644

[6] International Biochar Initiative, https://biochar-international.org/faqs/#1521824701674-1093ca88-fd85, (last visit 19/01/2019)

[7] Kan T., Strezov V., Evans J.E., (2016), *Lignocellulosic biomass pyrolysis: a review of product properties and effects of pyrolysis parameters*, Renewable and Sustainable Energy Reviews, 57:1126-1140

[8] Demirbas A., (2009), *Pyrolysis mechanisms of biomass materials*, Energy Sources, Part A, 31(13): 1186-1193

[9] McKendry P., (2002), *Energy production from biomass (part 1): overview of biomass,* Bioresource Technology 83:37-46

[10] Demirbas A., (2006), *Production and Characterization of Bio-Chars from Biomass via Pyrolysis*, Energy Sources Part A, 28(5): 413-422

[11] Wilson K., White D., (1987), *The Anatomy Of Wood*, London: Stobart Davies Ltd

[12] Basu P., (2010), *Pyrolysis Torrefaction,* In: Basu P., Biomass gasification and pyrolysis: practical design and theory, Kidlington, Oxford: Elsevier, 65-84

[13] Demirbas A., (2009*), Pyrolysis of Biomass for Fuels and Chemicals*, Energy Sources Part A, 31(12):1028-1037

[14] Wunna K., Nakasaki K., Auresenia J.L., Abella L.C., Gaspillo P.D., (2017), *Effect of alkali pretreatment on removal of lignin from sugarcane bagasse*, Chemical Engineering Transactions, 56:1831-1836

[15] Lebow T.S., Cooper P., Lebow K.P., (2006), *Study Design Considerations in Evaluating Environmental Impacts*, In: Townsend T.G., Solo-Gabriele H., Environmental Impacts of Treated Wood, New York: Taylor and Francis Group, 79-96

[16] Peydecastaing J., (2008*), Chemical modification of wood by mixed anhydrides,* [dissertation], Université de Toulouse

[17] Parham R.A., Gray R. L., (1984), *Formation and structure of wood,* In: Rowell R., The Chemistry of Solid Wood, Washington D.C.: American Chemical Society, 3-56

[18] Fengel D., Wegener G., (1989), *Wood: chemistry, ultrastructure, reactions*, Second Edition, Berlin: Walter de Gruyter

[19] De Wild P. J., (2011), *Biomass Pyrolysis for Chemicals*, [dissertation], University of Groningen, The Netherlands

[20] Demirbas A., Arin G., (2002), *An overview of biomass pyrolysis,* Energy Sources, 24(5):471-482

[21] Van de Velden M., Baeyens J., Brems A., Janssens B., Dewil R., (2010), *Fundamentals, kinetics and endothermicity of the biomass pyrolysis reaction*, Renewable Energy, 35:232-242

[22] Stefanidis S.D., Kalogiannis K.G., Iliopoulou E.F., MIchailof C.M., Pilavachi P.A., Lappas A.A., (2014), *A study of lignocellulosic biomass pyrolysis via the pyrolysis of cellulose, hemicellulose and lignin*, Journal of Analytical and Applied Pyrolysis, 105:143-150

[23] Yang H., Yan R., Chen H., Ho Lee D., Zheng C., (2007), *Characteristics of hemicellulose, cellulose and lignin pyrolysis*, Fuel, 86:1781-1788

[24] Kan T., Strezov V., Evans T.J., (2016), *Lignocellulosic biomass pyrolysis: a review of product properties and effects of pyrolysis parameters*, Renewable and Sustainable Energy Reviews 57:1126-1140

[25] Dhyani V., Bhaskar T., (2018), *A comprehensive review on the pyrolysis of lignocellulosic biomass,* Renewable Energy, 129:695-716

[26] Cha J.S., Park S.H., Jung S., Ryu C., Jeon J., Shin M., Park Y., (2016), *Production and utilization of biochar: a review*, Journal of Industrial and Engineering Chemistry, 40:1-15

[27] Mašek O., Luque, (2016), Biochar in thermal and thermochemical biorefineries-Production of biochar as a coproduct, In: Luque R., Sze Ki Lin C., Wilson K., Clark J., *Handbook of Biofuels Production - Processes and Technologies,* Second Edition, Elsevier

[28] Chhiti Y., Kemiha M., (2013), T*hermal Conversion of Biomass, Pyrolysis and Gasification: A Review*, The International Journal of Engineering And Science, 2(3):75-85

[29] Bridgwater A.V., (2012), *Review of fast pyrolysis of biomass and product upgrading*, Biomass and Bioenergy, 38:68-94

[30] Lv G., Wu S., Yang G., Chen J., Liu Y., Kong F., (2013), *Comparative study of pyrolysis behaviours of corn stalk and its three components*, Journal of Analytical and Applied Pyrolysis, 104:185-193

[31] Kim K.H., Kim JY., Cho TS., Choi J.W., (2012), *Influence of pyrolysis temperature on physicochemical properties of biochar obtained from the fast pyrolysis of pitch pine (Pinus rigida)*, Bioresource Technology, 118:158-162

[32] Kleber M., Hockaday W., Nico P.S., (2015), *Characteristics of biochar: physical and structural properties*, In: Lehmann J., Joseph S., Biochar for Environmental Management: Science, Technology and Implementation, Second Edition, Oxon and New York: Routledge, 91-103

[33] Caguiat J.N., Yanchus D.S., Gabhi R.S., Kirk D.W., Jia C.Q., (2018), *Identifying the structures retained when transforming wood into biocarbon*, Journal of Analytical and Applied Pyrolysis, 136: 77-86

[34] Leng L., Huang H., (2018), *An overview of the effect of pyrolysis process parameters on biochar stability*, Bioresource Technology, 270:627-642

[35] Keiluweit M., Nico P.S., Johnson M.G., Kleber M., (2010), *Dynamic molecular structure of plant biomass-derived black carbon (biochar),* Environmental Science & Technology, 44:1247-1253

[36] Amin F.R., Huang Y., He, Y. et al., (2016), *Biochar applications and modern techniques for characterization*, Clean Technologies and Environmental Policy, 18:1457-1473

[37] Mašek O., (2013), Biochar and carbon sequestration, In: Belcher C.M., *Fire Phenomena and the Earth System: An Interdisciplinary Guide to Fire Science*, John Wiley & Sons Ltd, 309-322

[38] Lal R., (2008), *Carbon sequestration*, Philosophical Transactions of the Royal Society B: Biological Sciences, 363:815-830

[39] http://www.allpowerlabs.com/news/copandcarbon.html (last visit 02/02/2019)

[40] Matthews J.A., (2008), *Carbon-negative biofuels*, Energy Policy, 36:940-945

[41] Blakeslee T. R., (2009), *Biochar: the key to carbon-negative biofuels*, Renewable energy world, https://www.renewableenergyworld.com/articles/2009/04/biochar-the-key-to-carbon-negative-biofuels.html (last visit 02/02/2019)

[42] Wang B., Gao B., Fang J., (2018), *Recent advances in engineered biochar productions and applications*, Critical Reviews in Environmental Science and Technology, 47(22):2158-2207

[43] Brassard P., Godbout S., Pelletier F., Raghavan V., Palacios J.H., (2018), *Pyrolysis of switchgrass in an auger reactor for biochar production: A greenhouse gas and energy impacts assessment*, Biomass and Bioenergy, 116:99-105

[44] Goodenough J.B., Abruna H., Buchanan M., (2007), *Basic research needs for electrical energy storage*, Report of the Basic Energy Sciences Workshop for Electrical Energy Storage, 18-22

[45] Pandolfo A.G., Hollenkamp A.F., (2006), *Carbon properties and their role in supercapacitors*, Journal of Power Sources, 157:11-27

[46] Tyagy A., Gupta R.K., (2015), *Carbon nanostructures from biomass waste for supercapacitors,* In: Krishnamoorthy S., Nanomaterials A Guide to Fabrication and Applications, 1st Edition, CRC Press Taylor and Francis Group

[47] Gabhi R.S., Kirk D.W., Jia C.Q., (2017), *Preliminary investigation of electrical conductivity of monolithic biochar*, Carbon, 116:435-442

[48] Péréz-Rodríguez S., Torres D., Lázaro M.J., (2018), *Effect of oxygen and structural properties on the electrical conductivity of powders of nanostructured carbon materials*, Powder Technology, 340:380-388

[49] Wu X., Shi X., Yao M., Liu S., Yang X., Zhu L., Cui T., Liu B., (2017), *Superhard three-dimensional carbon with metallic conductivity*, Carbon, 123:311-317

[50] Sebastian D., Ruiz A.G., Suelves I., Moliner R., Lazaro M.J., (2013), *On the importance of the structure in the electrical conductivity of fishbone carbon nanofibers*, Journal of Materials Science, 48:1423-1435

[51] Wallace G.G., Moulton S.E., Higgins M., Kapsa R.M.I., (2012), Carbon, In: Organic Bionics, Wiley-VCH Verlag GmbH & Co. KGaA, 41-79

[52] Terrones M., Botello-Mendez A.R., Campos-Delgado J., Lopez-Urias F., Vega-Cantú Y.I., Rodriguez-Macias F.J., Elias A.L., Munoz-Sandoval E., Cano-Marquez A.G., Charlie J., Terrones H., (2010), *Graphene and graphite nanoribbons: morphology, properties, synthesis, defects and applications*, Nano Today, 5:351-372

[53] Song J., Chen C., Zhu S., Zhu M., Dai J., Ray U., Li Y., Kuang Y., Li Y., Quispe N., Yao Y., Gong A., Leiste U.H., Bruck H.A., Zhu J.Y., Vellore A., Li H., Minus M.L., Jia Z., Martini A., Li T., Hu L., (2018), *Processing bulk natural wood into a high-performance structural material*, Nature, 554:224-228

[54] Song J., Chen C., Wang C., Kuang Y., Li Y., Jiang F., Li Y., Hitz E., Zhang Y., Liu B., Gong A., Bian H., Zhu J.Y., Zhang J., Li J., Hu L., (2017), *Superflexible wood*, ACS Applied Materials & Interfaces, 9:23520-23527

[55] Li Y., Liu H., (2000), *High-pressure densification of wood residues to form an upgraded fuel*, Biomass and Bioenergy, 19:177-186

[56] Jenkins S.H., (1930), *The determination of cellulose in straws*, Rothamsted Experimental Station, Harpendem, Herts

[57] Gao L., Guo W., Luo S., (2018), *Investigation in compressed moso bamboo (Phyllostachys pubescens) after hot-pressing molding*, Journal of Wood Science

[58] Nagle D.C., Byme C.E., (2000), *Carbonized wood and materials formed thereform*, US6051096A

[59] Brewer C.E., Brown R.C., (2012), *Biochar*, In: Comprehensive Renewable Energy, Volume 5, Elsevier, 357-384

[60] Krotz L., Giazzi G., (2014), Thermo Scientific FLASH 2000 CHNS Analyzer: Stability, Linearity, Repeatability and Accuracy, Application Note 42213

[61] Ferrari A.C., Robertson J., (2000), Interpretation of Raman spectra of disordered and amorphous carbon, Phys. Rev. B, vol. 61, no. 20, pp. 14095-14107

[62] Menind A., Križan P., Šooš L., Matúš M., Kers J., (2012), *Optimal conditions for valuation of wood waste by briquetting*, 8th International DAAAM Baltic Conference, Tallin, Estonia

[63] Basile L., (2016), *Evolution of electrical and structural properties of monolith biochar during pyrolysis*, Master thesis, Politecnico di Torino

[64] Péréz-Rodríguez S., Torres D., Lázaro M.J., (2018), *Effect of oxygen and structural properties on the electrical conductivity of powders of nanostructured carbon materials*, Powder Technology, 340: 380-388

[65] Wang T., Camps-Arbestain M., Hedley M., (2013), *Predicting C aromaticity of biochars based on their elemental composition*, Organic Geochemistry, 62: 1-6

[66] Wu M., Han X., Zhong T., Yuan M., Wu W., (2016), *Soil organic carbon content affects the stability of biochar in paddy soil*, Agriculure, Ecosystems & Environment, 223:59-66

[64] Ferrari A.C., (2007), *Raman spectroscopy of graphene and graphite: Disorder, electron-phonon coupling, doping and nonadiabatic effects*, Solid state communication, 143:47-57

ACKNOWLEDGEMENTS